Strategies for Utrophin Upregulation

Zakaria Orfi

Division of Experimental Medicine

McGill University

Montreal, Quebec, Canada

May, 2016

A thesis submitted to McGill University in partial fulfillment of the requirements of the degree of Doctorate of Philosophy

Table of Contents

Abstract

Duchenne Muscular Dystrophy (DMD) is the most common X-linked lethal disorder caused by a genetic defect in the dystrophin gene. A substantial, ectopic expression of utrophin, which is a close analogue of dystrophin, in the extra-synaptic sarcolemma of dystrophin-deficient muscle fibers, can prevent deleterious effects of dystrophin deficiency. Our aim is to up-regulate the expression of this dystrophin-related gene in DMD, thereby complementing the lack of dystrophin function. To achieve utrophin up-regulation, we engineered several zinc finger proteins (ZFPs), and tested their ability to target and upregulate the human utrophin A promoter. In parallel, we used genome editing tools, such as the zinc fingers nuclease (ZFN), and the Clustered, Regularly Interspersed, Short Palindromic Repeats (CRISPR), to target and modify the endogenous utrophin A promoter. Although results of ZFPs coupled to the trans-activator domain VP16 have shown a moderate up-regulation of the endogenous utrophin in HEK 293T cells, the screening of ZFN and CRISPR/Cas9 systems have shown these to have a great efficacy in inducing DNA double-strand breaks at utrophin A promoter. The co-transfection of HEK 293T cells with the CRISPR/Cas9 system and a donor plasmid harboring the Cytomegalovirus and chicken beta actin (CAG) promoter flanked between utrophin A arms triggered the integration of the CAG promoter sequence into the endogenous human utrophin A promoter region through a homology-directed repair mechanism. Integration of the CAG promoter within the utrophin A promoter region led to a substantial up-regulation of the endogenous utrophin gene in these cells.

Résumé

La Dystrophie Musculaire de Duchenne (DMD) est une maladie létale causée par le dysfonctionnement du gène codant pour la dystrophine située sur le chromosome X. La surexpression de l'utrophine (protéine analogue à la dystrophine) dans les muscles déficients de la dystrophine, peut prévenir l'effet néfaste liée à cette anomalie. Notre but est de sur-exprimer l'utrophine chez des patients atteints de la DMD afin de défier l'absence de la dystrophine. Pour cela, des protéines à doigts de zinc (ZFP) ont été synthétisées et leur capacité à activer le promoteur A de l'utrophine a été testé. En même temps, la nucléase à doigts de zinc (outils de correction génomique) ainsi que le système 'Courtes répétitions palindromiques groupées et régulièrement espacées ' (CRISPR) ont été utilisés pour modifier le promoteur A de l'utrophin endogène. Bien que le ZFP couplé au domaine trans-activateur de VP16 a montré une surexpression modérée de l'utrophine endogène dans les cellules HEK 293T, le criblage de ZFN et le système CRISPR/Cas9 a démontré quant à lui une grande efficacité à induire des cassures sur le double brin d'ADN au niveau du promoteur A de l'utrophine. La co-transfection des cellules HEK 293T avec le système CRSIPR/Cas9 ainsi que le plasmide donneur possédant le promoteur chimère de la β-actine de poulet fusionné a l'enhancer du promoteur précoce de cytomégalovirus (CAG) flanqué entre les deux bras du promoteur A de l'utrophine induit la voie de la réparation homologue dirigée qui induit à son tour l'intégration du CAG dans le promoteur A de l'utrophine humaine endogène. Les résultats ont confirmé que l'intégration de CAG au niveau du promoteur A de l'utrophine, permet une surexpression stable de l'utrophine endogène.

Acknowledgements

First and foremost, I want to express my deep gratitude toward my supervisor and mentor **Dr Josephine Nalbantoglu** for her support and guidance. It has been an honor to be her Ph.D. student. She has taught me, how good biotechnology and molecular biology is done. I appreciate all her contributions of time, ideas, and funding to make my Ph.D. experience productive and stimulating. Her love for science and research was contagious and motivational for me, even during tough times during my Ph.D.

I would like to express my gratitude to the members of my committee; Dr Elena Torban, Dr Renald Gilbert, and Dr Kenneth Hastings, for their academic guidance which helped develop my skills and critical thinking as well.

I would like also thank my colleagues in the Nalbantoglu's lab, SongSong Geng, Nadia Houri and Nancy Larochelle for their help guidance and kindness. Special thanks to **Nancy** for her help with experiments.

I had the privilege of receiving studentships and travel awards during my doctoral studies. I am grateful to the CIHR Neuroinflammation Training Program and McGill University for enriching my graduate student experience.

Last but definitely not least, a special thank you to my wife, my parents, my brother and my sisters for their encouragement and their faith in me. I love you!

"And remember! Your Lord caused to be declared: If ye are grateful, I will add more unto you." — Surah Ibrahim

List of Figures

Abbreviations

AAV	Adeno-Associated-Virus
BCA	BiCinchoninic acid
BMC	Becker muscular dystrophy
BMD	Becker Muscular Dystrophy
CAG	Cytomegalovirus and chicken beta actin
cDNA	Complementary DNA
CMV	Cytomegalovirus
CRISPR	Clustered Regularly Interspaced Short Palindromic Repeats
crRNA	CRISPR RNA
DAPs	Dystrophin associated proteins
DMD	Duchenne Muscular Dystrophy
DNA	Deoxyribonucleic acid
ECM	extracellular matrix
GCs	Glucocorticoids
GRMD	Golden Retriever Muscular Dystrophy Dog
HDR	Homologous Direct repair
HFMD	Hypertrophic feline muscular dystrophy
IPS cells	Induced Pluripotent Stem cells
Kb	kilobase
KDa	kilodalton
Mb	Mega-bases
MMP	Metalloprotease
NHEJ	Non Homologous End Joining
NO	Nitric oxide
PCR	Polymerase chain reaction
PMOs	Phosphorodiamidate morpholino oligomer
RNA	Ribonucleic acid
ROS	Reactive oxygen species
ROS	Reactive oxygen species
RT-PCR	Reverse transcription-PCR
SR	Sarcoplasmic reticulum
tracrRNA	Transactivating RNA)
WGA	Wheat germ agglutinin
ZFN	Zinc finger nuclease
ZZ	Zinc finger

Contribution of Authors

The majority of the experimental work presented in this thesis was performed by the candidate, Zakaria Orfi.

The thesis was written by Zakaria Orfi and edited by the candidate's supervisor, Dr. Josephine Nalbantoglu.

Chapter 1: Introduction

Duchenne Muscular Dystrophy

Human skeletal muscle is a complex and heterogeneous tissue composed of approximately 434 muscles, serving a multitude of functions, and contributing to over 40 % of total body weight. This complex tissue can be severely affected by inherited or sporadic monogenic disorders, leading to muscular dystrophies, which are characterized by progressive muscle wasting and weakness, typically causing premature death. Muscle degeneration has a negative impact on ambulation, posture, cardiac and respiratory functions. Many genes associated with muscular dystrophies encode proteins of the plasma membrane and extracellular matrix [1]. Duchenne Muscular Dystrophy (DMD) is the most common and severe form of muscular dystrophy. It was first described in 1852 by Dr. Edward Meryon and Guillaume Duchenne de Boulogne, as a pseudo-hypertrophic muscular paralysis, then named Duchenne Muscular Dystrophy. Joseph Sarrazin was the first patient diagnosed with DMD. According to Dr Duchenne, Joseph was normal at birth, but at the age of 2 years his lower extremities grew abnormally in volume, despite lacking power since birth and rarely being exercised. All of Joseph's movements were weak, and he could not walk except with legs spread apart for lateral balance. Three years later, Joseph's condition badly deteriorated, with weakness spreading to the whole body. The child was bedridden by age 12 despite treatment with electrotherapy and massage. He died of tuberculosis at age 14 [2].

Duchenne summarized 12 of his case studies and noted that there were six principal diagnostic features of DMD:

1. Loss of muscle strength, usually in the lower extremities.

2. Spreading of the lower limbs upon standing and walking.

3. Abnormal development of volume in lower extremities.

4. Progressive course of the disease.

5. Decrease in electro-muscular contractility.

6. Absence of fever.

DMD is considered one of the most common X-linked degenerative childhood muscle diseases, affecting approximately 1 in 3500 male births [3]. The life span of most DMD patients is shortened and affected patients die in their early twenties due to respiratory complications or cardiac dysfunction [4].

A milder dystrophy, called Becker Muscular Dystrophy (BMD), was described by the German physician Peter Becker in 1950 [5]. Similar to DMD, BMD has the same inheritance pattern, but is less severe, allowing longer survival. BMD symptoms appear at about age 12 or even later and BMD patients are bedridden at age of 25-30. Unlike DMD, most of BMD (70%) results from in-frame mutations, which produce internal deletion or duplication within the dystrophin gene. Though the beginning of symptoms and the progression of the disease are delayed in BMD, the clinical course is similar to the DMD [6, 7].

Dystrophin gene and protein

The Dystrophin Gene

Although most DMD patients are males, the *dystrophin* gene was localized on chromosome Xp21 in female patients. The position of DMD gene was determined by studying large deletions

of X chromosome in abnormal karyotypes of nine rare females with DMD [8]. Several studies have shown that DMD patients have X chromosome breakpoints in position Xp21, which provided strong evidence that this sub-band contains the DMD locus [9, 10]. Moreover, BMD was localized to the same region [11]. The dystrophin gene is one of the largest genes with 2.5 Mega-bases (Mb) of DNA, composed of 79 exons, and representing 1.5% of the X chromosome. The 14Kb cDNA was first cloned using human fetal muscle cDNA library [12, 13]. The dystrophin mRNA is expressed mainly in skeletal and cardiac muscle, with lesser amounts in the brain. The spatiotemporal dystrophin gene expression is controlled by seven independently regulated promoters. Three of them are upstream promoters and express the full length dystrophin: the Brain (B), Muscle (M), and Purkinje (P) promoters, which reflects the major tissues in which the dystrophin promoter is more active [14]. Unlike external promoters, the four internal promoters which can be referred to as retinal (R), brain-3 (B3), Schwann cell (S), and general (G), generate shorter dystrophin transcripts that encode truncated C-terminal isoforms. These promoters utilize a unique first exon that splices in to exons 30, 45, 56, and 63, respectively, and generate truncated protein of 260 kDa [15], 140 kDa[16], 116 kDa[17], and 71 kDa[18]. The alternative splicing might regulate the binding affinity of isoforms to the dystrophin associated complex [19, 20].

The majority of DMD cases are transmitted from the carrier mother to her son; however, 1/3 of cases are sporadic [21]. Unlike BMD, which generally exhibits in-frame dystrophin mutations, approximately 65% of DMD are characterized by large deletions of the dystrophin gene [22], and approximately 15-30% are the result of point mutations [23]. However, the size and position of the deletion within the dystrophin gene often does not correlate with the clinical phenotype

observed. This can be explained by the open reading frame mechanism of the truncated dystrophin RNA. In fact, depending on the predicted stability of dystrophin, it has been possible in many cases to predict whether a young DMD patient is likely to develop BMD or DMD [24]. Also it has been shown that the severity of DMD is generally correlated with the amount of dystrophin present at in the muscle-fiber membrane [25].

The Dystrophin Protein

The diagnostic marker of DMD is the absence of the cytoskeletal protein dystrophin, which is an essential component of the dystrophin glycoprotein complex (DGC) [26]. Dystrophin is a large protein composed of 3,685 amino acid residues (427kDa), and localized at the cytoplasmic face of the sarcolemma membrane (Figure 1) [27]. Because dystrophin is a member of the β-spectrin/α-actinin protein family [28], it acts as a bridge linking the actin cytoskeleton to the extracellular matrix (ECM), which leads to sarcolemmal stability during muscle contraction and can also coordinate signal transducers at the sarcolemma [29]. Based on its primary structure, dystrophin can be organized into four distinct regions: (1) The actin-binding domain at the NH2 terminus, (2) The central rod domain, (3) The cysteine-rich domain, and (4) The C-terminal domain. The first part of the dystrophin primary structure is the NH2-terminal end, which consists of 240 amino acids that form an actin binding domain followed by several repeating units known as spectrin-like repeats. The second and largest segment consists of the rod domain, which is composed of 24 repeating units interspaced by four proline rich hinge regions. The repeating units might bring more flexibility and elasticity to dystrophin during muscle contraction [30]. The third domain is a cysteine rich domain composed of three sub-domains: (1) WW (tryptophan), (2) ZZ (Zinc finger), and (3) EF (α-helices) domains. The WW is a globular

domain that binds to proline-rich substrates and binds also to the carboxy-terminus of beta-dystroglycan [31, 32]. The ZZ domain is also part of the cysteine-rich domain and holds a number of conserved cysteine residues that interact with calmodulin [33]. The fourth and last domain is the C-terminal domain, which is composed of 420 amino acids which can be an alternatively spliced region. Like the rod domain, the C-terminal domain also has two coiled-coil motifs [34, 35]. Dystrophin localization and structure are mandatory for sarcolemma stability. Dystrophin acts as a molecular 'shock absorber' that can reduce eccentric stress during contraction or flexion through its interaction with several proteins called Dystrophin Associated Proteins (DAPs) [36]. The DAP complex was first identified when dystrophin was enriched in muscle membrane fractions eluted from a wheat germ agglutinin (WGA) column, which is known for its high affinity to N-acetyl-glycosamine, a common component of glycans; thus, dystrophin was found to be associated with a glycoprotein complex [25, 37]. DAP is composed of three distinct complexes: 1) The dystroglycan complex, 2) The sarcoglycan-sarcospan complex, and 3) The cytoplasmic dystrophin-containing complex [38]. Based on their location within the sarcolemma and their physical association with each other, these complexes can be mapped in the following order: The extracellular dystroglycan complex which is composed of α-dystroglycan and β-dystroglycan binds to laminin-2 via α-dystroglycan (αDG), leading to the attachment of the entire complex to the extracellular matrix; while, the β-dystroglycan (βDG) in the sarcolemma interacts with both the sarcoglycan-sarcospan sub-complex, composed of the sarcospan-sarcoglycans (α, β, γ, δ,) complex, and the WW domain and EF hands of dystrophin [39, 40]. The third complex, the cytoplasmic dystrophin-containing complex, is composed of dystrophin, syntrophins (syn) and α-dystrobrevin (αDB). The C-terminal region of dystrophin

forms the binding site with two syntrophin subunits (α1 and β1) and the cytoplasmic protein dystrobrevin; while the dystrophin N terminus interacts with cytoskeletal actin [34]. The dystrobrevins and syntrophins can directly interact with each other, and the syntrophins also bind nitric oxide synthase (NOS) [41].

Figure 1 Schematic model of dystrophin and utrophin- associated protein complexes

The dystrophin and utrophin proteins bind similarly to cytoskeletal actin through their N-terminal domain and the ECM through their C-terminus, acting as a bridge linking the internal cytoskeleton and the extracellular matrix. The central rod domain is formed by triple-helical segments similar to the repeat domains of spectrin which are interrupted by four hinge regions. The C-terminal region binds β-dystroglycan as well as the syntrophins and α-dystrobrevin. Adapted from (Kay E. Davies *et al* 2015) [42].

Figure 1

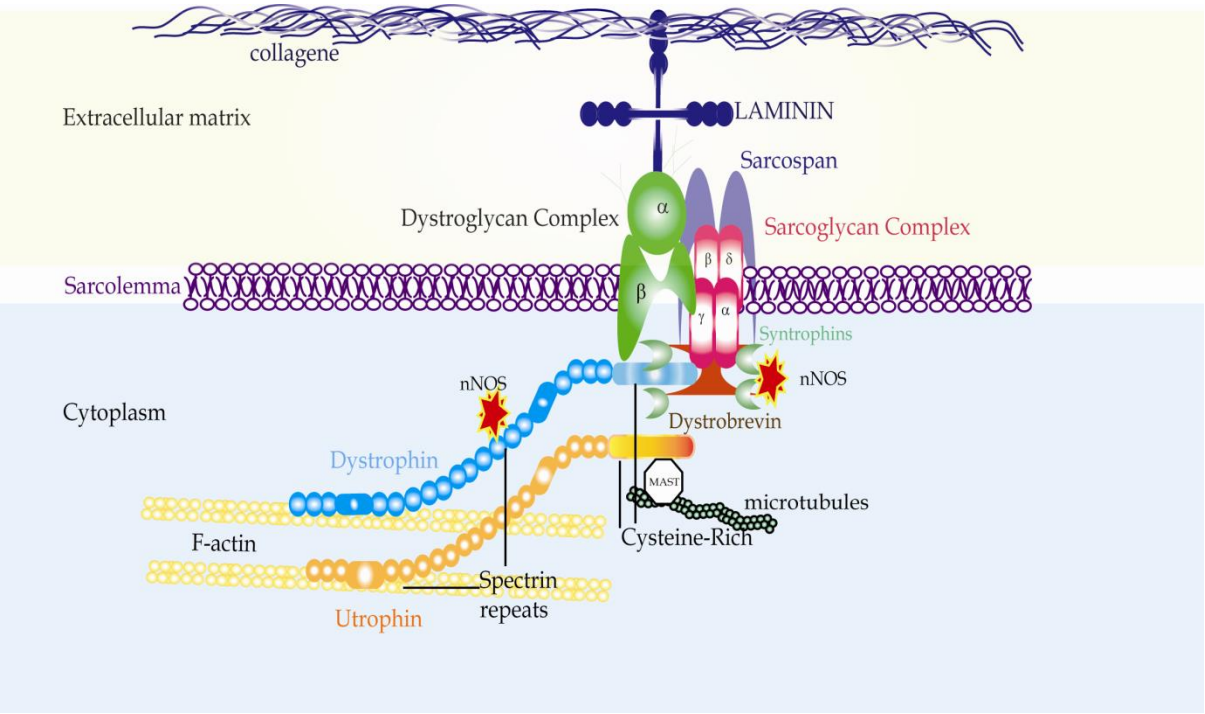
collagene
Extracellular matrix
LAMININ
Sarcospan
Dystroglycan Complex
α
Sarcoglycan Complex
β
δ
Sarcolemma
β
γ
α
Syntrophins
nNOS
nNOS
Cytoplasm
Dystrobrevin
Dystrophin
MAST
microtubules
F-actin
Cysteine-Rich
Spectrin
repeats
Utrophin

The Animal Models of DMD

The study of dystrophin gene in DMD patients allowed the discovery of its orthologue in mammalians. Disruptions of the dystrophin gene in these animals produced animal models for DMD, which can be used to study in detail the pathophysiology of the disease in humans. The choice of the animal model in experimental and pre-clinical trials is made according to the advantages and disadvantages they each provide [43]. To date, there are several mammalian models of DMD that have been used to better understand the pathophysiological process of DMD and to develop various types of therapeutic approaches leading to clinical trials.

The Dystrophin-Deficient *mdx* Mouse

The *mdx* mouse, an X chromosome-linked mouse mutant (gene symbol, *mdx*), first identified by Bulfield *et al* [44]. Later on, another group have shown that the *mdx* phenotype is due to a point mutation that converts a CAA (Glutamine) to a TAA stop codon in exon 23 [45]; the full-length dystrophin is absent in *mdx* mice, which leads to a truncated and unstable dystrophin unable to attach to the sarcolemma membrane, causing *mdx* muscle pathology. Although the absence of dystrophin does not affect the life span *mdx* mice [46], they have similar biochemical and histological defects as compared to human DMD patients; they exhibit severe muscle dysfunction, elevated serum creatine kinase and pyruvate kinase levels [47]. At birth, few myofibers are affected but necrosis occurs and it is more frequent during a crisis period at day 20 [48]. After the crisis period, the intensity of fiber necrosis decreases in frequency and occurs at low level during the life of the animal [48]. The *mdx* mouse has strong advantages as an animal

model including easy maintenance and breeding; as a result, the *mdx* mouse has been a key resource in the exploration of dystrophic pathophysiology.

Another *mdx* model that phenocopies the human DMD is the dystrophin and utrophin double knock out (*mdx*/*utnr*$^{-}$) mouse [49]. Unlike dystrophin-deficient *mdx* mice, which appear physically normal despite their underlying muscle pathology, the (*mdx*/*utnr*$^{-}$) mice show many signs typical of human DMD: they show severe progressive muscular dystrophy that results in premature death, and they have ultra-structural neuromuscular and myotendinous junction abnormalities [50]. Thus, the *mdx*/*utnr*$^{-}$ mouse is considered a more robust model of DMD.

The Dystrophin-Deficient Dog

The Golden Retriever Muscular Dystrophy Dog (GRMD) is a well characterized canine model of DMD [51]. Because of an RNA processing error that results from a single base change in the 3' consensus splice site of intron 6, there is loss of exon 7, which leads to absence of dystrophin protein [52]. The biggest advantage of GRMD is that their phenotype is closer to human DMD, with early onset muscle weakness, lethal respiratory distress, and cardio-myopathy. However, there are some disadvantages of this animal model including intra-variability between individuals, and considerable cost to maintain and breed the dogs.

The Dystrophin-Deficient Cat

The hypertrophic feline muscular dystrophy (HFMD) is characterized by a deletion of the exon 1 dystrophin muscle and Purkinje promoters [53]. The HFMD phenotype is characterized by marked muscle hypertrophy, necrosis, but less fibrosis [54]. The cat is considered a poor model of DMD because it has limited pathological similarity to DMD, and combines the practical disadvantages of being a large and affecting animal [55].

The Dystrophin-Deficient Pig

Porcine DMD model has been identified by genome-wide association analysis, which revealed spontaneous point mutation in the dystrophin gene (C>T, R1958W) in exon 41. Affected pigs show a reduction of 70% of dystrophin protein in both skeletal and cardiac muscles [56]; as a result, scientists have generated a genetically modified porcine model of DMD with deletion in exon 52 of the dystrophin gene [57].

The Dystrophin-Deficient Rat

Recently, a new rat model of DMD was generated using the Clustered Interspaced Short Palindromic Repeats (CRISPR)/Cas9 system. The CRISPR system targeted two exons in the rat dystrophin gene, which resulted in the absence of dystrophin expression in the F0 generation. The affected rats exhibited a decline in muscle strength, and the emergence of degenerative/regenerative phenotypes in the skeletal muscle, heart, and diaphragm. Because rats are bigger than mice and smaller than dogs, maintenance is easier in a laboratory setting. These advantages make *Dmd*-rats useful for developing therapeutic methods to treat DMD [58].

Pathophysiology of Duchenne Muscular Dystrophy

Although no standard model can explain the exact pathophysiology of DMD, multiple models have been explored to explain the chronology of muscle damage in a dystrophin-deficient environment including the membrane fragility, the impaired calcium homeostasis, and the proteolysis theories (Figure 2) [59].

Membrane fragility

Several studies have shown that loss of function mutations in any of the genes encoding Dystrophin Associated Proteins (DAP) might have a similar phenotype to what is seen in dystrophin mutations. The similarity of phenotypes is likely explained by the destabilization of the entire DAP that results from a deficiency in only one member [60-62]. Dystrophin as a member of the DAP plays a structural role by linking the extracellular matrix to the cytoskeletal actin, which may help in maintaining the integrity of the muscle fiber membrane. An electron microscopy study in 1975 was used to describe the ultra-structural features of DMD muscle. The electron microscopy results have shown disrupted sections or delta lesions on the sarcolemma membrane of DMD cells [63]. This observation gave rise to the theory of membrane fragility, which postulates that the primary pathology of DMD muscle might be due to the fragility and leakiness of the cell membrane [64]. In confirmation of this theory, several studies have shown elevated muscle enzymes such as creatine kinase in the serum of dystrophic patients, which might be interpreted as evidence of sarcolemmal fragility in dystrophic muscle [65]. Moreover, the membrane fragility hypothesis became more reliable when Petrof *et al* demonstrated a significant correlation between eccentric contractions and membrane impermeable dye uptake in *mdx* muscle; unlike the normal control there were about fivefold more dye-positive fibers in *mdx* muscle under all the stress stimulation protocols [66]. Therefore, in dystrophin-deficient muscle, it is proposed that contraction stress leads to membrane tears, which might lead to calcium disequilibrium between extracellular and intracellular compartments.

Calcium homeostasis

Membrane disruption in dystrophin-deficient myofibers is usually associated with abnormal cytosolic calcium. In fact, several studies have shown elevated calcium in muscle fibers from DMD patients and *mdx* mice [67, 68]. Unlike normal controls, DMD muscle biopsies showed an increase in the number of fibers positive for a histochemical calcium stain [69]. Together, these results indicate that calcium might play a role in the pathophysiological processes leading to cell death [70]. Spectroscopic studies have shown that the total calcium content of DMD muscle was significantly elevated, about 50% higher in DMD patients [71]. Although the early spectroscopic studies can't distinguish between internal and external calcium, technical advances using fluorescent calcium chelators has allowed distinction between intra- and extracellular calcium; two groups have shown that the intracellular calcium content of DMD myotubes and *mdx* myofibers was twofold higher compared to the controls [72, 73]. However, other groups have found no change in calcium concentration [74, 75]. These contradictory results could be explained either by difficulties in methodological application of the fluorescent calcium chelator technique [76] or by an effect of mechanical stress during cell extraction and preparation. To further confirm that mechanical stress might lead to intracellular calcium disequilibrium, a study was conducted where intracellular calcium activity was recorded in human muscle cells in culture: normal (control) and dystrophic (DMD) cells. Internal calcium concentrations were the same in controls and noncontracting DMD cells, but large increases were observed when myotubes were co-cultured with rat spinal cord explants to improve the maturation of human myotubes and promote spontaneous contractions [77, 78]. In contrast, in the presence of contractile activity inhibitors the myotubes did not exhibit an increase in free cytosolic calcium.

Although early studies speculated that extracellular calcium simply enters dystrophic fibers through micro-lesions in the sarcolemma, the data suggest that contraction is a dominant factor contributing to calcium abnormalities in DMD cells instead of membrane tears [77]. For more precise measurement of calcium influx, the manganese quenching technique has been used to trace calcium entry into a myofiber, which has shown that calcium entry in *mdx* myotubes and fibers is about twofold compared to normal controls [79, 80]. Moreover, using the patch clamp technique, it has been shown that leak channel (calcium channel) activity is threefold greater in *mdx* myotubes compared to the normal once, suggesting that voltage independent channels might be responsible for extra calcium influx into *mdx* myotubes [81, 82]. Moreover, high levels of cytosolic calcium may also cause abnormal mitochondrial function in dystrophic myotubes, which can enhance the production of reactive oxygen species (ROS) [83-85].

ROS effect on dystrophic cells

There is strong evidence that oxidative stress can contribute to the dystrophic phenotype [86]. In fact, the levels of most antioxidant enzyme and reactive oxygen species (ROS) concentrations are significantly elevated in both DMD patients and *mdx* mice [87-89]. Moreover, treatment of *mdx* mice with antioxidants, such as *N*-acetylcysteine [89] or green tea extract [90], lowered muscle damage and increased muscle force production. Therefore, calcium entry may stimulate production of ROS by several cellular mechanisms, including mitochondria [85] and NAD(P)H oxidase [91], which might lead to calcium re-entry via lipid peroxidation, or by promoting the release of calcium from the sarcoplasmic reticulum (SR) via calcium release channels (ryanodine receptors, RyRs) giving rise to an intracellular positive feedback loop for damaging calcium and ROS signals. ROS production may also have downstream consequences by activating calcium-

dependent proteases, such as calpain, resulting in proteolysis of cellular constituents. Moreover, cytosolic calcium and ROS overload impair mitochondrial oxidative phosphorylation [92] and can directly affect the contractile properties of muscle cells [93]. Elevated ROS in dystrophic cells can be explained also by the reduction of nitric oxide synthase nNOS from the sarcolemma, which acts as a scavenger of ROS via nitric oxide production [94]. Moreover, ROS production might promote satellite-cell proliferation through activation of Wnt/β-catenin signaling pathway during adult skeletal muscle regeneration [95, 96]. In addition, Wnt7a activates the planar cell polarity pathway consisting of PAR-3 and PKCl asymmetrically to drive the symmetric expansion of satellite stem cells, and regulating the acquisition of distinct daughter cell fates.[97]. Recently, a study has indicated that in the absence of dystrophin, expression of (MAP)/microtubule affinity–regulating kinase2 (Mark2) protein is down-regulated, leading to an abnormal distribution of the cell polarity regulator PAR-3 on satellite cell, which causes in loss of their asymmetric divisions, and reduces their capacity to form myogenic progenitors [98, 99]. Therefore, muscle wasting in DMD is not only caused by myofiber fragility, but also by impaired regeneration owing to intrinsic satellite cell dysfunction [98].

Muscle degeneration from Free Radicals

It has been shown that nNOS is part of the DAP complex. Loss of dystrophin leads to either a reduction, or no change in nNOS in the cytosol; instead, all data show that there is a large loss of nNOS from the sarcolemma [100]; an absence of nNOS from the sarcolemma leads to a significant decrease of nitric oxide (NO) production in dystrophic muscles, which might affect several downstream pathways. NO can promote muscle growth through activation of satellite cells, which are in a quiescent state in skeletal muscle. Increase in NO synthesis can increase

satellite cell proliferation either by activation of metalloprotease (MMP) [101] or through cell polarity by activating Vanl2 and Wnt signaling pathways [102]. Moreover, loss of nNOS from dystrophic muscle leads to significant reduction of cGMP and increases cytosolic calcium and impairs glycolysis, which increases muscle fatigability [103]. Furthermore, NO acts as a vasodilator and a key modulator of vascular tone [104]. Loss of nNOS from dystrophic muscle can also amplify the early inflammatory response to injury [105].

Proteolysis

The data above suggest that loss of dystrophin leads to membrane lesion, which will activate calcium leaking channels. Increased cytosolic calcium content in turn will trigger a series of pathogenic events including calcium-activated proteolysis, signaling perturbations, and mitochondrial death [106, 107]. In fact, it has been shown that calcium alone is sufficient to induce muscular dystrophy *in vivo* [108]. Steady up-regulation in cytosolic calcium concentration leads to activation of proteases, particularly calpains, which can destroy the membrane constituents and will trigger calcium entry. This vicious circle leads to cell death [109, 110]. Using hydrolysis of a fluorogenic calpain substrate it has been confirmed that proteolysis is faster in *mdx* myotubes than controls, which can be stopped by inhibiting calcium leak channel activity and lowering external calcium concentration [111]. Moreover, a variety of proteolysis inhibitors indicated that most of the extra proteolysis was due specifically to calpains and not to lysosomal or proteosomal pathways [112]. Loss of dystrophin leads to the collapse of the entire DAP complex which in turn triggers the function of several downstream signaling events, thereby contributing to disease progression.

Figure 2 Mechanisms for membrane disruption in dystrophic muscle.

(Left part) A model of dystrophin and associated protein complexes in normal muscle.

Absence of dystrophin leads to sarcolemmal disruptions and muscle degeneration (right part). In the absence of dystrophin, tears may simply develop as a result of the mechanical stress. An increase in free radicals (pink triangles) is thought to be caused by the displacement of NOS from the plasma membrane. The high levels of free radicals in dystrophic muscle are thought to contribute to muscle degeneration via the oxidation of muscle membranes and recruitment macrophages. Calcium-sensitive pathways also contribute to muscle degeneration in muscular dystrophy. Calcium (red spheres) may enter through membrane lesions or through calcium channels. Calcium dysregulation may also lead to abnormal mitochondrial function as well as the activation of the calcium-dependent protease calpain to degrade muscle membrane proteins. Redrawn from (GQ. Wallace and Elizabeth M. McNally *et al* 2009) [113].

Figure 2

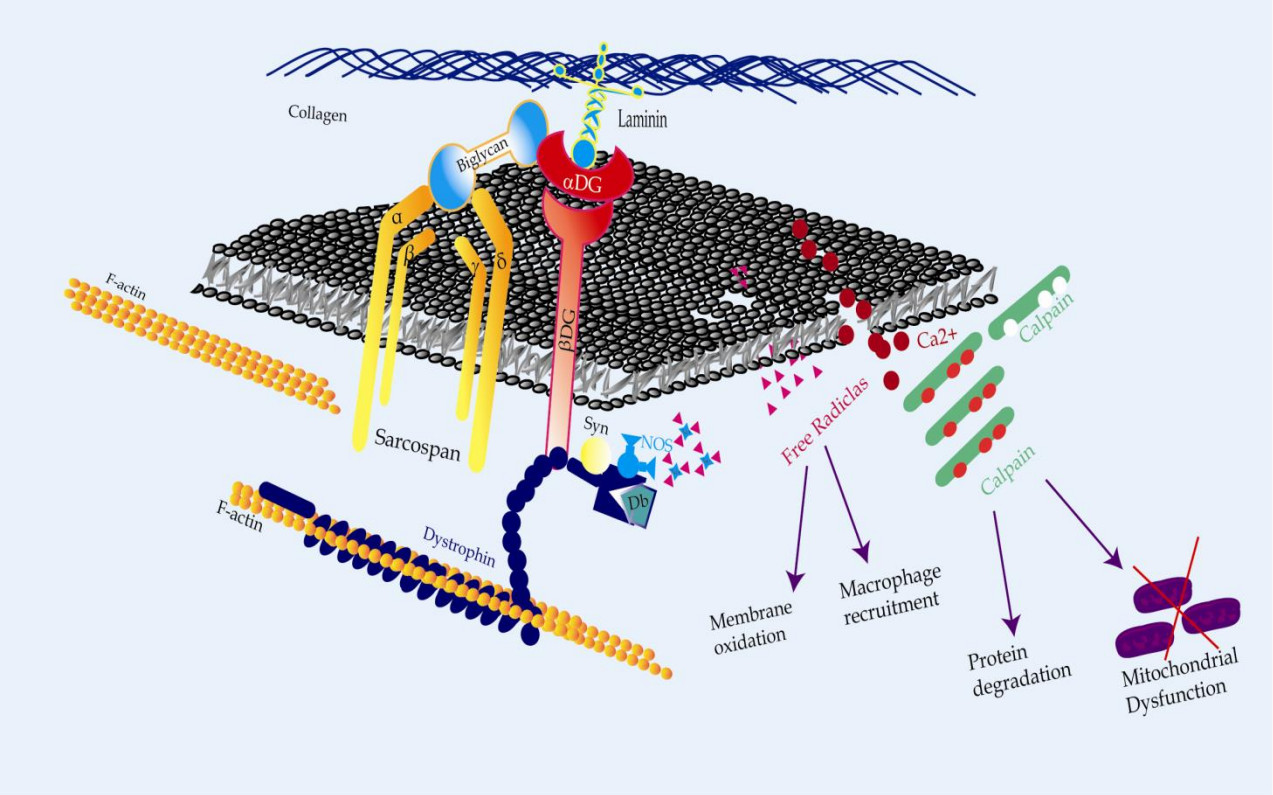
Collagen
Laminin
Biglycan
αDG
α
β
γ
δ
βDG
F-actin
Sarcospan
Syn
NOS
Db
F-actin
Dystrophin
Free Radicles
Ca2+
Calpain
Calpain
Membrane oxidation
Macrophage recruitment
Protein degradation
Mitochondrial Dysfunction

Experimental Treatment

The discovery of the *dystrophin* gene and its implications for DMD has been known for over 30 years [12], yet no effective treatment is available to halt, prevent or reverse the progression of DMD. Different therapeutic strategies for DMD are currently being explored, including pharmacological, molecular and cellular-based approaches. Most of the pharmacological treatments seem less effective since they mainly target the secondary features of dystrophin deficiency including inflammation, fibrosis, and muscle regeneration [114]. However, molecular and cellular based strategies, including gene therapy, exon-skipping, and mutation suppression, which are primarily targeted at replacing/restoring the mutated DMD gene, have shown more potential to rescue the dystrophic phenotype [115].

Therapies targeting secondary features of DMD

Although most of the symptomatic management offered to DMD patients, including pharmacotherapy, rehabilitation, and surgical management, has improved lifespan from late childhood to early adulthood, their objectives are limited in regards to slowing disease progression, preventing scoliosis and optimizing the respiratory and cardiac function. To date, the only available drug therapies for DMD are the Glucocorticoids (GCs) including prednisone and its derivative prednisolone, and deflazacort, which are considered the first-line therapy available to improve muscle growth, delay muscle necrosis, and improve respiratory function [116, 117]. However, the exact cellular mechanism on the beneficial effect of GCs is still unknown [118]. In fact, studies using cDNA microarray genotyping steroid-treated *mdx* mice have shown an up-regulation of structural protein genes, signalling genes and genes involved in immune response [119]. GCs treated *mdx* mice have shown increased taurine and creatine levels,

an indicator of muscle repair [120]. Long-term dexamethasone treatment has mediated utrophin accumulation in DMD muscle cells [121]. Moreover, because of their anti-inflammatory and immunosuppressive actions, GCs promote myoblast proliferation and reduce muscle necrosis [122, 123]. Other than weight gain, mild hypertension, cataract formation, short stature and a delayed puberty, no severe side effects have been observed in DMD patients in either short or long term studies; thus, the benefits of the drug outweigh the risks [124]. Physical therapy has also helped maintain flexibility and mobility. Since respiratory and cardiac diseases are the major cause of mortality and morbidity in DMD patients, cardiac and respiratory care is highly efficient in increasing survival rates and longevity [125, 126]. In addition to GCs, other drugs have emerged to target the secondary features of dystrophin deficiency. The aim of these approaches is to inhibit necrosis, increase cellular adhesion and maintain muscle stability. It is known that necrosis and inflammation are the major parameters leading to muscle damage. Indeed, inhibition of the NF-κB signaling pathway by injecting the NEMO-binding domain (NBD) significantly reduced skeletal muscle damage in the *mdx* mouse [127]. Moreover, reduction of inflammation and necrosis using the anti-TNFα antibody (Remicade) leads to a clear delay and reduction of muscle breakdown in young *mdx* mice [128]. Since NOs activity is down regulated in DMD, inhibition of the GMP-hydrolyzing phosphodiesterase (PDE) activity will selectively increase nNOS expression through the GMP signaling pathway. In fact, pre-clinical studies in the *mdx* mice have shown that PDE5A inhibitors tadalafil and sildenafil protect the dystrophin-deficient skeletal muscle and restore blood supply to skeletal muscles after exercise [129]. In addition, over-expression of α7BX2 integrin chain in order to reinforce the attachment of muscle fiber to the basal lamina in *mdx*/*utr* (-/-) mice has improved their life span threefold, reduced the

development of muscle disease, and maintained mobility [130]. Furthermore, in exploratory studies blocking the myostatin protein, which is a negative regulator of skeletal muscle growth, in *mdx* mice, *mdx* /myo (-/-) mice were stronger and more muscular than the *mdx* controls [131, 132]. Although therapies targeting secondary symptoms of DMD have shown significant improvements in DMD patients, recent experimental DMD therapeutics are directed toward molecular and cellular-based strategies, which have shown some promise in preclinical studies. The gene and cell based strategies involve the manipulation of the cellular machinery at the level of gene transcription, mRNA processing or translation.

Therapies targeting primary features of DMD

A. Dystrophin modulation strategies

Since dystrophin is known as the principal suspect causing DMD, the most straightforward approach to therapy would be to restore or reintroduce a wild-type, or normal, copy of the mutated dystrophin gene. However, as the dystrophin gene (2.2 Mb) and the cDNA (14 kb) are exceptionally long, direct replacement of the dystrophin gene is challenging.

B. Dystrophin gene product modifiers

Stop codon reading through

About 13% of patients with DMD have a nonsense mutation in the dystrophin gene [133]. During translation some drugs have shown their ability to skip the mRNA stop codon by introducing an amino acid at the premature stop codon, and as a result, the mRNA translation is continued. Gentamicin is an aminoglycoside antibiotic, which can interact with the 40S ribosomal subunit [134] to introduce an amino acid at the mRNA stop codon, therefore, allowing the translation of full-length protein. This approach was tested in *mdx* mice and the results have

shown a 20% increase in dystrophin positive fibers. However, in human DMD patients, there was an increase of 15% or less [135]. The difference in dystrophin expression between *mdx* mice and DMD patients might be explained by the presence of different gentamicin isomers, which are not all active. Although gentamicin could be considered as a potential up regulator of dystrophin in patients with stop codon mutations, it exhibits some kidney toxicity [136]. Ataluren (PTC124) is a newly identified drug acting similarly to gentamicin, except that PTC124 interacts with the 60S ribosomal subunit [137]. Although PTC124 was well tolerated in clinical trials, the 30 m and 6-minute walk tests were similar to the placebo. Therefore, the positive effect of PTC124 on DMD patients was negligible [138].

Exon skipping

Since BMD patients have a truncated but partially functional dystrophin [24], antisense oligonucleotides (AOs), which are able to force the cellular machinery to 'skip over' a targeted exon, can restore the open reading frame and allow the expression of an internally truncated but partially functional dystrophin in DMD patients. Based on the fact that the majority of DMD cases arise from partial out-of-frame deletions in the dystrophin gene [139], the exon skipping approach is currently one of the most attractive approaches for the treatment of DMD. The principal of antisense-mediated exon skipping is based on the use of modified and complementary small RNAs or DNAs called antisense oligonucleotides (AONs), which are able to bind and modulate splicing of dystrophin pre-mRNA. In order to make the oligonucleotide resistant to nucleases and improve their affinity to RNA, two types of modified antisense AONs have been generated. First, the 2'O-methyl-phosphorothioate AONs (2OMPs) were obtained by changing the negative oxygen with a sulfur atom and adding a methyl group to the hydroxyl

group at the second position of the ribose. Second, the phosphorodiamidate morpholino oligomer PMOs has a morpholine ring that replaces the ribose and a nitrogen atom replaces the oxygen present in the phosphodiester link. The annealing of AOs to the selected splicing motifs will mask the target exon; and therefore, this will restore the reading frame and generate a truncated but partly functional dystrophin protein (i.e. result in BMD). The antisense-mediated exon skipping was first tested on cells derived from *mdx* mice [140], with the modified oligonucleotides being directed against both splicing sites of the *mdx* dystrophin exon 23. As a result, exon 23 was omitted, which lead to the generation of an in-frame dystrophin transcript with a small internal deletion [141]. Moreover, AOs have ameliorated the disease phenotypes of the *mdx/utr -/-* dKO mice, which lack both utrophin and dystrophin gene and display more similar muscle pathology to that of the DMD patients [142]. The most common deletion in DMD patients is an eight exon deletion ranging from exons 45 to 52 [143], and for this reason, clinical trials are currently concentrating on this target. In fact, transfection of specific AON-induced skipping of exon 46 was achieved in muscle cells; as a result, the reading frame was restored and dystrophin synthesis induced in more than 75% of transfected myotubes. Moreover, immunohistochemical analyses have shown a significant increase in dystrophin levels in DMD myotubes. This study has shown that 2OMPs treatment can restore dystrophin expression in DMD myotubes, which would probably be used as therapeutic in DMD patients with exon 45 deletions [144]. Although all preclinical results indicate that the exon skipping approach holds a lot of promise for DMD patients, in 2013, GlaxoSmithKline (GSK) and Prosensa announced that GSK's Phase III clinical trial failed to meet the primary endpoint of a statistically significant improvement in the 6-minute walk test compared to placebo.

C. Dystrophin gene therapy and gene replacement strategies

Although the first clinical trial of gene therapy in 1990 has shown a strong interest for this therapeutic approach, which presented the proof-of-concept for the feasibility to treat a genetic disorder by gene therapy without major side effects [145], the death patients in 1999 and 2002 respectively due to a massive immune reaction against the capsid of the infused viral vector, and acute leukemia, caused a major setback for this approach [146, 147]. However, the death incidence of gene therapy is still much lower than the pharmacological approach. Thus, gene therapy is still an attractive approach to cure many hereditary diseases such as DMD.

DMD is caused by recessive and monogenic mutations in the dystrophin gene. Several experimental approaches in dystrophic animals showed that expression of dystrophin can be restored in the sarcolemma of muscle fibers after gene transfer, regardless of the dystrophin mutation type [148-150]. In fact, a significant reversal of dystrophic symptoms was observed in transgenic mice expressing approximately 20% of the wild type level of dystrophin [151]. Therefore, gene replacement therapy is considered the most practical strategy to treat the dystrophic pathology. Gene replacement therapy is based on introducing the lacking dystrophin gene using various vectors to the target muscle cells in order to overcome the harmful effects of gene mutation. Thus, the main challenge for gene replacement therapy is to find a safe vector capable of a widespread and efficient delivery of the dystrophin gene to all muscles. However, as the dystrophin gene (2.2 Mb) and the cDNA (14 kb) are exceptionally long, and there is a large mass of skeletal muscles to be treated, direct replacement of the dystrophin gene is challenging. Two major approaches have been used to transfer genes into muscles either using “naked” DNA plasmid or viruses.

Dystrophin plasmid injection

Injection of “naked” dystrophin plasmid DNA to muscles through systemic delivery leads to expression of full-length dystrophin cDNA in about 40% of *mdx* mouse diaphragm fibres [152, 153]. Because plasmid injection can evade potential immune response, this approach has shown some potential as a safe gene therapy for DMD; however, it is incapable of sustained transgene translation in DMD [154].

Adenovirus and adeno-associated virus injections

Viral vectors are an alternative option in gene therapy. Nevertheless, several factors should be taken in considerations for the choice of the viral vector including the target cell, immunogenicity, and required duration of transgene expression. In order to deliver the 14 kb dystrophin cDNA into the nuclei of muscle cells, vectors with large capacity are needed. Adenoviruses are non-enveloped icosahedral viruses with a linear double stranded DNA of 35kb in length. Because adenovirus can infect muscle, lung, brain, and heart cells, they are attractive vectors for gene therapy. Although the first and second generation adenoviral vectors (E1/E3 deleted) with a capacity of 8 kb cannot carry the dystrophin cDNA, the third generation 'gutless' vectors with capacity of ~34 kb overcome this restriction by removing all adenovirus genes [155]. Unlike the first generation adenovirus which induces mouse immune response [151], the third generation adenovirus had reduced host immune response and improved persistence of transgene expression in muscle [156, 157]. However, another crucial problem needed to be overcome: adenoviruses were not highly infective for mature muscle fibers [158]. They are too large to easily cross the dense basal lamina that surrounds mature myofibres and there are fewer adenoviral attachment receptors on the surface of mature myofibres [159].

Adeno-associated viruses (AAVs) are single stranded DNA viruses discovered as contaminants from adenovirus preparations. They are considered the first choice vector for gene transfer to muscle for several reasons: they can infect a variety of post mitotic cells, such as skeletal muscle and heart. They also have the capacity to deliver their genome to the nucleus. Although AAVs have many different serotypes, they are characterized by their reduced inflammatory and immunological responses; however, immune response might arise against the transgene product [160]. The serotypes1, 2, 6, 8 and the 9 are more frequently used for muscle gene therapy; however, they have a limited cloning capacity of 4.6 kb [161]. Based on observation of the milder BMD phenotype with internally deleted dystrophin at 46%, micro and mini dystrophin transgenes have been developed and delivered through AAVs. In fact, injection of AAVs carrying micro-dystrophin (μDys) into *mdx* mouse led to 80% dystrophin positive fibers [162, 163], which restored the DAP complex at the myofiber sarcolemma. The first AAV clinical gene therapy trial for DMD was performed with six DMD boys using rAAV2.5 CMV Delta 3990 mini-dystrophin. While no trangene expression was detected, dystrophin-specific T cells were detected after treatment, providing evidence of transgene expression even when the functional protein was undetectable in skeletal muscle [164]. This result indicates the necessity of either screening DMD patients for immunity to dystrophin or treating them transiently with immunosuppressant drugs before their treatment with AAV mini-dystrophin gene therapy. Recently, an innovative method for the delivery of the full-length dystrophin gene has been developed using three independent AAV vectors carrying "in tandem" sequential exonic parts of dystrophin sequence via their inverted terminal repeat sequences, which may lead to functional improvement [165].

D. Dystrophin genome editing using CRISPR- Cas9 System

Genome editing is based on the use of engineered nucleases composed of sequence-specific DNA-binding domains fused to a nonspecific DNA cleavage module [166]. These engineered nucleases enable efficient and precise genetic modifications by inducing targeted DNA double-strand breaks (DSBs) that trigger the cellular DNA repair mechanisms, including error-prone nonhomologous end joining (NHEJ) and homology- directed repair (HDR) [167]. Recently, the bacterial Clustered Regularly Interspaced Short Palindromic Repeats (CRISPR)/ CRISPR-associated (Cas9) system has emerged as an effective genome editing tool, allowing successful correction of dystrophin mutation in the germ line of *mdx* mice [168], human DMD patient myoblasts, and in Induced Pluripotent Stem cells (IPS) [169, 170]. Although the dystrophin gene has been successfully corrected, immune response to the newly corrected gene product, and the wide range of mutations in the dystrophin gene might be an obstacle for this strategy [171].

E. Cell-based therapy

Cell-based therapy involves the injection of normal cells into a dystrophic area in the hope that normal cells will fuse and correct the diseased muscles. These cells can be either muscle precursor cells or stem cells that have the ability to differentiate into muscle cells. One of the most successful procedures so far has been the transplantation of myoblasts into diseased tissue.

Myoblast injection

In this experiment, injection of normal myoblasts results in a phenomenon known as ‘gene complementation’, which results in the expression of both exogenous and host genes in the myofibre syncytium [172]. Although good transplantation results have occurred in *mdx* mice [173, 174], in clinical trials only one patient out of 11 had 10.3% of muscle fibers expressing

donor-derived dystrophin after myoblast transfer [175]. The explanation behind the unexpected result has been attributed to poor immunosuppression combined with insufficient numbers and distribution of transplanted cells [176, 177]. It is clear now that the success of myoblast transplantation is closely related to the choice of immunosuppressive drug used [178].

Stem cell injection

Besides satellite cells which are responsible for the growth and maintenance of skeletal muscle, there are other stem cells found in skeletal muscle that have myogenic potential including muscle-derived stem cells (MDSCs), muscle side-population cells and muscle-derived CD133+ progenitors. Intravenous injection of *mdx* and GRMD dogs with stem cells derived from a dystrophin positive donor leads to dystrophin positive myofibers [179]. Sadly, this procedure displays low efficiencies in term of level of dystrophin expression [180]. However, another type of stem cell has been proposed as a potential therapeutic option.

Induced Pluripotent Stem (IPS) cells injection

The proposed stem cells are the Induced Pluripotent Stem (IPS) cells, which can be generated from the tissues of the DMD patients using defined factors [181]. Because IPS cells can be isolated directly from DMD patients and still maintain their pluripotency, genetically corrected IPS cells might be applicable to autologous transplantation as *ex vivo* gene therapy [182]. In fact, several studies were able to differentiate the corrected IPS cells toward skeletal muscle cells and successfully detect the expression of full-length dystrophin protein [170, 183]. These results present an important proof of concept for developing IPS cell-based gene therapy for DMD disease.

F. Utrophin modulation strategies

The utrophin gene is large, approximately 900 kb in size [184] and is located in region 2 of the long arm of human chromosome 6 [185]. The utrophin mRNA and protein are broadly expressed; indeed, the name utrophin is derived from ubiquitously transcribed dystrophin-related protein [186]. It is expressed in skeletal muscle, nerves, blood vessels, and myofibres. Unlike developing myofibres, where utrophin is present throughout the sarcolemma, in the adult myofibres, utrophin expression is restricted to the neuromuscular and myotendinous junctions (NMJs and MTJs) [187-189]. The transcribed mRNA produces a 13-kb transcript [185] and a protein of approximately 400 kD protein [190]. The utrophin gene produces two mRNA isoforms that differ in their N-termini, utrophin-A and utrophin-B, which are transcribed from two different promoters A and B [191]. Utrophin is expressed in both slow and fast muscle fibers; however, it is expressed at greater levels in slow fibres [192, 193] . It has been shown that utrophin A promoter is active in skeletal myofibres and upregulated in the absence of dystrophin, and hence is considered the more relevant therapeutic target, while the B promoter is active in the heart, lungs, and in endothelial cells, for example, endomysial blood vessels [191, 194]. Indeed, one of the most promising approaches for DMD therapy is based on increasing the levels of utrophin. The primary structure of utrophin, 3433 amino acids, displays about 80% homology with dystrophin and the protein performs similar functions [195]. Similar to dystrophin, utrophin shares many of the same binding partners. It has been shown that the C-terminus of utrophin binds to members of the DAP, such as α-dystrobrevin-1, and β-dystroglycan, and also binds to cytoskeletal F-actin [39, 196]. Elevated and re-localized utrophin to the sarcolemma in some DMD cases, added to the strong similarities in sequence and structure between utrophin and

dystrophin, prompted the hypothesis that utrophin up-regulation could substitute the absence of dystrophin at the sarcolemma [197, 198]. In fact the therapeutic effect of up-regulating extra-synaptic utrophin was tested by Tinsley et *al* in 1996 [199], and revealed that mini-utrophin over-expression in transgenic *mdx* mice is sufficient to rescue the dystrophic *mdx* phenotype. These transgenic mice were found to have a lower amount of fibrosis/necrosis and normal serum creatine kinase levels in addition to complete restoration of the dystrophin complex to the sarcolemma [200, 201]. These results were confirmed in studies involving a transgenic *mdx* mouse named Fiona that expressed full-length utrophin in skeletal muscle at a level fourfold higher than non-transgenic *mdx* mice. These transgenic mice were found to attain a complete reversal of the dystrophic phenotype. Therefore, up-regulation of utrophin could have powerful therapeutic effects in DMD patients.

Up-regulation of the endogenous utrophin A promoter

As mentioned above, the utrophin gene is controlled from two distinct promoters, utrophin A and utrophin B [202]. The utrophin A promoter resides within a methylation-sensitive CpG island region characterized by the absence of the TATA or CAAT motifs [202, 203], whereas the utrophin B promoter is found within a large intron 50 kb downstream of exon 2 and generates a transcript with a unique exon 1 that splices into exon 3 of the utrophin gene [191]. Synapse-specific expression of utrophin A is mediated, in part, via the binding of the ETS-factors GABP alpha and beta to the N-box [204], which is a characteristic of the promoter of other neuromuscular junction proteins such as the acetylcholine receptor subunit [205, 206]. In addition, the GC-elements near the N-box are bound by Sp1 and Sp3 factors, which have a zinc finger DNA-binding domain, and interact with GABP alpha and synergize in the transcriptional

activation effected by GABP [207]. The utrophin A promoter can also be activated by peroxisome proliferator-activated receptors (PPARs), nuclear receptor transcription factors that also activate the slow muscle program [208]. Calcineurin and NFAT, together with GABP and the transcriptional co-activator proliferator-activated receptor gamma co-activator 1-α (PGC1α), also contribute to the expression of utrophin at the NMJs of both fast and slow fibres [209-211]. Moreover, glucocorticoid treatment leads to increased levels of utrophin, but it is unclear whether this is primarily due to promoter activation or posttranslational upregulation [212, 213]. The expression of utrophin is also controlled by both 3' untranslated region (UTR) [192, 193] and the phosphatase calcineurin, its calcium-dependent regulator calmodulin, and the transcription factor nuclear factor of activated T cells (NFAT), as part of the slow muscle gene program [209].

Several studies have tried to activate the endogenous utrophin A promoter in extra-synaptic nuclei through treatment with heregulin, which acts via the N-box motif of the utrophin A promoter [214], and l-arginine, which results in an increase in utrophin expression through increased nNOS production [215]. Moreover, delivery of full length utrophin or TAT-micro-utrophin, a recombinant utrophin protein modified with the HIV-derived TAT protein transduction domain, improves specific force production and lead to reduced serum levels of creatine kinase [216]. In addition, overexpression of RhoA, a small GTPase, in skeletal muscle leads to an up-regulation and proper distribution of utrophin protein at the plasma membrane without any effect on utrophin transcription [217]. Lately, Kay Davies's group has screened 5,000 small compounds in H2K *mdx* myoblast cell line, which led to the discovery of an active molecule called SMT C1100, which is considered as the first orally bioavailable small molecule

utrophin up-regulator. Preliminary results showed therapeutic potential of this molecule as assessed by its prevention of pathology in *mdx* mice [218]. Recently, it has also been reported that the transcription factor homeobox protein engrailed-1 (EN-1) binds and activates the utrophin A promoter [219].

Engineering of Zinc Finger Proteins targeting utrophin A promoter

Transcription factors play a crucial role in controlling gene expression, Zinc Finger Proteins (ZFPs) are the largest transcription factor family in the human genome [220].Over the past decade, early studies of chromatin structure led to the discovery of the nucleosome structure, which is composed of eight histone proteins and about 146 base pairs of DNA [221, 222]. The DNase I can cut between the nucleosome structure in active chromatin, and it is assumed that these cleaved sequences may bind transcription factors [223]. The nucleosome study of the 5S RNA genes in *Xenopus laevis* led to the discovery of the first eukaryotic transcription factor, TFIIIA [224]. The TFIIIA structure has a remarkable nine repeating motifs, later labeled zinc finger because it contained a zinc (Zn) atom and can "grab" the DNA [225]. Prolonged proteolysis of TFIIIA has shown that TFIIIA contains a repetition of nine "finger" units, each of them composed of 30-amino acids, which can fold around the zinc ion and form a ββα structure. Each consecutive finger is linked by five intervening amino acids. The structure of each zinc finger has a conserved structure in the pattern of cysteines- histidines (Cys-Cys…His-His). The folding structure of the finger is maintained by a zinc ion that interacts with the two invariant pairs of cysteines and histidines [226]. The precise pattern of zinc finger amino acids that interact with DNA has been characterized by studying the crystal structure of the transcription factor Zif268. The Zif268 interacts with the DNA major groove through specific hydrogen-bond from

amino acids at helical positions –1, 3, and 6 to three successive nucleotides on one strand of the DNA [227]. The zinc finger module can function as a monomer and bind to three adjacent nucleotides, or as a multimeric protein in which several zinc fingers are linked together in extended arrays that recognize unique DNA sequence of different lengths; such artificial zinc-fingers (ZFs) are often fused to either trans activator or inhibitor effector domains [228]. Zinc finger proteins can be designed for specific recognition of predetermined DNA sequences. In order to select specific ZFPs from a predicted library, several methods have been used including phage display selection, ribosomal selection, yeast one- and two-hybrid system [229-231]. Data obtained from phage selection, ribosomal selection, and from the known binding specificities of naturally occurring zinc fingers have been used to make 'rationally designed' zinc fingers. The first ZFP libraries were established by Barbas *et al* in 2003 [232]. This modular design offers a large number of combinational possibilities for the specific recognition of DNA. Since the interaction of ZFP and DNA has been solved by the design and the selection of several ZFPs libraries, it is possible to target virtually any DNA sequence using pre-made zinc-finger modules. Because of their small size and low immunogenicity, engineered ZF proteins have been used to target different endogenous genes. Moreover, the potential of zinc finger proteins for therapeutic application are currently under investigations in clinical trials [233]. Recently, generation of engineered zinc finger transcription factors designed to target a specific region in the utrophin A promoter led to significant enhancement of muscle function with decreased necrosis and restoration of the dystrophin-associated proteins [234, 235].

Utrophin A Promoter Modifiers

There are several ways to modulate utrophin levels, including gene therapy, stabilization of the protein/RNA and transcriptional up-regulation of utrophin RNA. Although gene replacement therapy for human monogenic diseases such as DMD has shown its therapeutic efficacy in a number of experimental studies [236], the size of targeted gene either dystrophin or utrophin have shown some limitations of this transfer technology. Therefore, several therapeutic approaches have recently explored a different approach. Genome editing is an innovative technology for genome manipulation which was first discovered thirty years ago in yeast when an endonuclease I-Scel was used in combination with a donor vector to manipulate the LacZ gene conversion [237, 238]. Similar processes have been noticed in mammalian cells [239]. Genome manipulation takes advantage of the double strand breaks occurring either naturally or induced by specific endonucleases. The induced DSBs are repaired through two pathways; the first is the Homologous Direct Repair (HDR) which is a high fidelity process in which the undamaged chromatin sister serves as template to repair the DSBs [240]. The second pathway is the Non-Homologous End Joining (NHEJ) mechanism, which is considered an error prone pathway leading to small insertion or deletion mutations [241]. In order to use an endonuclease as a genome editing tool, it must exhibit a combination of qualities: specific recognition of target sequences coupled with modularity and adaptability for retargeting new sequences.

Zinc Finger Nuclease strategy

Zinc Finger Nucleases (ZFNs) combine both properties 1) the DNA binding specificity and flexibility of ZFPs and 2) a cleavage activity of the modified FokI domains that function as obligate homodimers [242]. Recently, ZFNs have been used in gene editing of specific targets

for either gene knockout or gene integration [243]. Applications of gene editing using ZFNs can be useful in several fields including biotechnology (cellular and animal engineering), agriculture (crops and animals improvement) [244, 245], and finally medicine (gene therapy) [246, 247]

CRISPR/Cas9 strategy

Targeted genome editing using engineered nucleases provides a powerful tool for precise deletions, insertions and specific sequence changes in different animals and cell types [248]. Because of its simple way of inducing genome editing, the Clustered Regularly Interspaced Short Palindromic Repeats (CRISPR) has revolutionized the genome editing field. The CRISPR system was first discovered in 1987 by Nakata and colleagues while studying the *iap* enzyme involved in isozyme conversion of alkaline phosphatase in E. Coli; the sequence of this proteolytic gene revealed repetitive palindromic elements that shared no homology with any known genes [249]. The function of these repetitive sequences remained a mystery [250] until 2005 when three independent groups discovered that these bacterial CRISPR spacers shared a high degree of homology with bacteriophages [251, 252]. The bioinformatics analysis of these spacer sequences has shown a key role in bacteriophage resistance [252, 253]. Recently, combination of the CrRNA and TrcRNA into a customized guide RNA (gRNA) that can be delivered under the control of a unique U6 promoter followed by the Cas9 endonuclease in a single plasmid has simplified the CRISPR technology as a genome editing tool [254].

Rationale and objectives

The rescue of the DMD phenotype is correlated with the levels of expressed utrophin in *mdx* mice [255]. Therefore, a substantial, ectopic expression of utrophin can prevent deleterious effects of dystrophin deficiency. In previous work, our group and others have shown that artificial zinc finger transcription factors targeting murine utrophin A promoter can lead to its endogenous up-regulation and can improve the *mdx* phenotype [234, 256]. The aim of this study is to design tools to up-regulate the endogenous utrophin. In this study we took 2 approaches: first, we designed a new panel of specific custom-designed transcription factors with zinc finger (ZF) motifs that can target specific sites in the human utrophin A promoter, then we tested their ability of stimulating the endogenous human utrophin gene expression. The second approach is based on modifying the endogenous utrophin promoter using genome editing tools. In order to modify the endogenous utrophin promoter, we engineered both Zinc Finger Nuclease (ZFN) and Clustered Regularly Interspaced Short Palindromic Repeat (CRISPR Cas9+sgRNA) expression plasmids. The engineered plasmids were then tested for their ability of targeting and cleaving the human utrophin A promoter. We have also designed a donor plasmid that has the CMV early enhancer/chicken beta actin (CAG) promoter flanked by the human utrophin A promoter sequences, in order to insert a strong promoter into the human utrophin genomic locus.

Chapter 2: Materials and Methods

Zinc Finger Protein

Design and Synthesis of Zinc finger proteins

The identification of potential ZFP target sites was selected using the ZiFiT software, which can be accessed from the Zinc Finger Consortium website (http://www.zincfingers.org). In order to design a three zinc finger protein, the upstream region of human utrophin A promoter sequence was selected from the NCBI web site http://www.ncbi.nlm.nih.gov. The numbering corresponds to the human utrophin promoter sequence EMBL accession N: X95523 [202]. The upstream promoter sequence was then pasted to be analyzed into the text box labeled 'sequence', and then the Tool-Gen option to design a three zinc finger protein was selected. After clicking on Submit, the output provided the nucleotide position and the sequence of the target site as well as a list of fingers for array assembly. Each finger is color-coded to match the nucleotide triplet it recognizes.

Sub-cloning of ZFP into Pc3XB vector

A library of plasmids coding for a single Zinc Finger protein was purchased from Tool-Gen consortium, with each plasmid having the same backbone but carrying different ZFP; for example, pc3XB-F1,-F2 and-F3 encode individual hypothetical finger modules. Each finger coding sequence is flanked on the 5'end by unique *XbaI* and *XmaI* sites and on the 3'end by unique *AgeI*, *BsgI* and *BamHI* sites. The configuration of unique flanking restriction sites in all pc3XB based plasmids permits any two fingers (e.g., F1 and F2) to be joined together by ligating a finger F1-encoding vector backbone (linearized by digestion with *AgeI* and *BamHI*) to a finger F2-encoding fragment (released from the plasmid by digestion with *XmaI* and *BamHI*). The

resulting plasmid encodes a two-finger (F1 followed by F2) array which again is flanked on the 5' end by *XbaI* and *XmaI* and on the 3' end by *AgeI, BsgI* and *BamHI*. A third finger (F3) can be added to the array by ligating an F1/F2-encoding AgeI/BamHI-digested vector backbone to a F3-encoding *XmaI/BamHI*-digested fragment [257].

Mammalian Expression Vector PST-1374

The sub-cloned ZFP were cut using *XmaI/BamHI* and cloned into a new vector PST-1374, where a VP-16 trans-activating domain was cloned in frame downstream of F1-F2-F3 zinc finger. In order to track the expression of the PST-1374 an IRES-GFP gene was cloned downstream of the ZFP.

Cell lines, transient transfections and beta galactosidase reporter assay

The human HEK 293T cell line was grown in Dulbecco modified Eagles medium (DMEM) (Gibco Corporation, Grand Island, NY, USA) supplemented with 10% foetal calf serum. Transient co-transfection experiments in the 293T cell line were carried out using Lipofectamine 2000 according to the manufacturer's instructions. Cell extract was prepared and assayed for beta galactosidase activity according to the manufacturer's instructions (Galacton-*Star*, Life Technologies) using a Bio-orbit 1200 luminometer. The total protein in the extracts was quantified using a BCA assay, and equal amount of protein used on western blot to quantify the ZFP expression level, using the VP16 antibody (Santa Cruz Biotechnology). The specific activity was measured by normalizing the beta galactosidase activity against the VP16 expression.

Activation of Endogenous utrophin A Promoter in Vitro

HEK 293T cells were plated at a density of 10^6 cells in a 6 well plate. Then, plasmids encoding ZFP were transfected into the cells using Lipofectamine 2000 (Life Technologies) according to

the manufacturer's recommendations. 48 hours after transfection, selection was started and kept for at least 3 weeks in the presence of blasticidin (5ug/ml) (Sigam Aldrish). Under these conditions, the control cells died within 5 days, and the transfected ones were kept under selection for a month and a half before testing their expression of the recombinant protein by Western blotting for VP16.

Analysis of human utrophin mRNA Levels

Total RNA was extracted from HEK 293T cells expressing either PST1374-ZFP or the negative control pST1374-GFP-VP16 using the TRIzol reagent according to the manufacturer's instructions (Life Technologies). One μg of total extracted RNA was reverse transcribed using oligo (dT) primers and M-MLV (Moloney Murine Leukemia Virus) (Life Technologies) in a final volume of 20μl at 37°C for 50 min. A real-time PCR assay was performed in a 96-well format using the ABI Prism 7000 Sequence Detection System (Applied Biosystems, Foster City, CA). Primers for human utrophin A, and for human glyceraldehyde-3-phosphate dehydrogenase (GAPDH) (housekeeping gene) were synthesized from Alpha DNA.

Human UTRN For: GCCAATTCCAAGTTCCATTAAATC

Human UTRN Rev: CAGTAGAACACACAGTCAGCACTCAA

Human GAPDH For: CATCAATGACCCCTTCATTGAC

Human GAPDH Rev: CGCCCCACTTGATTTTGGA

PCR mixtures containing either the cDNA template from the HEK 293T cells expressing ZFP, or HEK 293T expressing GFP-VP16 cells as a negative control were run on the ABI 7000 Real

Time PCR machine. The results were analysed using the Applied Biosystems analysis software. The data are expressed as the ratio between utrophin and GAPDH mRNA expression. The gene expression ratio between utrophin and GAPDH is shown as the mean ± SEM from three independent experiments performed in triplicate. *$P < 0.05$ and***$P < 0.01$ indicate statistical significance by t-test.

Zinc Finger Nuclease

Design and cloning of Zinc Finger Nuclease

The design of zinc finger nuclease was performed similarly to the design of zinc finger proteins with some modifications. Briefly, the targeted sequences of utrophin A promoter was selected and introduced into the ZiFiT software. Then, the output gave the predicted zinc finger to be produced. Unlike ZFP, the predicted ZFN have two pairs of ZFN each one targeting an opposite strand of DNA and interspaced with 6-bp [258]. Each predicted ZFN was sub-cloned first in the pX3B plasmid, and then cloned in the pst1374 plasmid which expresses the FokI nuclease. The FokI nucleases are catalytically active only as dimers. Finally, both ZFN left and right were then cloned into a Psyc plasmid, which harbors an A2P sequence; as a result, both ZFN left and right are expressed as polycistronic mRNA under the control of one CMV promoter.

T7E1 cleavage assay and Indel mutation detection

A 2.3 kb human utrophin A promoter PCR products were amplified using the primers:

P1: TCAAACACTCCAATGTGGCCTTATTATCTA

P2: TAAAGCTTGGAGAAGCAGACACGAAC

25uL aliquots of the PCR product were added to 1× Buffer 2 New England Biolabs (NEB), denatured at 95°C for 5 minutes, slowly cooled to room temperature to allow annealing and formation of hetero-duplexes. The individual preps were then treated with 5 units of T7E1 (NEB) for 30 minutes at 37°C. Digested products were separated on a 1% agarose gel (1×TBE). The band intensity was analyzed using ImageJ (NIH) in order to calculate mutation frequencies we used the following formula:

$$\% \text{ Indel} = 100*(1- (1-(b + c)/ (a+ b+ c))^{1/2}$$

Where **a** represents the intensity of the undigested PCR product, and **b** and **c** are the intensities of each cleavage products. To better characterize the mutations, the 2.3Kb amplification bands were cloned into the pcDNA3 plasmid, followed by a single clone Sanger sequencing and aligned to observe the individual Indel mutations.

CRISPR/Cas9 system

sgRNA Design

The online software http://crispr.mit.edu/ was used to design and predict the sgRNAs targeting 2.3Kb of human utrophin A promoter region. The designed oligos were based on the target site sequence (20bp), which has to be flanked on the 3' end by a Proto-spacer Adjacent Motif (PAM) of 3bp NGG sequence. All sgRNAs with a predicted activity score greater than 0.9 were ranked according to the least possible number of potential off-target sites. The best predicted sgRNAs were ordred from Alpha DNA (Canada), and cloned into the Px261 plasmid.

Plasmids

- CRISPR plasmids (PX261) and (pX330) were provided by Dr. Feng Zhang and are also available through Addgene # 42230 / # 42229) [259].
- The PGl4:14 human utrA::luciferase plasmid was provided by Dr. Tejvir S. Khurana [260]
- UTR-CAG-UTR-Luciferase plasmid was obtained by cloning the Cytomegalovirus Enhancer/Chicken β-Actin (CAG) promoter into the PGl14 human UTRN-Luciferase.

First the PGl14: UTRN-Luciferase was cut with Sma1 and treated with calf intestinal phosphatase; meanwhile, a Cytomegalovirus Enhancer/Chicken β-Actin (CAG) promoter fragment was imported from the CAG-GFP plasmid using HincII restriction enzyme. After gel purification and T4 DNA ligation the CAG promoter was inserted into the utrophin A promoter region between the N-box and E-Box motifs as confirmed by sequencing.

- The Donor plasmid UTR-CAG-UTR-GFP was generated by replacing the luciferase reporter gene by the Green Fluorescent Protein (GFP) sequence.

Luciferase assay

HEK 293T cells were seeded at equal density into 6 wells plates. In each well HEK 293T cells were either transfected with the UTRN-Luciferase or the UTR-CAG-UTR-Luciferase plasmids using polyethylenimine (PEI): One day before transfection, $0.5x10^6$ HEK 293T cells were seeded in 6 well dish using DMEM/10% FBS medium**.** Next day, in a sterile tube (1ug) of plasmid DNA was diluted in serum-free media. After that, 1ug/uL of PEI was added to the diluted DNA and mixed well by pipeting. Finally, the mixture was incubated for 15 minutes at RT and added to the cells. After 24h post-transfection cells were harvested for either luciferase

measurement using luciferase assay kit (Promega), following the manufacturer's indications or total RNA extraction using TRIZol (Invitrogen) followed by RT-qPCR reaction as indicated in the section on analysis of mRNA.

Homologous Direct Repair induction

In a 6 well plate HEK 293T cells were co-transfected with both plasmids CRISPR-Cas9 and donor UTR-CAG-UTR-GFP using the polyethylenimine (PEI). In order to inhibit the NHEJ pathway and increase the frequency of HDR pathway repair, transfected cells were treated with 1μM SCR7 (S7742-5MG; Cedarlane, CA) for 24h. 78h post-transfection cells were transferred to a 10 cm dish, and selected with 1 ug/mL puromycin for 7 days.

PCR genotyping

In total 18 clones survived and were independently expanded. Duplicates of each single clone were obtained. The first duplicated plate was conserved for cell expansion, and the second one used for PCR genotyping. The extracted genomic DNA of each single clone was then PCR genotyped using about 50–200 ng of the genomic DNA as template. Detection of Knocked in cells was done by amplifying a 1.1Kb fragment, which has primers that cover both the (CAG) end region and the genomic utrophin region as well.

F1: GCGGCTCTAGAGCCTCTGCTAA

F2: GGGGAGCTAAACTGAGGCCCC

The cycling program was as follows: 95.5C for 5 min followed by 35cycles of 95.5C for 20s, 70C for 30s and 72C for 60s. The PCR product was run on a 1% agarose gel. Positive clones were expected to have a 1.1Kb fragment amplified.

RNA extraction and real-time RT-PCR analysis

Total RNA was extracted from HEK 293T cells treated either UTR-CAG-UTR-GFP and CRISPR-Cas9 or the negative control using the TRIzol reagent according to the manufacturer's instructions (Life Technologies). One μg of RNA was reverse transcribed using oligo (dT) primers and M-MLV (Moloney Murine Leukemia Virus) (Life Technologies) in a final volume of 20μl at 37°C for 50 min. A real-time PCR assay was performed in a 96-well format using the ABI Prism 7000 Sequence Detection System (Applied Biosystems, Foster City, CA). Primers for human utrophin A and for human glyceraldehyde-3-phosphate dehydrogenase (GAPDH) (housekeeping gene) were synthesized by Alpha DNA.

Human UTRN For: GCCAATTCCAAGTTCCATTAAATC

Human UTRN Rev: CAGTAGAACACACAGTCAGCACTCAA

Human GAPDH For: CATCAATGACCCCTTCATTGAC

Human GAPDH Rev: CGCCCCACTTGATTTTGGA

PCR mixtures containing either the cDNA template from the selected HEK 293T cells treated withUTR-CAG-UTR-GFP+CRSIPR-Cas9, or non-treated HEK 293T cells as a negative control were run. The results were analysed using the Applied Biosystems analysis software. The data are expressed as the ratio between utrophin and GAPDH mRNA expression. The gene expression ratio between utrophin and GAPDH is shown as the mean ± SEM. from three independent experiments performed in triplicate. *$P < 0.05$ and***$P < 0.01$ indicate statistical significance by t-test.

Analysis of utrophin Protein Levels

HEK293T cells were lysed with RIPA buffer (50 mM Tris HCl [pH 7.4], 150 nM NaCl, 1 mM EDTA, 1% deoxycholate, 1%Triton X-100 supplemented with phosphatase and protease inhibitor cocktails (Roche), and the protein concentration was measured by bicinchoninic acid (BCA) assay. 35 µg of protein lysates were resolved by western blot on 5% acrylamide gel, transferred overnight to nitrocellulose membranes, and probed for utrophin, and vinculin (V9131 Sigma). The western blot band intensity was analyzed using ImageJ (NIH).

Results

Chapter 3: Zinc Finger Protein mediates utrophin up-regulation

Design and Characterization of ZFPs Targeting the Proximal Utrophin A Promoter

Zinc Finger Proteins (ZFPs) are the largest group of all transcription factors involved in controlling gene expression [261]. The C2H2 zinc-finger structure is composed of a repeated 28–30 amino acid sequence forming short beta hairpin, and an alpha helix. The secondary structure of the C2H2 zinc finger is stabilized by zinc tetrahedral binding to two cysteine and two histidine residues [262]. The alpha helix harbors seven amino acids which recognize the three base pairs (3bps) in the major groove of double stranded DNA [263]. In 1994 the first engineered ZFP was characterized by Klug and colleagues [264]. Since then, engineered ZFPs have emerged as very useful tools, designed by three major strategies including: 1) engineering of ZFPs by modular design; 2) the OPEN strategy (Oligomerized Pool Engineering); and 3) the selection of ZFPs from degenerated zinc finger libraries. Because each finger binds its 3-bp subsite as an independent module, modular design is considered relatively simple to accomplish ZFP engineering [265]. The aim of this project was to target and up-regulate human utrophin expression using a new generation of engineered ZFPs [266]. Potential ZFPs targeting human utrophin A were identified and selected using the ZiFiT software. In order to design a three-module ZFP, the DNase I accessible sites of human utrophin A promoter sequence [267] were analysed by the software, and the output showed several potential 9-bp targeted sequences (Figure 3.A). The selection of the predicted 9bps was based on two parameters: 1) The ZFP should have a low affinity score and 2) high GNN score as reported on the ZFP design

instructions (figure 3.B) [266]. In order to design zinc finger artificial transcription factors, the DNA-binding domains were linked to a trans-activation domain provided by the VP16 protein of the herpes simplex virus; the fusion protein was guided by a nuclear localization signal (NLS) to ensure nuclear trafficking (CMV-NLS-ZFP-VP16). The negative control plasmid was obtained by replacing the zinc finger DNA binding domain by the green fluorescent protein GFP (CMV-NLS-GFP-VP16) (Figure 4B). Individual zinc-finger DNA binding domains that could putatively bind the human utrophin A promoter were sub-cloned first into the pX3CB plasmid according to Keith *et al* protocol (Figure 4A) [257]. After the cloning of the predicted ZFPs into the Pst1374 plasmid, the biological activities of the artificial transcription factors were further characterized by a series of *in vitro* experiments. First, the expression of each ZFP was assessed by western blotting using anti-VP16 antibody. In addition, the nuclear localization of ZFP was revealed by immuno-staining of HEK 293T cells (Figure 5A, B). Moreover, the sequencing results confirmed that the cloned ZFPs were identical to the predicted ZFPs (Figure 5C).

Trans-activation of the human utrophin A promoter

For our initial studies, HEK 293T cells were first co-transfected with both plasmids: the engineered ZFPs and the 1.3kb human utrophin A promoter fragment driving expression of the beta galactosidase reporter [268]. Cells were harvested 48h post transfection and assayed for beta galactosidase activity, and western blotted for VP16 expression. The analysis of beta galactosidase activity showed that the increase of activity was dependent on the presence of the ZFPs. The specific activity was deduced by normalizing the beta galactosidase activity against the VP16 expression. The screening of several ZFP constructs led to the characterisation of potential ZFPs that are able to induce beta galactosidase up-regulation as shown in Figure 6.

The up-regulation of human endogenous utrophin gene

To assess the effect of transfected ZFP on endogenous utrophin expression, we generated stably selected HEK 293T cell line expressing the most promising ZFP based on the up-regulation of the beta galactosidase reporter, especially the ZF51, which had previously shown a significant increase of murine utrophin [269]. During initial experiments under blasticidin selection, we observed that after a few passages the cells lost ZFP expression as assessed by western blot analysis. We then decided to insert an IRES-GFP into the ZF51 construct in order to track its expression via fluorescence microscopy. After cloning the IRES-GFP into the Pst1374-ZF51-VP16, a beta galactosidase assay was performed to ensure that the IRES-GFP has no effect on the ZFP activity. As shown in Figure 7A, the IRES-GFP did not interfere with ZF51 activity, as it could still activate the human utrophin A promoter linked to the reporter gene. The ZF51-IRES-GFP transfected cells were FACS sorted, and total mRNA was then harvested. The RT-qPCR analysis showed only a 1.3 the fold increase in the utrophin A mRNA level (Figure 7B).

Because the human utrophin A promoter is highly rich in CpG islands and has several DNA methylation spots, the endogenous chromatin environment could be silenced via DNA methylation. To further improve the regulatory effects of ZFP, we considered epigenetic factors such as DNA methylation. In order to overcome epigenetic modification of utrophin A promoter, we treated the stably selected ZF51-IRES-GFP-293T HEK cells for 5 days with 40 uM of azacytidine, which is a chemical analogue of the cytosine nucleoside; its incorporation into DNA leads to a covalent binding with DNA methyltransferases, and its DNA methyltransferase function is blocked. In addition, the covalent protein adduction will trigger DNA damage signaling, resulting in the degradation of trapped DNA methyltransferases [270]; as a result, the

utrophin promoter will be less methylated, allowing the ZF51 to induce the endogenous utrophin A promoter activation. Treatment of selected ZF51-IRES-GFP 293T HEK cells with azacytidine did lead to a slight increase in utrophin mRNA expression (Figure 7C). According to the above results we can conclude that ZF51 treatment led to a very high upregulation of the 1.3Kb utrophin A short promoter carried on a plasmid backbone, but only modest increase of transcription of the endogenous promoter with the context of chromatin.

Figure 3 Graphical representation of the human utrophin A promoter and the predicted sequences of the three zinc finger proteins

Several transcription factors bind to the utrophin A promoter such as AP1, Sp1 and Sp3; this region also contains a myogenic regulatory E-box and a synaptic regulatory N-box. **(A)** The red square represents the predicted ZFP targeted sequences on the upstream human utrophin A promoter. The transcription initiation site is also included. **(B)** Example of (ZiFiT) software output from the finger search page when human utrophin A promoter sequence (X95523) is provided as a target sequence.

Figure 3

A

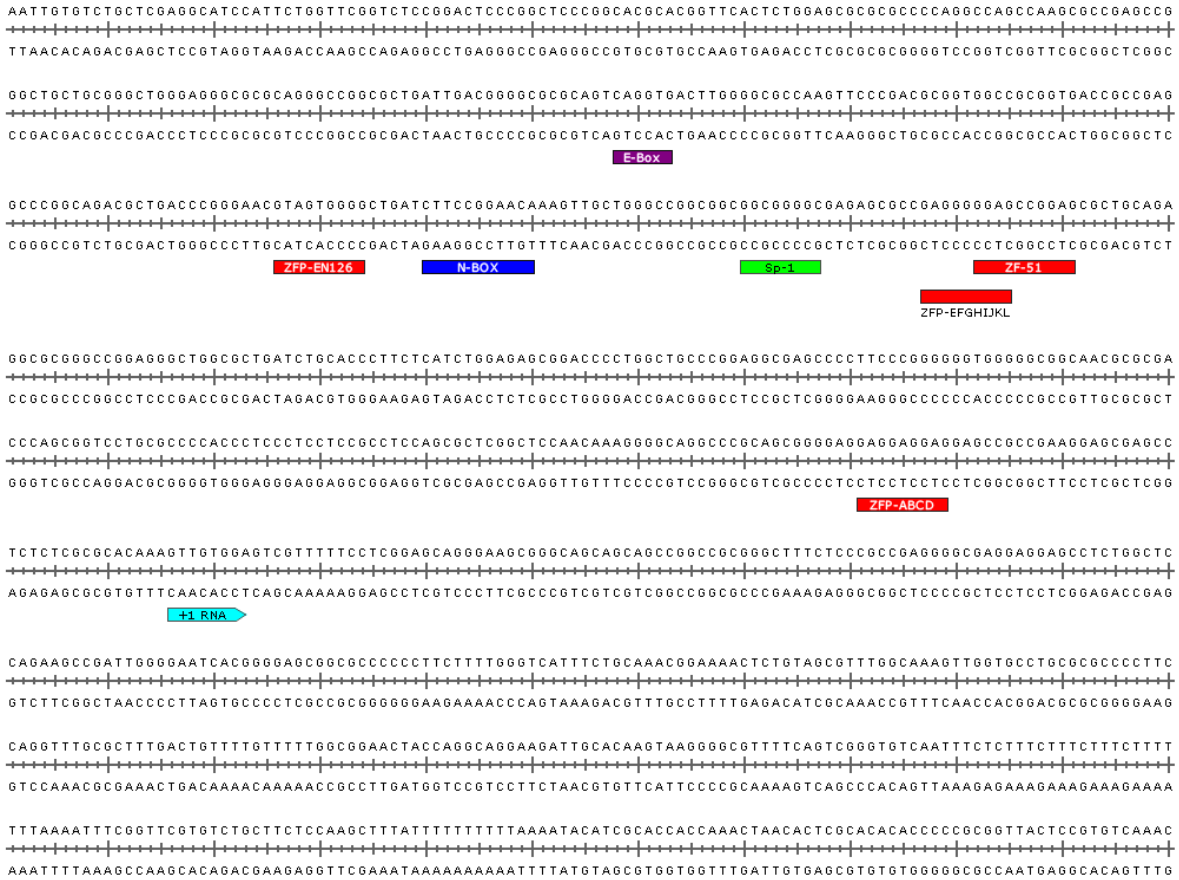

Figure 3

B

```
9 gGAGGAGGAGg 19 | GNN Score: 0.59 | Affinity Score: 1.21
9 cCTCCTCCTCc 19
```

FINGER	HELIX	TRIPLET	REFERENCE NUMBER	MODULE SOURCE
F1	KSSNLRR	GAG	ZF113	ToolGen
F1	QSFNLRR	GAG	ZF115	ToolGen
F1	RKSNLIR	GAG	ZF135	ToolGen
F1	SGSNFTR	GAG	ZF136	ToolGen
F2	KSSNLRR	GAG	ZF113	ToolGen
F2	QSFNLRR	GAG	ZF115	ToolGen
F2	RKSNLIR	GAG	ZF135	ToolGen
F2	SGSNFTR	GAG	ZF136	ToolGen
F3	KSSNLRR	GAG	ZF113	ToolGen
F3	QSFNLRR	GAG	ZF115	ToolGen
F3	RKSNLIR	GAG	ZF135	ToolGen
F3	SGSNFTR	GAG	ZF136	ToolGen

```
6 cGAGGGGGAGc 16 | GNN Score: 0.59 | Affinity Score: 2.25
6 gCTCCCCCTCg 16
```

FINGER	HELIX	TRIPLET	REFERENCE NUMBER	MODULE SOURCE
F1	KSSNLRR	GAG	ZF113	ToolGen
F1	QSFNLRR	GAG	ZF115	ToolGen
F1	RKSNLIR	GAG	ZF135	ToolGen
F1	SGSNFTR	GAG	ZF136	ToolGen
F2	RKDHLTR	GGG	ZF131	ToolGen
F2	RSDKLNR	GGG	ZF133	ToolGen
F2	RRSHLTR	GGG	ZF134	ToolGen
F3	KSSNLRR	GAG	ZF113	ToolGen
F3	QSFNLRR	GAG	ZF115	ToolGen
F3	RKSNLIR	GAG	ZF135	ToolGen
F3	SGSNFTR	GAG	ZF136	ToolGen

Figure 4 Cloning strategy of ZFP from individual finger modules into Pst1374 plasmid.

(A) Each finger coding sequence is flanked on the 5′ end by unique *Xba*I and *Xma*I sites and on the 3′ end by unique *Age*I, and *Bam*HI sites. The configuration of unique flanking restriction sites in all pc3XB-based plasmids permits any two fingers (e.g., F1 and F2) to be joined together by ligating a finger F1-encoding vector backbone (linearized by digestion with *Age*I and *Bam*HI) to a finger F2-encoding fragment (released from the plasmid by digestion with *Xma*I and *Bam*HI). The resulting plasmid encodes a two-finger (F1 followed by F2) array which again is flanked on the 5′ end by *Xba*I and *Xma*I and on the 3′ end by *Age*I, and *Bam*HI. (Ligation of compatible *Xma*I and *an AgeI* overhang destroys both sites). A third finger (F3) can be added to the array by ligating an F1/F2-encoding *Age*I/*Bam*HI-digested vector backbone to a F3-encoding *Xma*I/*Bam*HI-digested fragment [257]. **(B)** Schematic illustration of ZFP-VP16 transcription factor construct: the ZFP-VP16 expression cassette was driven by the CMV promoter and guided by a nuclear localization signal (NLS). The plasmid also contained an IRES-GFP. (see Material and methods section for more details).

Figure 4

A

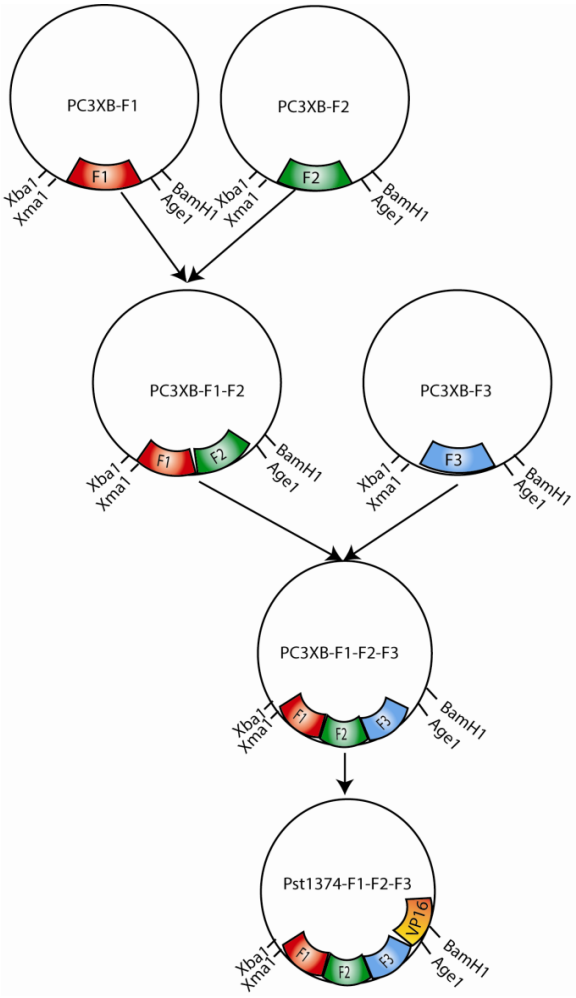
PC3XB-F1
PC3XB-F2
F1
F2
Xba1
Xma1
BamH1
Age1
PC3XB-F1-F2
PC3XB-F3
F3
PC3XB-F1-F2-F3
Pst1374-F1-F2-F3
VP16

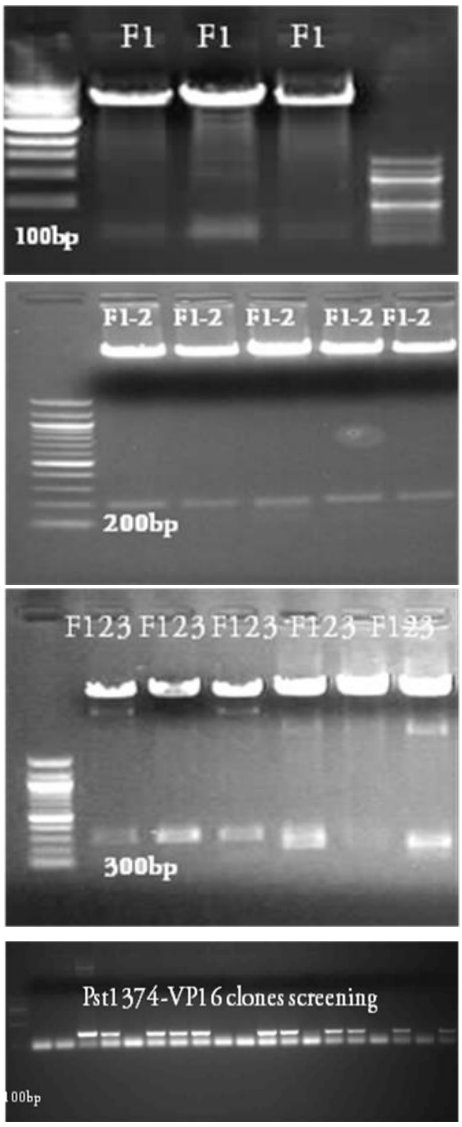
F1 F1 F1
100bp
F1-2 F1-2 F1-2 F1-2 F1-2
200bp
F123 F123 F123 F123 F123
300bp
Pst1374-VP16 clones screening
100bp

B


CMV
NLS
F1
F2
F3
Vp16
IRES-GFP
CMV
NLS
GFP
Vp16

Figure 5 Expression of various ZFPs in HEK 293T cells.

(A) Western blotting with an anti-VP16 antibody was used after transient transfection of different ZFPs (ZFP1, ZFP2 and ZFP3) into the HEK 293T cells. The beta tubulin anti body served as a loading control.

(B) Nuclear localization of ZFP- VP16 and GFP-VP16 fusion protein in HEK 293T transfected cells was detected by immunocytochemistry with an anti-VP16 antibody, nuclei were stained with Hoechst.

(C) Example of Sanger sequencing results: nucleotide and amino acid sequences of a predicted three-zinc finger gene. The α-helix portions present in each finger domain are ZF-115 ZF-134-ZF135.

Figure 5

A

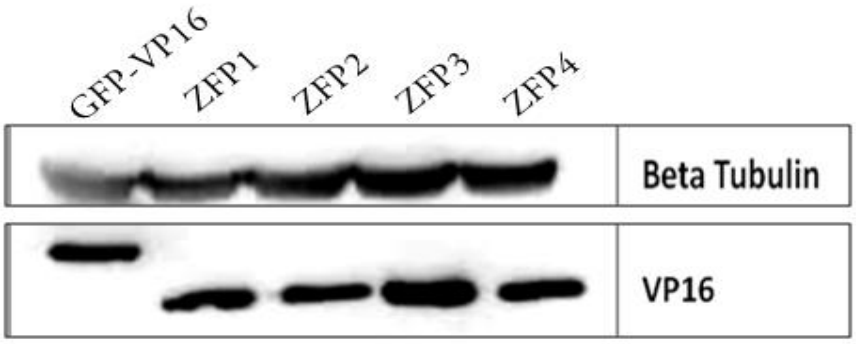
GFP-VP16
ZFP1
ZFP2
ZFP3
ZFP4
Beta Tubulin
VP16

B

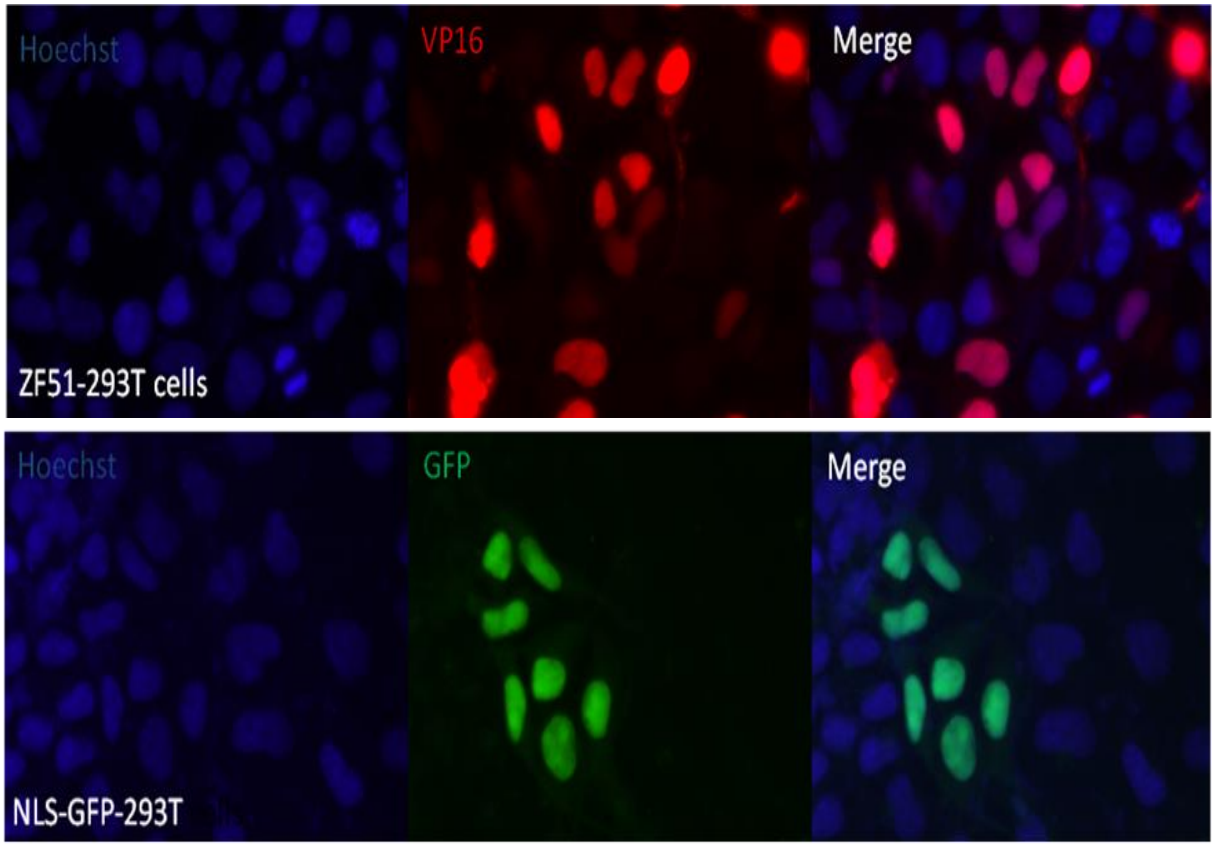
Hoechst
VP16
Merge
ZF51-293T cells
Hoechst
GFP
Merge
NLS-GFP-293T

Figure 5

C

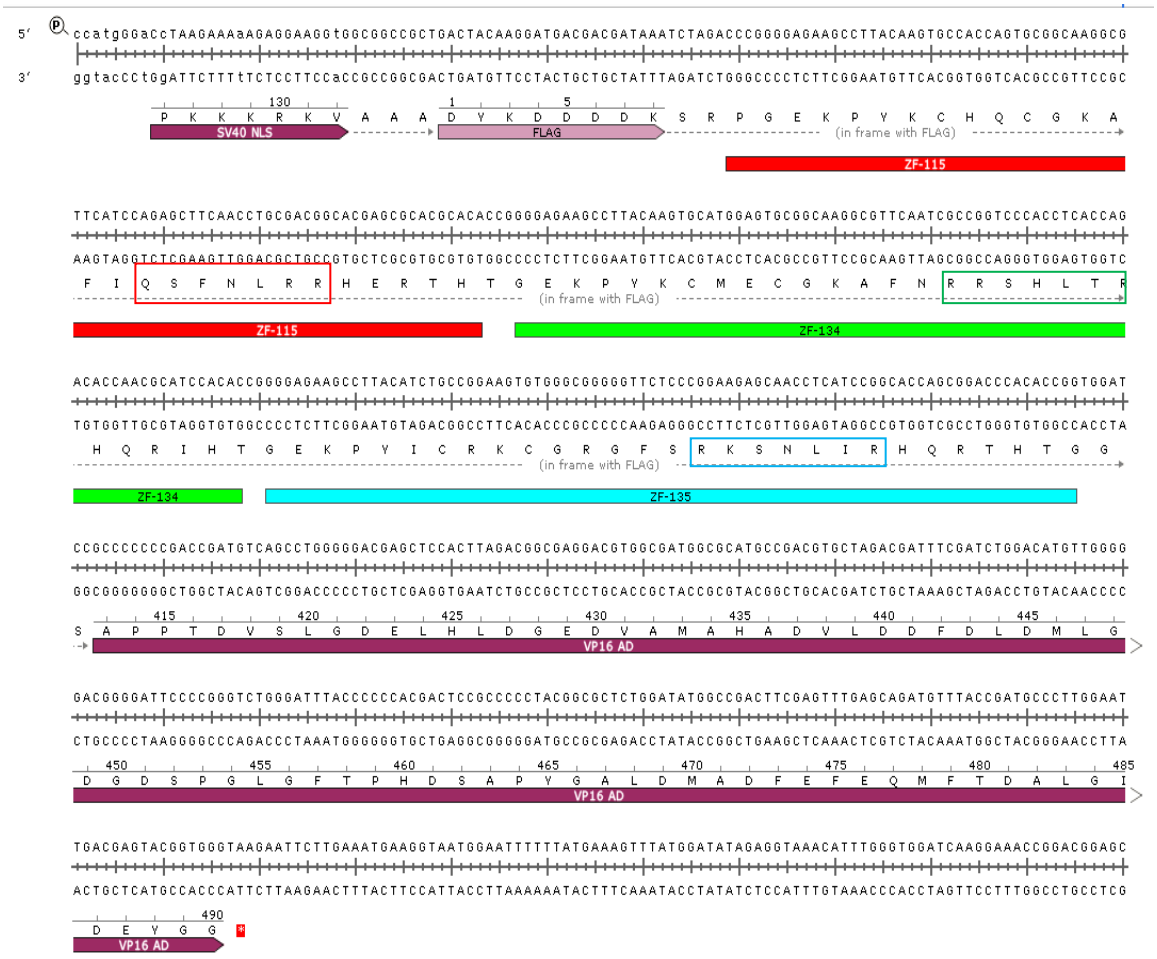
5′ ccatgGGAccTAAGAAAAAGAGGAAGGtGGCGGCCGCTGACTACAAGGATGACGACGATAAATCTAGACCCGGGGAGAAGCCTTACAAGTGCCACCAGTGCGGCAAGGCG
3′ ggtacCCtGgATTCTTTTtTCTCCTTCCaCCGCCGGCGACTGATGTTCCTACTGCTGCTATTTAGATCTGGGCCCCTCTTCGGAATGTTCACGGTGGTCACGCCGTTCCGC
P K K K R K V A A A D Y K D D D D K S R P G E K P Y K C H Q C G K A
SV40 NLS
FLAG
(in frame with FLAG)
ZF-115
TTCATCCAGAGCTTCAACCTGCGACGGCACGAGCGCACGCACACCGGGGAGAAGCCTTACAAGTGCATGGAGTGCGGCAAGGCGTTCAATCGCCGGTCCCACCTCACCAG
AAGTAGGTCTCGAAGTTGGACGCTGCCGTGCTCGCGTGCGTGTGGCCCCTCTTCGGAATGTTCACGTACCTCACGCCGTTCCGCAAGTTAGCGGCCAGGGTGGAGTGGTC
F I Q S F N L R R H E R T H T G E K P Y K C M E C G K A F N R R S H L T R
(in frame with FLAG)
ZF-115
ZF-134
ACACCAACGCATCCACACCGGGGAGAAGCCTTACATCTGCCGGAAGTGTGGGCGGGGGTTCTCCCGGAAGAGCAACCTCATCCGGCACCAGCGGACCCACACCGGTGGAT
TGTGGTTGCGTAGGTGTGGCCCCTCTTCGGAATGTAGACGGCCTTCACACCCGCCCCCAAGAGGGCCTTCTCGTTGGAGTAGGCCGTGGTCGCCTGGGTGTGGCCACCTA
H Q R I H T G E K P Y I C R K C G R G F S R K S N L I R H Q R T H T G G
(in frame with FLAG)
ZF-134
ZF-135
CCGCCCCCCCGACCGATGTCAGCCTGGGGGACGAGCTCCACTTAGACGGCGAGGACGTGGCGATGGCGCATGCCGACGTGCTAGACGATTTCGATCTGGACATGTTGGGG
GGCGGGGGGGCTGGCTACAGTCGGACCCCCTGCTCGAGGTGAATCTGCCGCTCCTGCACCGCTACCGCGTACGGCTGCACGATCTGCTAAAGCTAGACCTGTACAACCCC
415 420 425 430 435 440 445
S A P P T D V S L G D E L H L D G E D V A M A H A D V L D D F D L D M L G
VP16 AD
GACGGGGATTCCCCGGGTCTGGGATTTACCCCCCACGACTCCGCCCCCTACGGCGCTCTGGATATGGCCGACTTCGAGTTTGAGCAGATGTTTACCGATGCCCTTGGAAT
CTGCCCCTAAGGGGCCCAGACCCTAAATGGGGGGTGCTGAGGCGGGGGATGCCGCGAGACCTATACCGGCTGAAGCTCAAACTCGTCTACAAATGGCTACGGGAACCTTA
450 455 460 465 470 475 480 485
D G D S P G L G F T P H D S A P Y G A L D M A D F E F E Q M F T D A L G I
VP16 AD
TGACGAGTACGGTGGGTAAGAATTCTTGAAATGAAGGTAATGGAATTTTTTATGAAAGTTTATGGATATAGAGGTAAACATTTGGGTGGATCAAGGAAACCGGACGGAGC
ACTGCTCATGCCACCCATTCTTAAGAACTTTACTTCCATTACCTTAAAAAATACTTTCAAATACCTATATCTCCATTTGTAAACCCACCTAGTTCCTTTGGCCTGCCTCG
490
D E V G G *
VP16 AD

Figure 6 Differential behaviour of ZFPs targeted to utrophin A promoter

(A) Activation of the transfected human utrophin A promoter reporter gene. The indicated ZFP-VP16 fusion plasmids were co-transfected with the utrophin-beta galactosidase reporter construct as described under "Experimental Procedures." The fold beta galactosidase reporter activation by the ZFPs was calculated in comparison with that of a control vector encoding GFP-VP16. **(B)** Detection of VP16 protein levels by western blot in HEK 293T cells transfected with different ZFP constructs. An anti-tubulin antibody was used as a loading control.

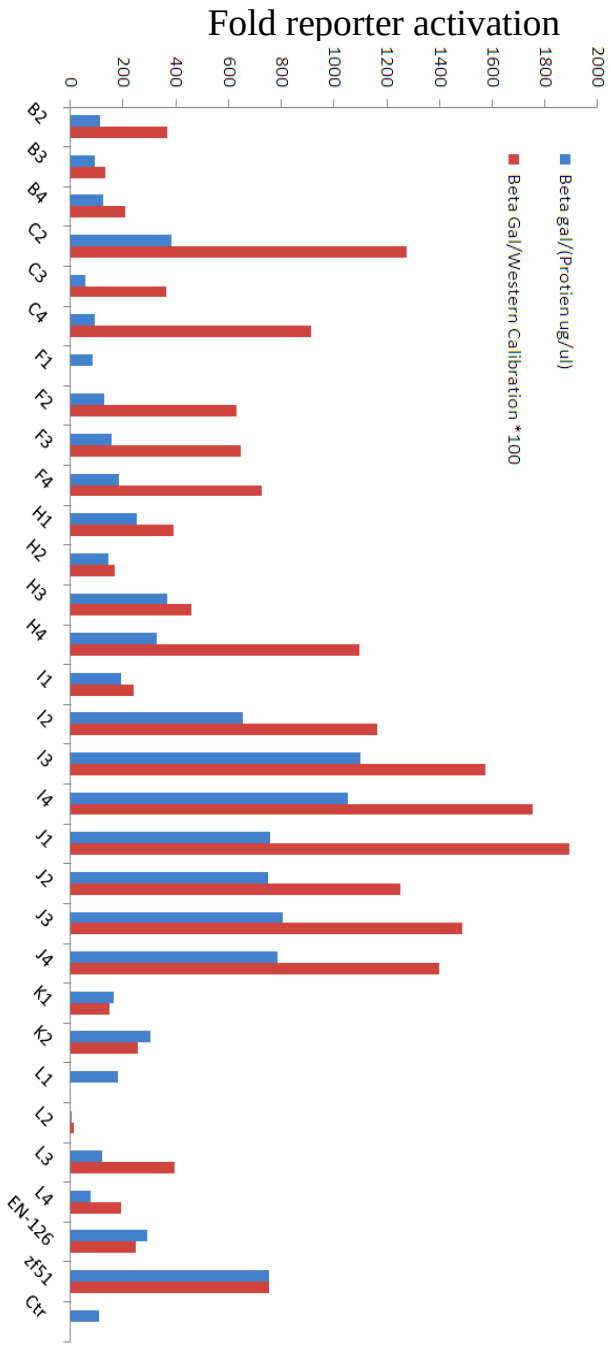
Fold reporter activation
0
200
400
600
800
1000
1200
1400
1600
1800
2000
B2
B3
B4
C2
C3
C4
F1
F2
F3
F4
H1
H2
H3
H4
I1
I2
I3
I4
J1
J2
J3
J4
K1
K2
L1
L2
L3
L4
EN-126
zf51
Ctr
Beta gal/(Protien ug/ul)
Beta Gal/Western Calibration *100

Figure 6 A

Figure 6 B

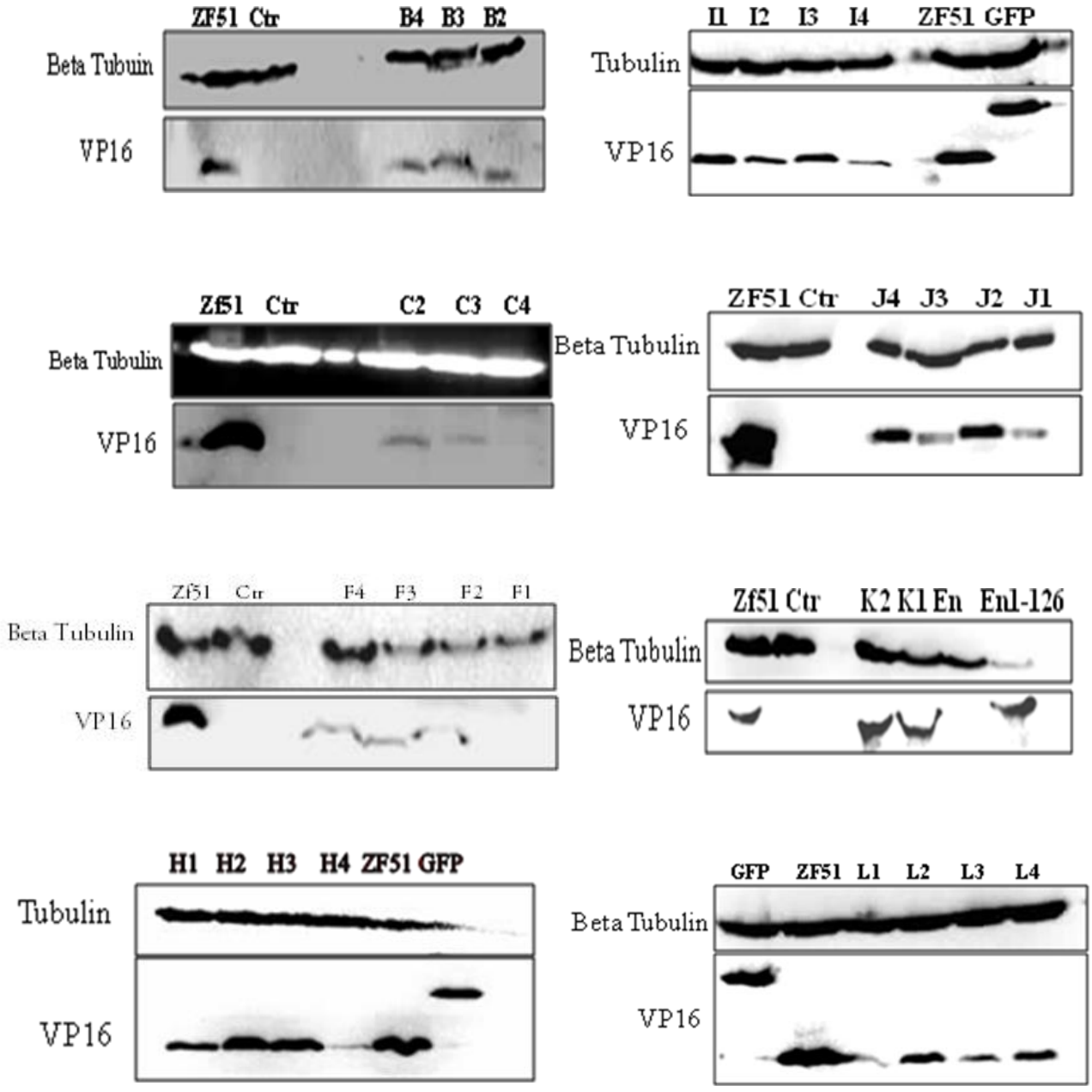
ZF51 Ctr
B4 B3 B2
Beta Tubuin
VP16
I1 I2 I3 I4 ZF51 GFP
Tubulin
VP16
Zf51 Ctr
C2 C3 C4
Beta Tubulin
VP16
ZF51 Ctr J4 J3 J2 J1
Beta Tubulin
VP16
Zf51 Ctr
F4 F3 F2 F1
Beta Tubulin
VP16
Zf51 Ctr K2 K1 En Enl-126
Beta Tubulin
VP16
H1 H2 H3 H4 ZF51 GFP
Tubulin
VP16
GFP ZF51 L1 L2 L3 L4
Beta Tubulin
VP16

Figure 7 Activation of the endogenous human utrophin gene by ZF51

(A) The histogram shows the fold induction of the utrophin-beta galactosidase expression using the ZF51-Pst and ZF51-IRES-GFP. Plasmid utrophin A promoter beta galactosidase was co-transfected either with the zinc finger ZFP51-Pst or ZF51- -IRES-GFP, or the control GFP-VP16 in HEK 293T cells. **(B)** The analysis by real-time PCR of the utrophin gene mRNA expression in HEK 293 T selected cells transfected with the ZF51 or control vectors. The ratio between the utrophin and GAPDH gene expression is shown as means ± S.D. from three independent experiments that were performed in triplicate. **(C)** The analysis by real-time PCR of the utrophin gene mRNA expression in HEK 293T FACS sorted cells transfected with the ZF51 or control vectors treated with azacytidine for 5 days. The ratio between the utrophin and GAPDH gene expression is shown as means ± S.D. from three independent experiments that were performed in triplicate.

Figure 7

A

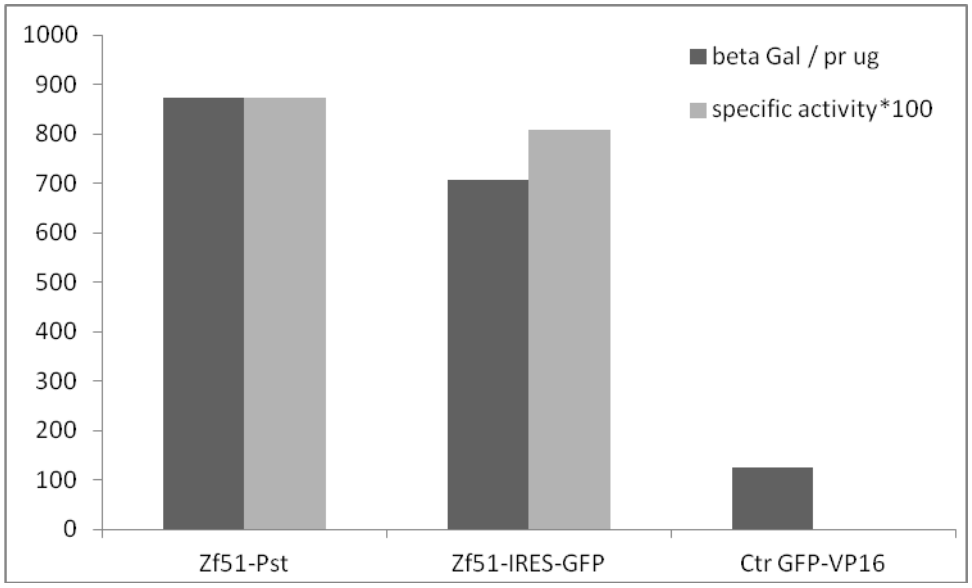
1000
900
800
700
600
500
400
300
200
100
0
beta Gal / pr ug
specific activity*100
Zf51-Pst
Zf51-IRES-GFP
Ctr GFP-VP16

B

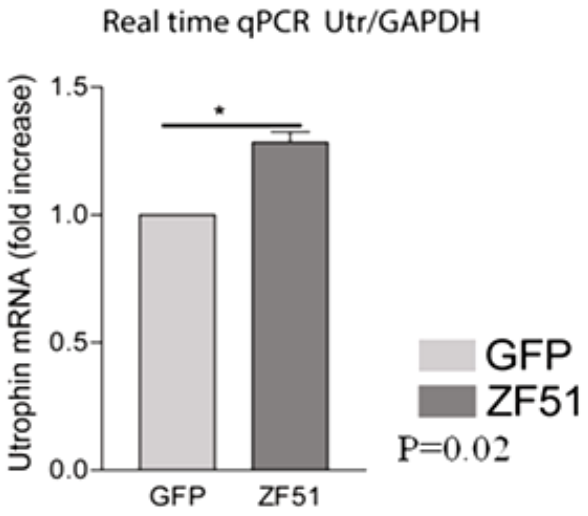
Real time qPCR Utr/GAPDH
Utrophin mRNA (fold increase)
1.5
1.0
0.5
0.0
*
GFP
ZF51
GFP
ZF51
P=0.02

C

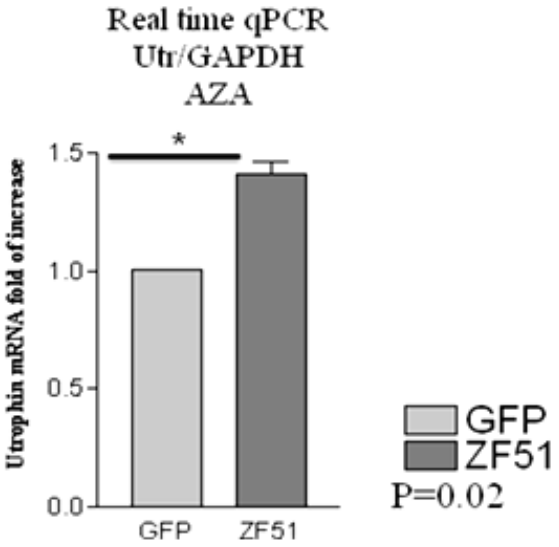
Real time qPCR
Utr/GAPDH
AZA
Utrophin mRNA fold of increase
1.5
1.0
0.5
0.0
*
GFP
ZF51
GFP
ZF51
P=0.02

Chapter 4: Zinc Finger Nuclease cleaves utrophin A promoter

Design and validation of ZFN targeting human utrophin A promoter

Genome editing with engineered site-specific nucleases has emerged as a new technology to selectively modify and correct genes [271]. Genome editing is based on the use of engineered nucleases composed of sequence-specific DNA-binding domains fused to a nonspecific DNA cleavage module [166]. The engineered nuclease will produce double-strand breaks (DSBs) in DNA at specific genomic locations, which will trigger gene repair machinery [272] including the Homologous Direct Repair (HDR) and the Non-Homologous End Joining (NHEJ) mechanism [241]. It is known that zinc finger proteins can be reprogrammed to target any DNA sequence; therefore, a fusion protein comprising such a programmable DNA-binding domain coupled to the FokI endonuclease could be used as a genome editing tool. Indeed, Zinc finger nucleases (ZFNs) are artificial DNA restriction enzymes that are composed of programmed DNA-binding zinc finger proteins fused to the nonspecific nuclease domain derived from FokI endonuclease [273]. Because the human utrophin A promoter structure has several Sp1/Sp3 zinc finger binding sites, ZFNs could be used as genome editing tools to target human utrophin A region [269], in order to subsequently insert an artificial promoter sequence to drive endogenous utrophin gene expression. To investigate the feasibility of a ZFN-mediated site-specific cleavage in human utrophin A promoter, we engineered ZFN expression plasmids using the same strategy described in chapter 3. We first selected the utrophin A promoter sequence and using the ZiFiT software we designed several ZFNs targeting the utrophin A promoter (Figure 8). In order to test the ability of ZFN to target and cleave the human utrophin A promoter DNA, predicted ZFNs were cloned into the Pst1374 plasmid which has a modified FokI nuclease that is catalytically active

only as homodimers [274]. Therefore, a ZFN target site consists of two ZF ‘half-sites’ on complementary DNA strands, separated by a ‘spacer’ of six base pairs, as shown in (Figure 8).

Effect of psyc-ZFNs on human utrophin A promoter

We used the psyc-97 backbone, which has the 2A peptide sequence to co-express ZFNs as two separate entities. It is known that psyc-97 express both GFP and Mcherry from the same transcript as two separate entities as shown in the first panel of Figure 9B [275]. In order to express both ZFNs from the same backbone, we first replaced the Mcherry sequence by the ZFNL (left) that targets the positive strand of the target site, and verified if we could detect expression of both ZFNL and the GFP. Indeed, the immunofluorescence shows that the (FLAG) of ZFNL is expressed with GFP as a bicistronic element and both are localized into the nuclei. Then we cloned the ZFNR (right) that targets the negative strand on the psyc-97 plasmid by replacing the GFP sequences. In fact, when ZFNR replaced the GFP sequence in psyc-97, the immunofluorescence results showed that the (FLAG) of ZFNR is expressed with Mcherry as bicistronic elements. Finally, we joined both ZFNL and ZFNR in one plasmid psyc-ZFNR-ZFNL (Figure 9A.B). When both ZFNs bind to the target sequence the dimerized FokI becomes active and causes genomic DNA cleavage, which in turn triggers the NHEJ mechanism leading to insertion/deletion (indel) mutations. The presence of indels can be detected by mismatch-sensitive T7E1 endonuclease assay. The T7E1 endunoclease recognizes mismatches in fragments produced following denaturation and annealing of PCR amplified fragments. As shows in Figure 9C there is an extra band of 400bp in the amplified genomic DNA of ZFN treated cells following T7E1 incubation, indicating that ZFN can induce DNA double-strand breaks in the utrophin A promoter genomic locus.

Figure 8 Targeting the human utrophin A Promoter with designed ZFNs.

(A) A 2.3Kb section of utrophin A promoter targeted by ZFNs. The DNA sequence of the primary binding site for each ZFN is boxed. ZFN-UTRN-R (blue box) and ZFN-UTRN-L (pink box) bind to 9bp, each ZF target complementary is inter-spaced with 6bp. ZFN-UTRN-R binds the 9 bp site AGA-GCG-GAC, whereas ZFN-UTRN-L binds to the 9-bp site AGA-AGG-GTG of the negative strand. **(B)** When the predicted three zinc fingers nuclease (left) ZF138-ZF132-ZF119-FokI, will meet the right three zinc finger ZF107-ZF130-ZF119-Fok1, the endonuclease FokI will form a dimer complex, and produce DNA double strand breaks (DSB).

Figure 8

A

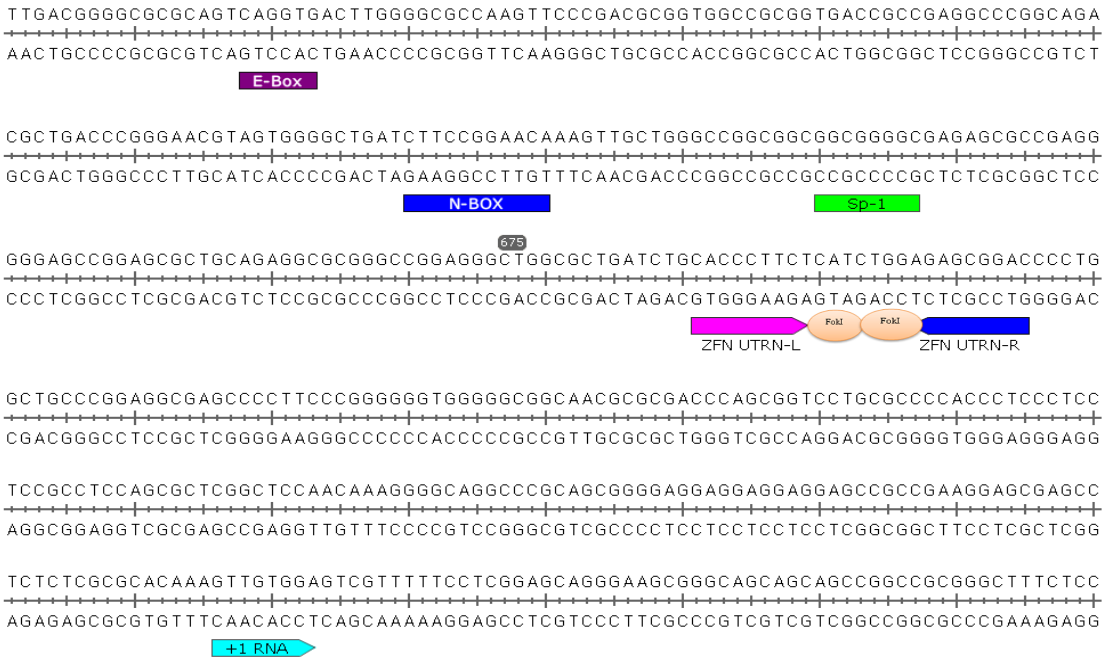
TTGACGGGGCGCGCAGTCAGGTGACTTGGGGCGCCAAGTTCCCGACGCGGTGGCCGCGGTGACCGCCGAGGCCCGGCAGA
AACTGCCCCGCGCGTCAGTCCACTGAACCCCGCGGTTCAAGGGCTGCGCCACCGGCGCCACTGGCGGCTCCGGGCCGTCT
E-Box
CGCTGACCCGGGAACGTAGTGGGGCTGATCTTCCGGAACAAAGTTGCTGGGCCGGCGGCGGCGGGGCGAGAGCGCCGAGG
GCGACTGGGCCCTTGCATCACCCCGACTAGAAGGCCTTGTTTCAACGACCCGGCCGCCGCCCCGCTCTCGCGGCTCC
N-BOX
Sp-1
675
GGGAGCCGGAGCGCTGCAGAGGCGCGGGCCGGAGGGCTGGCGCTGATCTGCACCCTTCTCATCTGGAGAGCGGACCCCTG
CCCTCGGCCTCGCGACGTCTCCGCGCCCGGCCTCCCGACCGCGACTAGACGTGGGAAGAGTAGACCTCTCGCCTGGGGAC
FokI
FokI
ZFN UTRN-L
ZFN UTRN-R
GCTGCCCGGAGGCGAGCCCCTTCCCGGGGGGTGGGGGCGGCAACGCGCGACCCAGCGGTCCTGCGCCCCACCCTCCCTCC
CGACGGGCCTCCGCTCGGGGAAGGGCCCCCCACCCCCGCCGTTGCGCGCTGGGTCGCCAGGACGCGGGGTGGGAGGGAGG
TCCGCCTCCAGCGCTCGGCTCCAACAAAGGGGCAGGCCCGCAGCGGGGAGGAGGAGGAGGAGCCGCCGAAGGAGCGAGCC
AGGCGGAGGTCGCGAGCCGAGGTTGTTTCCCCGTCCGGGCGTCGCCCCTCCTCCTCCTCCTCGGCGGCTTCCTCGCTCGG
TCTCTCGCGCACAAAGTTGTGGAGTCGTTTTTCCTCGGAGCAGGGAAGCGGGCAGCAGCAGCCGGCCGCGGGCTTTCTCC
AGAGAGCGCGTGTTTCAACACCTCAGCAAAAAGGAGCCTCGTCCCTTCGCCCGTCGTCGTCGGCCGGCGCCCGAAAGAGG
+1 RNA

B

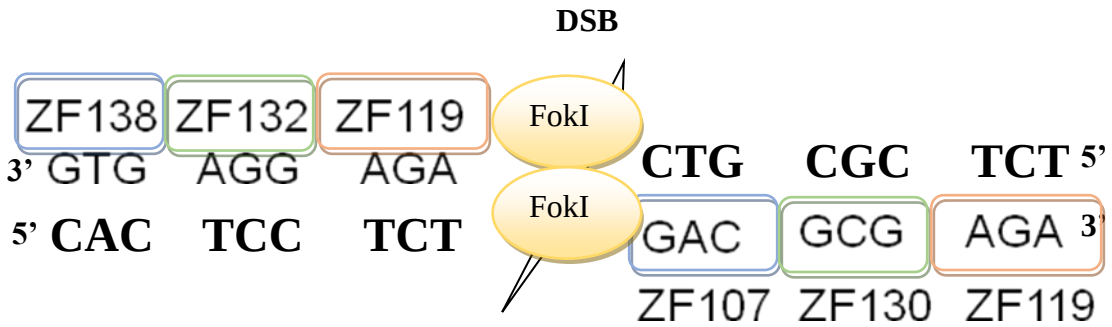
DSB
ZF138
ZF132
ZF119
FokI
FokI
3' GTG AGG AGA
5' CAC TCC TCT
CTG CGC TCT 5'
GAC GCG AGA 3'
ZF107 ZF130 ZF119

Figure 9 Cloning of ZFN into the psyc-97 plasmid.

(A) Schematic representations of psyc-97 plasmid that expresses both GFP and Mcherry from the same transcript as two separate entities, and psyc-ZFNL-ZFNR vector that co-expresses both ZFNs from the same transcript as two separate entities.

(B) In the first panel HEK 293T cells were transfected with psyc-97 plasmid. Because the GFP is linked to a nuclear localisation sequence (NLS), it is localized into the nucleus; however, the Mcherry is expressed all-over the cell. The second panel represents HEK 293T cells transfected with psyc-ZFNL (we replaced the Mcherry with the ZFNL, which has a FLAG tag). The immunofluorescent labelling shows that ZFNL with the (FLAG) tag is expressed bicistronically with GFP and both are localized to nuclei. In the third panel, ZFNR replaces the GFP in psyc-97, and immunofluorescent labelling shows that ZFNR with the (FLAG) tag is expressed with MCherry.

(C) Three days after transfection of HEK 293T cells with psyc- ZFNL-ZFNR, genomic DNA was isolated from transfected and non-transfected cells. A 2.3Kb PCR fragment of utrophin A promoter product was amplified from both treated and control cells for subsequent T7E1 assay.

(D) The frequency of allelic mutation in each pool of treated cells was determined using the T7E1 assay (gel). Bands migrating at 1.9kb and 400 bp represent the T7E1 digestion products of the parent amplicon. The bands were quantified by ethidium bromide staining and densitometry to determine the frequency of NHEJ.

Figure 9

A

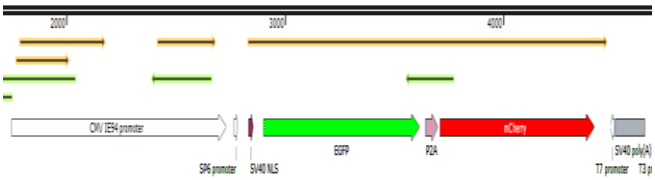

Psyc 97

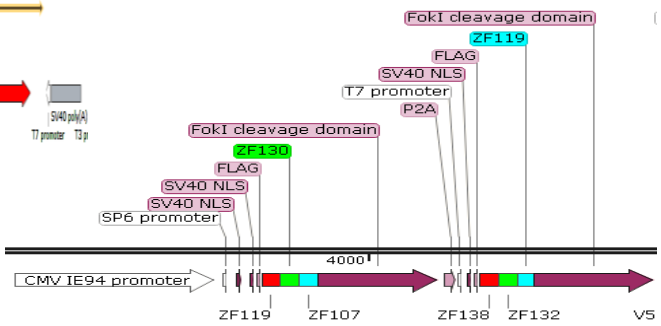

B

psyc ZFN R-L

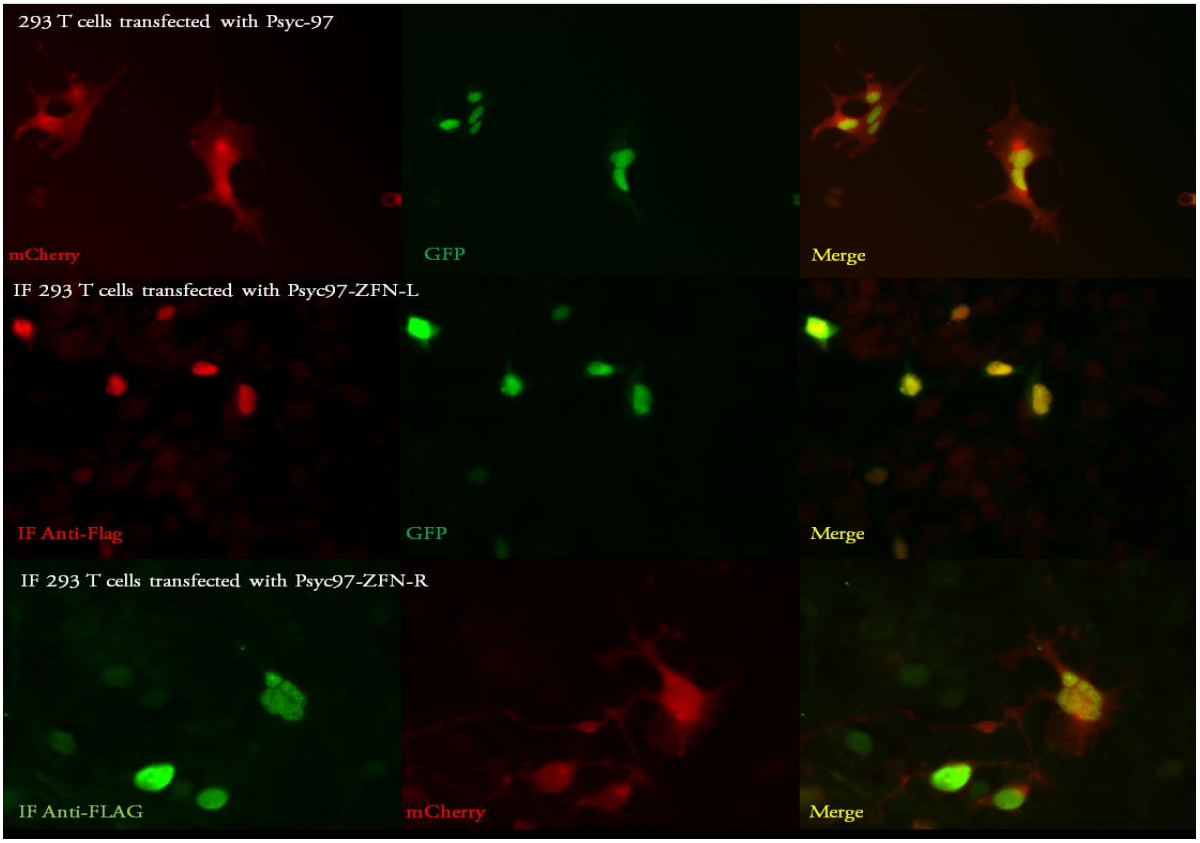

Figure 9

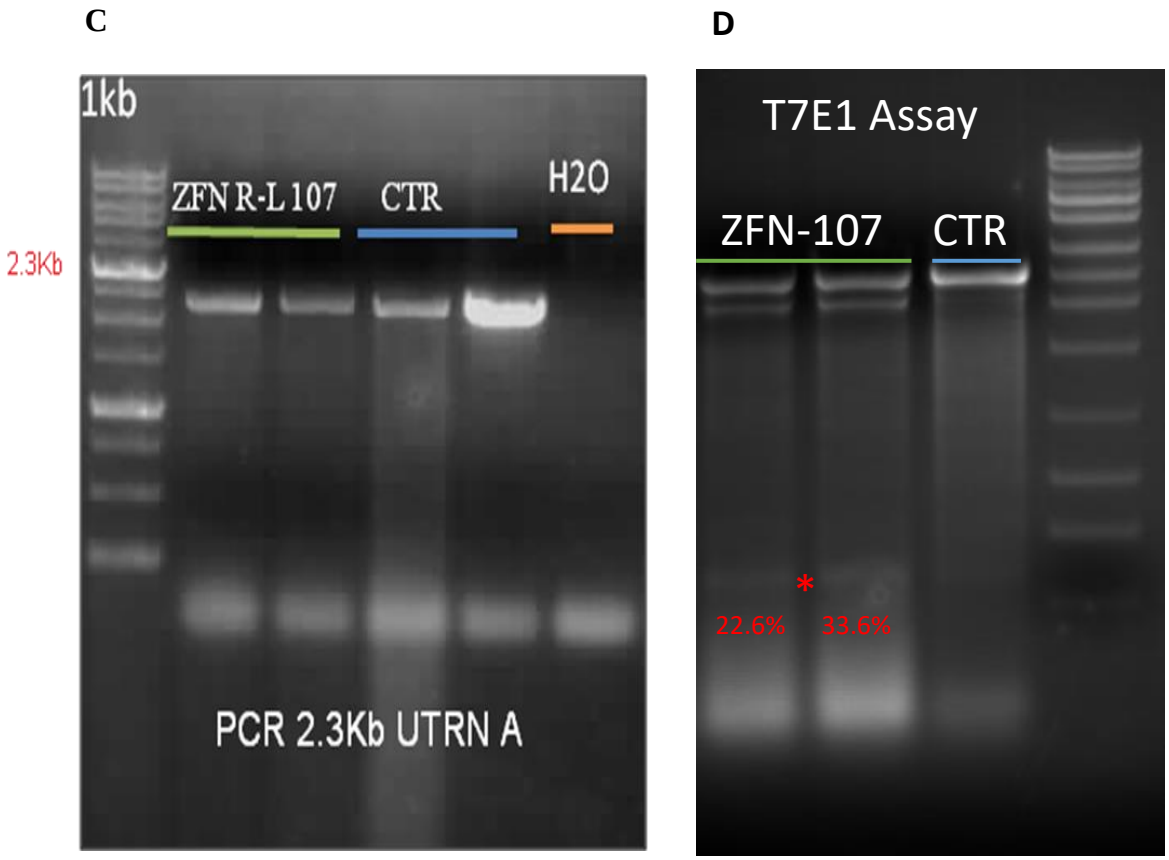
C
1kb
ZFN R-L 107
CTR
H2O
2.3Kb
PCR 2.3Kb UTRN A
D
T7E1 Assay
ZFN-107
CTR
*
22.6%
33.6%

Chapter 5: Use of CRISPR/Cas9 genome editing to up-regulate utrophin via HDR

CRISPR/Cas9 mediated genome editing of human utrophin A promoter in HEK 293 T cells.

The insertion of precise genetic modifications by CRISPR-Cas9 system is highly efficient in comparison to previous genome editing tools. The CRISPR-Cas9 systems (clustered, regularly interspaced, short palindrome repeats (CRISPR)–CRISPR-associated protein) is an innovative tool for genome engineering, enabling the induction of site-specific genomic (DSBs) by single guide RNAs (sgRNAs). The DSB will trigger DNA repair mechanisms such as (NHEJ) or (HDR). During the NHEJ repair pathway, the DSB is repaired by random insertion/deletion mutations at the site of junction. However, the HDR repair pathway can introduce precise point mutations or insertions in the presence of a repair template in the form of a donor plasmid, which allows high fidelity and precise editing (Figure 10).

Insertion of the CAG promoter into the human utrophin A promoter

In order to verify the effect of inserting a Cytomegalovirus Enhancer/Chicken β-Actin (CAG) promoter into the human utrophin A promoter, we have cloned the CAG promoter into the 2.3Kb utrophin A promoter driven luciferase reporter gene. The insertion of CAG within the human utrophin A region led to an over 1000-fold up-regulation of the downstream luciferase gene as shown in (Figure 11). Therefore, we pursued genome editing of the human utrophin gene locus to insert the CAG within the utrophin A promoter region.

Design and validation of CRISPR-Cas9 targeting human utrophin A promoter

In this study, we engineered (CRISPR Cas9+sgRNA) expression plasmids, and tested their ability to cleave human utrophin A promoter DNA. The online software http://crispr.mit.edu/ was used to predict the appropriate regions of human utrophin A promoter. The software output provided several sgRNA (20bp) oligos, which are flanked on the 3' end by a 3bp NGG PAM sequence. The choice of sgRNA is oriented by a high score and fewer off target frequencies. The best predicted sgRNA were ordered and cloned into the plasmid pX261 Cas9, which contains three expression cassettes. First, the guide RNA site is driven by a U6 promoter. Then, the hSpCas9 enzyme driven by the CBh promoter recognises the sgRNA and the DNA target sequence complex. Finally, there is a puromycin cassette used as a selection marker. In order to verify the activity of CRISPR Cas9 on utrophin A promoter, the sequenced (Px261-sgRNA) plasmids were transfected into HEK 293T cells, and stably selected (Figure 12).

Effect of CRISPR-CAS9 on human utrophin A promoter

Next, we verified if CRSIPR/Cas9 system can target and cleave the utrophin A promoter. We harvested the wild type and stably selected HEK 293T cells expressing (CRISPR Cas9 + sgRNA), and extracted the genomic DNA. It is known that DSBs are partially repaired by the NHEJ pathway; therefore, we performed the T7EI assay to detect the indels caused by the Cas9 endonuclease. The 2.3Kb fragment containing the target site of utrophin A promoter was PCR-amplified from the genomic DNA. T7EI digestion performed on the PCR fragment showed two

separate fragments of 700pb and 1.7Kb in the stably selected cells, but not in the wild type HEK 293T cells. (Figure 13)

Sequencing histogram of utrophin A promoter genomic DNA

These PCR amplicons were cloned into the PCDNA3.1 plasmid, and the positive clones were sequenced. The sequencing of 15 positive clones confirmed that short insertions and deletions had indeed occurred at the target site, indicating that (CRISPR Cas9 + gRNA) can target and induce DSB in human utrophin promoter A (Figure 13).

CRISPR/Cas9 induces homologous recombination in HEK 293 T cells

In order to induce the homologous recombination, we cotransfected HEK 293T cells with both plasmids: CRISPR/Cas9-sgRNA and the donor plasmid UTR-CAG-UTR-GFP. The co-transfected cells were treated with 1uM of Scr7 for 3days in order to block the NHEJ repair mechanism, and give more chance to the HDR mechanism. 3 days post-transfection, we started the selection with puromycin for 1 week. Single clones were expended separately as replicates. One part of the resistant clones was used to harvest the gDNA, and the other part was frozen as a backup. Using a PCR-based screening approach (Figure 14), we assessed whether the CAG promoter targeting construct had integrated at the utrophin A site in the genome. Among the 7 clones selected, we identified that four out of the seven were positive (Figure 14A). As shown, PCR of the wild-type locus has no band, whereas PCR of the knock-in allele results in 1100 bp band for clones resistant to puromycin. We thus genotyped the 4 clones and all of them resulted in complete knock-in of CAG promoter (Figure 14B).

Effect of CAG insertion into utrophin A promoter

To assess the effect of CAG insertion into the genomic utrophin region in the knock-in cells, we collected samples for Western blotting and mRNA analysis. These studies on positive clones of HEK 293T cells treated with CRISPR-Cas9 + Donor plasmid and non-treated control cells showed that utrophin mRNA is up-regulated up to 25 fold in clone A2, leading to a 13-fold increase in utrophin protein levels. Clones A5 and B6 had lower but still substantial increase in utrophin mRNA and protein (Figure 15).

CRISPR/Cas9 Off-target cleavage

Off-target cleavage is a serious barrier for engineered nuclease mediated genome editing [276]. The initial selection of the sRNA had identified 4 putative sites with 60% of homology to the target site at locus: Chr19:-15662158, Chr10:-13142194, Chr19:+18284579, Chr14:+94088868. In the stably transfected clones we amplified these putative target sequences, followed by sequencing. The analysis showed that in these clones, these putative target sequences did not have any indel mutations (Figure 16), which indicates that CRISPR/Cas9 targets utrophin A promoter with high precision.

Figure 10 CRISPR/Cas9 mediated genome editing of human utrophin A promoter in HEK 293 T cells

Human utrophin A promoter has several binding sites for the transcription factors **AP1**, **AP2**, **Sp1** and **Sp3**. This promoter region also contains a myogenic regulatory binding site **E-box** and a synaptic regulatory site **N-box**. The CRISPR-Cas9 target site is located between the **E-box** and the N-Box motifs. The sgRNA recognizes the genomic utrophin A promoter region and will guide the nuclease Cas9, which in turn will make double a strand break (DSB) on the target genomic DNA. The DSB will trigger DNA repair mechanisms such as non-homologous end joining (NHEJ) or Homologous Direct Repair (HDR). During the NHEJ repair pathway, the DSB is repaired by random indel mutations at the site of junction. Unlike NHEJ, the HDR repair pathway can introduce precise point mutations or insertions in the presence of a repair template in the form of a donor plasmid, which allows high fidelity and precise editing. The schematic diagram shows the strategy for CRISPR/Cas9 mediated knock-in of Cytomegalovirus Enhancer/Chicken β-Actin (CAG) promoter into the endogenous utrophin A promoter region in the presence of a dsDNA donor vector.

Figure 10

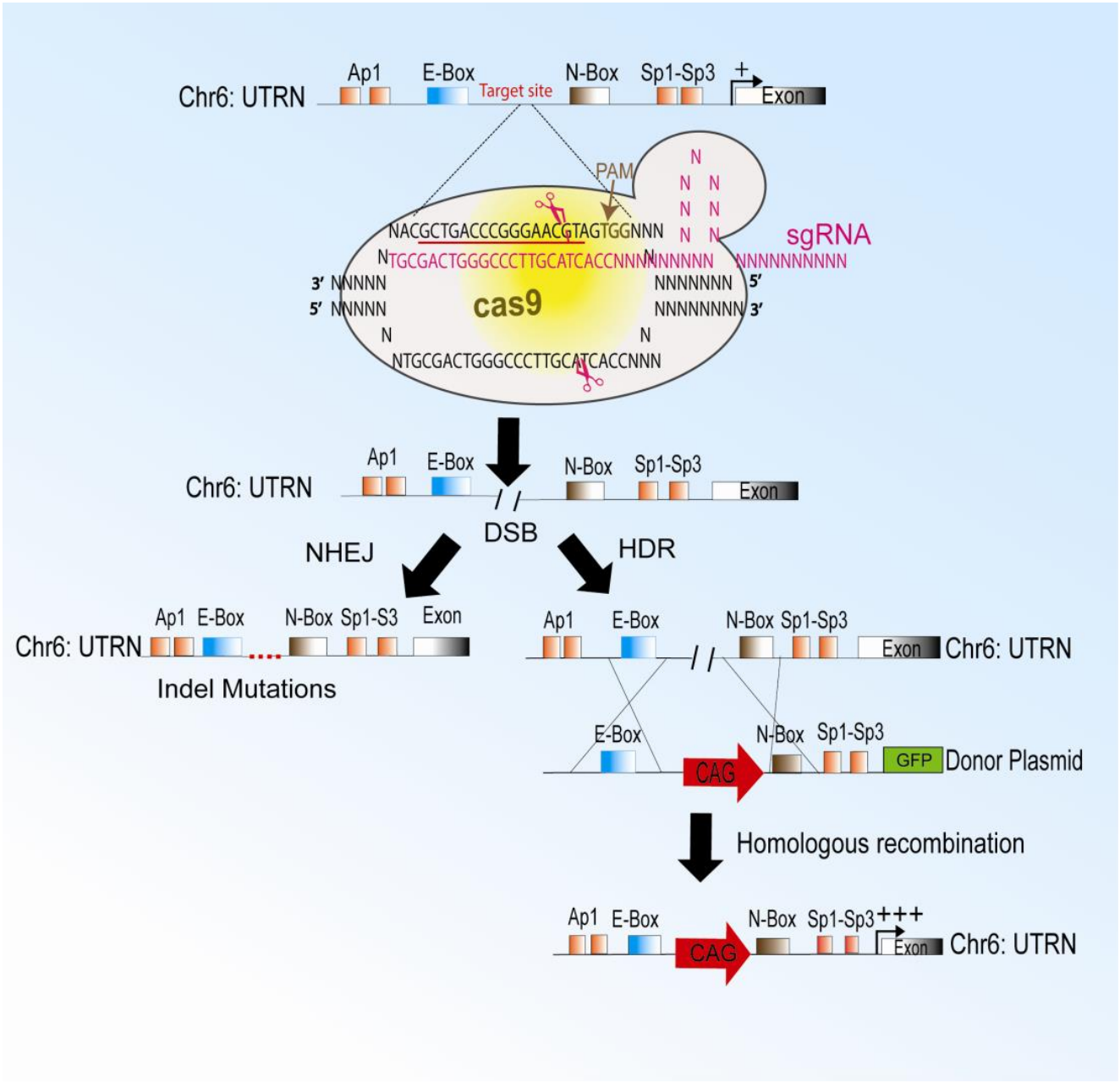
Chr6: UTRN
Ap1
E-Box
Target site
N-Box
Sp1-Sp3
+
Exon
PAM
N
N N
N N
N N
sgRNA
NACGCTGACCCGGGAACGTAGTGGNNN
NTGCGACTGGGCCCTTGCATCACCNNNNNNNNN
NNNNNNNNNN
3′ NNNNN
5′ NNNNN
cas9
NNNNNNN 5′
NNNNNNNN 3′
N
N
NTGCGACTGGGCCCTTGCATCACCNNN
Chr6: UTRN
Ap1
E-Box
N-Box
Sp1-Sp3
Exon
DSB
NHEJ
HDR
Chr6: UTRN
Ap1
E-Box
N-Box
Sp1-S3
Exon
Indel Mutations
Ap1
E-Box
N-Box
Sp1-Sp3
Exon
Chr6: UTRN
E-Box
N-Box
Sp1-Sp3
CAG
GFP
Donor Plasmid
Homologous recombination
Ap1
E-Box
CAG
N-Box
Sp1-Sp3+++
Exon
Chr6: UTRN

Figure 11 Insertion of the (CAG) promoter into the human utrophin A promoter

(A) Schematic representation of pGl4:14 utrophin A- luciferase plasmid, which has a 2.3Kb human utrophin A promoter driven luciferase reporter gene (kind gift from Tejvir S. Khurana), and pGl4:14 URTN-CAG-UTRN-luciferase plasmid, which was obtained by cloning the CAG promoter into the human utrophin A promoter region between the E-Box and the N-box motifs. **(B)** Both reporter constructs, utrophin luciferase (UTR-Lux) and the utrophin-CAG-utrophin luciferase (UTRN-CAG-UTRN-Lux) were transiently transfected into HEK 239T cell lines and assayed after 24 h of incubation. The insertion of CAG promoter into the utrophin promoter region leads to an increase in luciferase activity and luciferase mRNA 24h post-transfection.

Figure 11

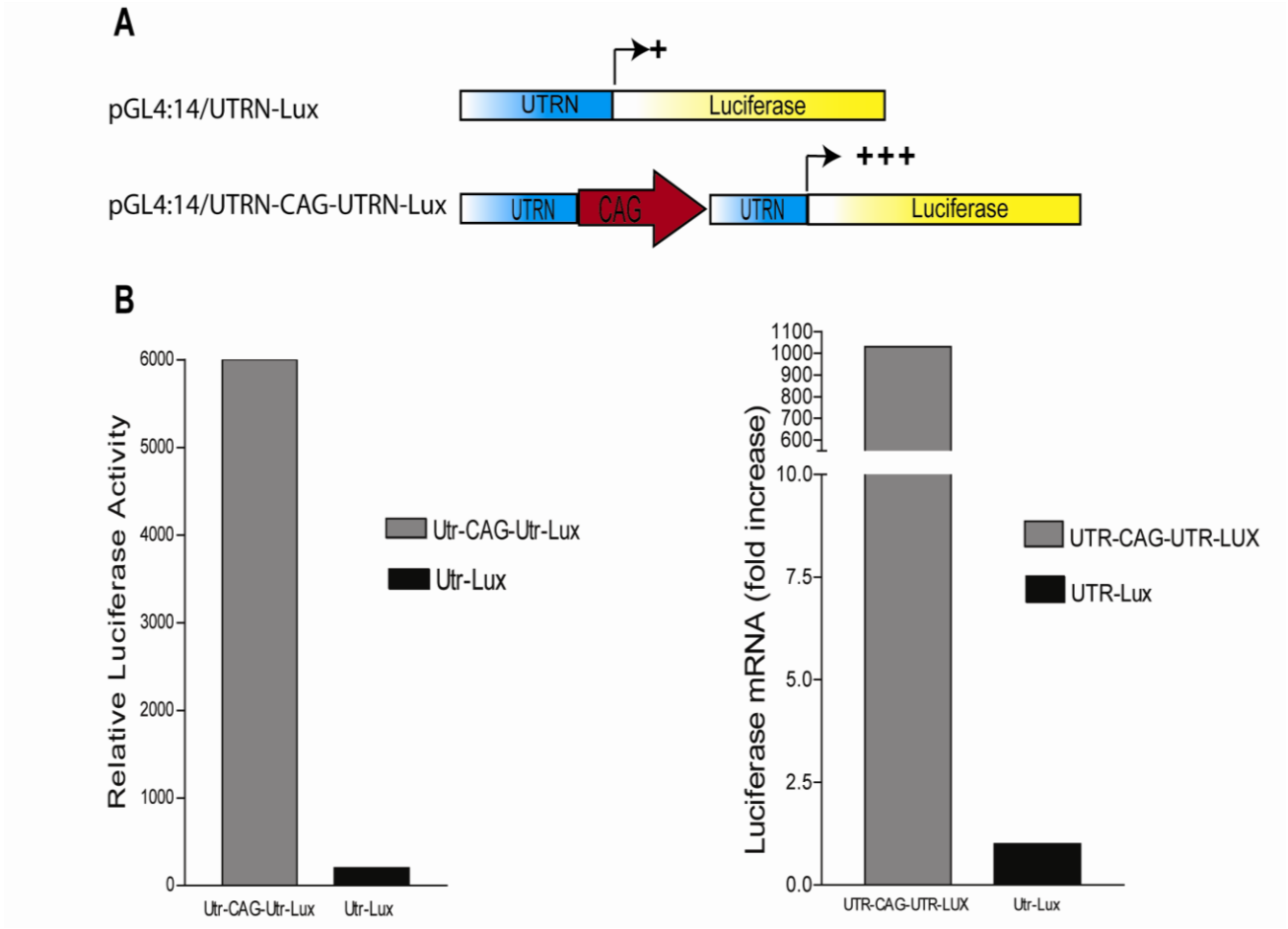
A
pGL4:14/UTRN-Lux
UTRN
Luciferase
+
pGL4:14/UTRN-CAG-UTRN-Lux
UTRN
CAG
UTRN
Luciferase
+++
B
Relative Luciferase Activity
6000
5000
4000
3000
2000
1000
0
Utr-CAG-Utr-Lux
Utr-Lux
Utr-CAG-Utr-Lux
Utr-Lux
Luciferase mRNA (fold increase)
1100
1000
900
800
700
600
10.0
7.5
5.0
2.5
0.0
UTR-CAG-UTR-LUX
Utr-Lux
UTR-CAG-UTR-LUX
UTR-Lux

Figure 12 Target identification in the 2.3 Kb fragments of human utrophin A and the best predicted sgRNAs.

(A) 2.3Kb human utrophin A sequence harboring the target site (blue) next to the PAM sequence (red).

(B) Best predicted sgRNA targeting human utrophin A promoter region has the best score of all predicted sgRNAs.

(C) Sanger sequencing of the cloned sgRNA in the Px261 plasmid showing the U6 promoter driven sgRNA.

Figure 12

A

P1

ATCAAACACTCCAATGTGGCCTTATTATCTATTTTGAAGGAGAAAATCTGAGTTTCATCAACTCAACCAGGATACAGTGAGTGATAA
GCAACTTTTGGTGTCTGCAAAATGATCAGTTAAAAAAAACCTGGGGGCTGGGCACGGTGGCTCATGCCTGTAATCCCAGCACTTT
GGGAGGCCCCGTCTCTACTAAAAATACAAAAAATTAGCAGGGCGTGGTGGTGGGCGCCTGTAGTCCCAGCTACTAGGGAGGCTG
AGGCAGGAGAATGGCGTGAACCCAGGAGGCGGAGCTTGCAGTGAGCGAGATCGCGCCACTGCACTGCAGCCTGGGCAACTGA
GAGAGACACTGTCAAAAAAAAAAAAAAAAGAAAGAAAGAAAGAAAGAAAAAATCCTGGAGTCCCTCTATGTGACCATACTCAG
CTAGCACTTGATCTGTTCTTTTCTTATGGCATTTATCTCCCGGATCTTGTATATACTTACTTGTTTACATGTCTTATCTCACCTACTACA
TTCCAAGTTCTTTAAGGGTAAGATCACTATCAGATTTATCTTTGCTTTACCCACAGAACCAGCAAACCTGACAGCCCTAAACTGATG
CTTGTTAAATGAATGAATGAAGTGAATGAATAAAATCATACCCATTTCAAGTTAATCCTTTGGATTTTATTTGGCTTATACGTAGAAA
ATCATCAAAAGGAAGGAAACTGTCCTAGAAACCTTACAAGGAAGAGTCTCTTTTGGGAATCTCCTACCTGCCCCCTCCCTGGAGC
ACTTAGGGATGGATGGGGGAAACTTTCACTATAACAAAAGGCGAGTAAACTCTTTCTGAAAATTAGTTTAAGGCCCCTAGTGGTTT
AATCTTTACTGCCGCGTAAATTAACTCAAATATTAAGCCAGCAATAAACCGGCGCTCCAGTATCAACCATCCTTTTCTCTGTTAATAC
GAACTAGGAACTCAGGTTGCTGTTTTCTTTCCCCTCCCACGTGTGCTGATCGTGTAAAAGAATCACAGGAACACACGAGCAATGA
AATGTGTAAATAAGAAAAATGCACACACATCACGAGCTCATTTCTTCCCAGATATTTTTTGGTCAACCTCTCAAGCTTGGAACAGG
CTCTATAACAGATGTGCGTTTGTGTGTGCATATTGGAAAACAGAAAAATAAGGTCAGCGCAAACACTACTTGTAATACAAACTAATG
TAAGAGAAAACTTCTTTTTCAATATTAACAACGACACTAGAGAAATAATGTAAAATAAATATACGGTTGGAACTAGGGGTAAAAAA
AAAATCAGCAACGTCAGCAAACTGAGATGGGGTGAGTTGGAAGGCAGATTGGAATTTATCTCTTAAAAAAATATCACCCTAACTAG
AGACCTGTTTTGCCTAAGGGGACGTGACTCACATTTTCGGATAATCTGAATAAGGGGAATTGTGTCTGCTCGAGGCATCCATTCTG
GTTCGGTCTCCGGACTCCCGGCTCCCGGCACGCACGGTTCACTCTGGAGCGCGCGCCCCAGGCCAGCCAAGCGCCGAGCCGGGC
TGCTGCGGGCTGGGAGGGCGCGCAGGGCCGGCGCTGATTGACGGGGCGCGCAGTCAGGTGACTTGGGGCGCCAAGTTCCCGA
CGCGGTGGCCGCGGTGACCGCCGAGGCCCGGCAGACGCTGACCCGGGAACGTAGTGGGGCTGATCTTCCGGAACAAAGTTGCTG
GGCCGGCGGCGGCGGGGCGAGAGCGCCGAGGGGGAGCCGGAGCGCTGCAGAGGCGCGGGCCGGAGGGCTGGCGCTGATCTG
CACCCTTCTCATCTGGAGAGCGGACCCCTGGCTGCCCGGAGGCGAGCCCCTTCCCGGGGGGTGGGGGCGGCAACGCGCGACCC
AGCGGTCCTGCGCCCCACCCTCCCTCCTCCGCCTCCAGCGCTCGGCTCCAACAAAGGGGCAGGCCCGCAGCGGGGAGGAGGAG
GAGGAGCCGCCGAAGGAGCGAGCCTCTCTCGCGCACAAAGTTGTGGAGTCGTTTTTCCTCGGAGCAGGGAAGCGGGCAGCAGC
AGCCGGCCGCGGGCTTTCTCCCGCCGAGGGGCGAGGAGGAGCCTCTGGCTCCAGAAGCCGATTGGGGAATCACGGGGAGCGGC
GCCCCCCTTCTTTTGGGTCATTTCTGCAAACGGAAAACTCTGTAGCGTTTGGCAAAGTTGGTGCCTGCGCGCCCCTTCCAGGTTT
CGCTTTGACTGTTTTGTTTTTGGCGGAACTACCAGGCAGGAAGATTGCACAAGTAAGGGGCGTTTTCAGTCGGGTGTCAATTTCTC
TTTCTTTCTTTCTTTTTTTAAAATTTCGGTTCGTGTCTGCTTCTCCAAGCTTTAT

P2

B

	Target site	PAM		score	sequence	
guide sequence:	ACGCTGACCCGGGAACGTAG	TGG	Guide #1	95	ACGCTGACCCGGGAACGTAG	TGG
on-target locus:	chr6:+144606123		Guide #4	93	GATCAGCCCCACTACGTTCC	CGG
number of offtarget sites: 27 (4 are in genes)			Guide #5	91	CGGCCACCGCGTCGGGAACT	TGG

C

cloning of sgRNA into the Px261 plasmid sequencing results.

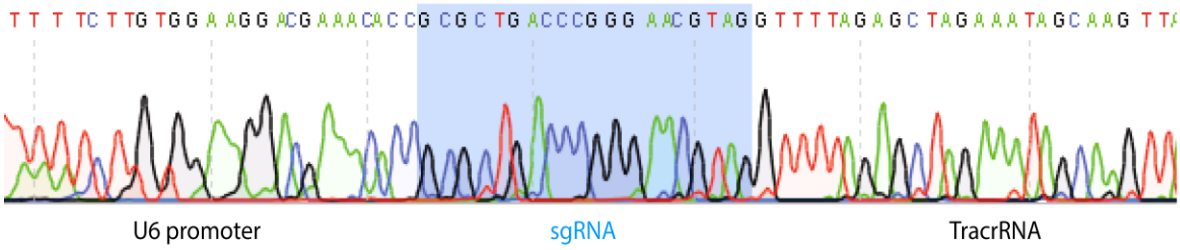

Figure 13 CRISPR/Cas9 mediated genome editing of human utrophin A promoter region

(A) 2.3Kb human utrophin A promoter fragment is amplified using p1 and p2 primers. The CRISPR-Cas9 target sequence is located at position 1.7Kb from primer p1 side and 0.7Kb from primer p2. **(B)** sgRNA oligonucleotides were cloned into the bicistronic expression vector (PX261) from Addgene. **(C)** T7E1 assays for Cas9-mediated indels at the human utrophin A promoter locus. Red arrowheads indicate the expected T7E1 fragments. **(D)** Deletions were confirmed by sequencing the PCR products spanning the expected cleavage sites. Electropherograms around the target sequences of wild-type and mutant utrophin A promoter region indicate that each DSB occurs exactly 3 bp upstream of the PAM sequence. Red triangles indicate deleted nucleotide(s). **(E)** Multiple sequence alignment analysis around the targeted DNA sequences of the wild type utrophin and 4 mutants indicates that CRISPR-Cas9 can target and cleave the human utrophin A promoter.

Figure 13

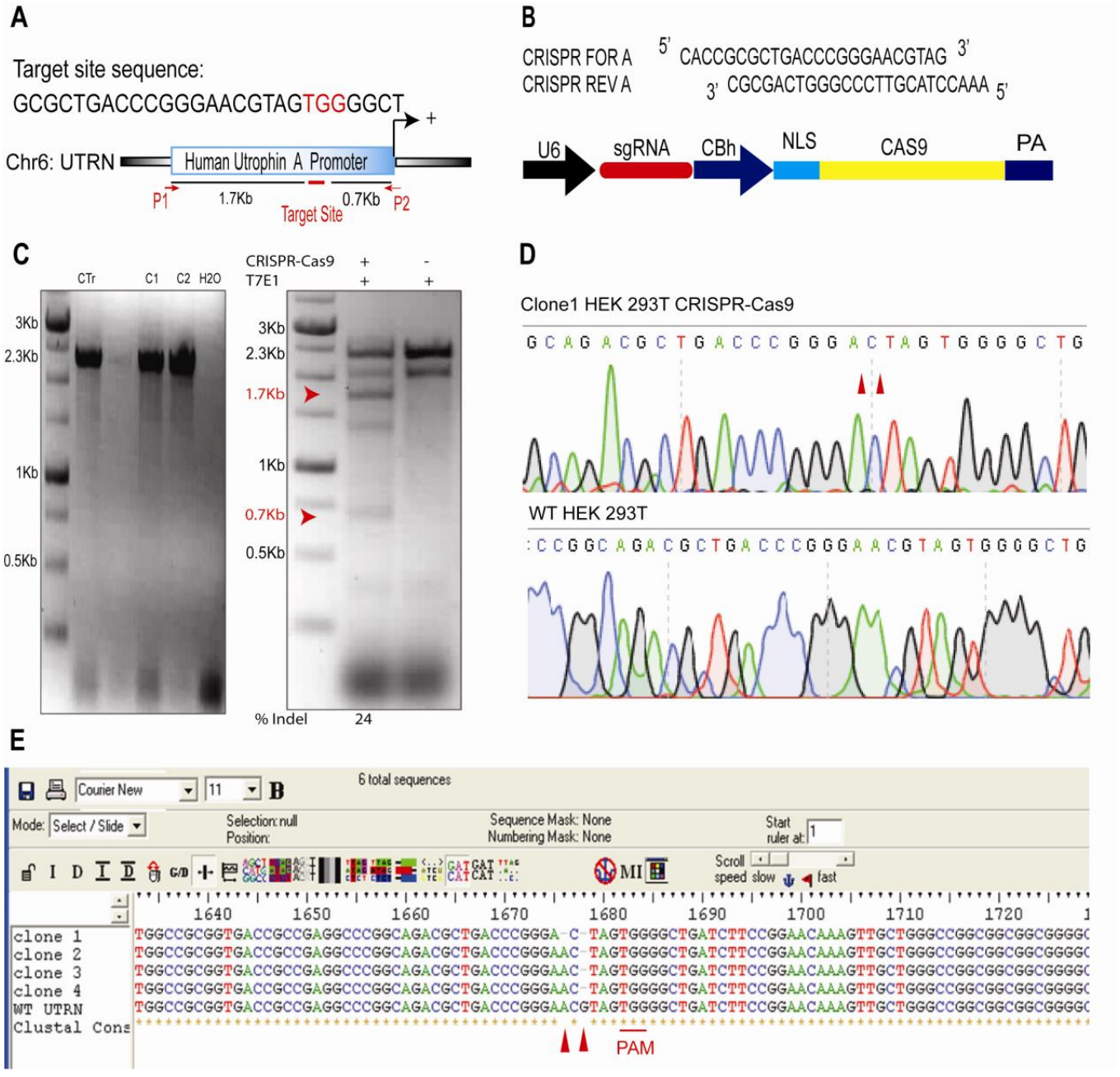
A
Target site sequence:
GCGCTGACCCGGGAACGTAGTGGGGCT
Chr6: UTRN
Human Utrophin A Promoter
P1
1.7Kb
0.7Kb
P2
Target Site
B
CRISPR FOR A 5' CACCGCGCTGACCCGGGAACGTAG 3'
CRISPR REV A 3' CGCGACTGGGCCCTTGCATCCAAA 5'
U6
sgRNA
CBh
NLS
CAS9
PA
C
CTr
C1
C2
H2O
CRISPR-Cas9
T7E1
3Kb
2.3Kb
1.7Kb
1Kb
0.7Kb
0.5Kb
% Indel
24
D
Clone1 HEK 293T CRISPR-Cas9
WT HEK 293T
E
6 total sequences
Courier New
Mode: Select / Slide
Selection: null
Position:
Sequence Mask: None
Numbering Mask: None
Start ruler at: 1
Scroll speed slow fast
1640
1650
1660
1670
1680
1690
1700
1710
1720
clone 1
clone 2
clone 3
clone 4
WT UTRN
Clustal Cons
PAM

Figure 14 Detection of CRISPR/Cas9-induced homologous recombination in HEK 293 T cells.

(A) Schematic representation of the predicted human utrophin A promoter region after insertion of the CAG promoter. Primer F1 covers the CAG part of the Donor plasmid, while F2 covers the genomic utrophin region of HEK 293T host cell. Single clone candidates for potential targeted integration of UTR-CAG-UTR donor plasmid are screened first by PCR. Gel electrophoretic pattern is shown of the PCR products corresponding to the junction region between the CAG promoter arm and the HEK 293T host genome. Lanes 1–7: PCR products derived from the genomic DNA of selected HEK 293T cells co-transfected with CRISPR-cas9 and the Donor plasmid. The clones A2-A5-B2 and B6 are positive clones as shown on the agarose gel. **(B)** Multiple sequence alignment between the clone A2 and the Donor plasmid shows that HDR occurred, and the CAG promoter is knocked in exactly at the expected position.

Figure 14

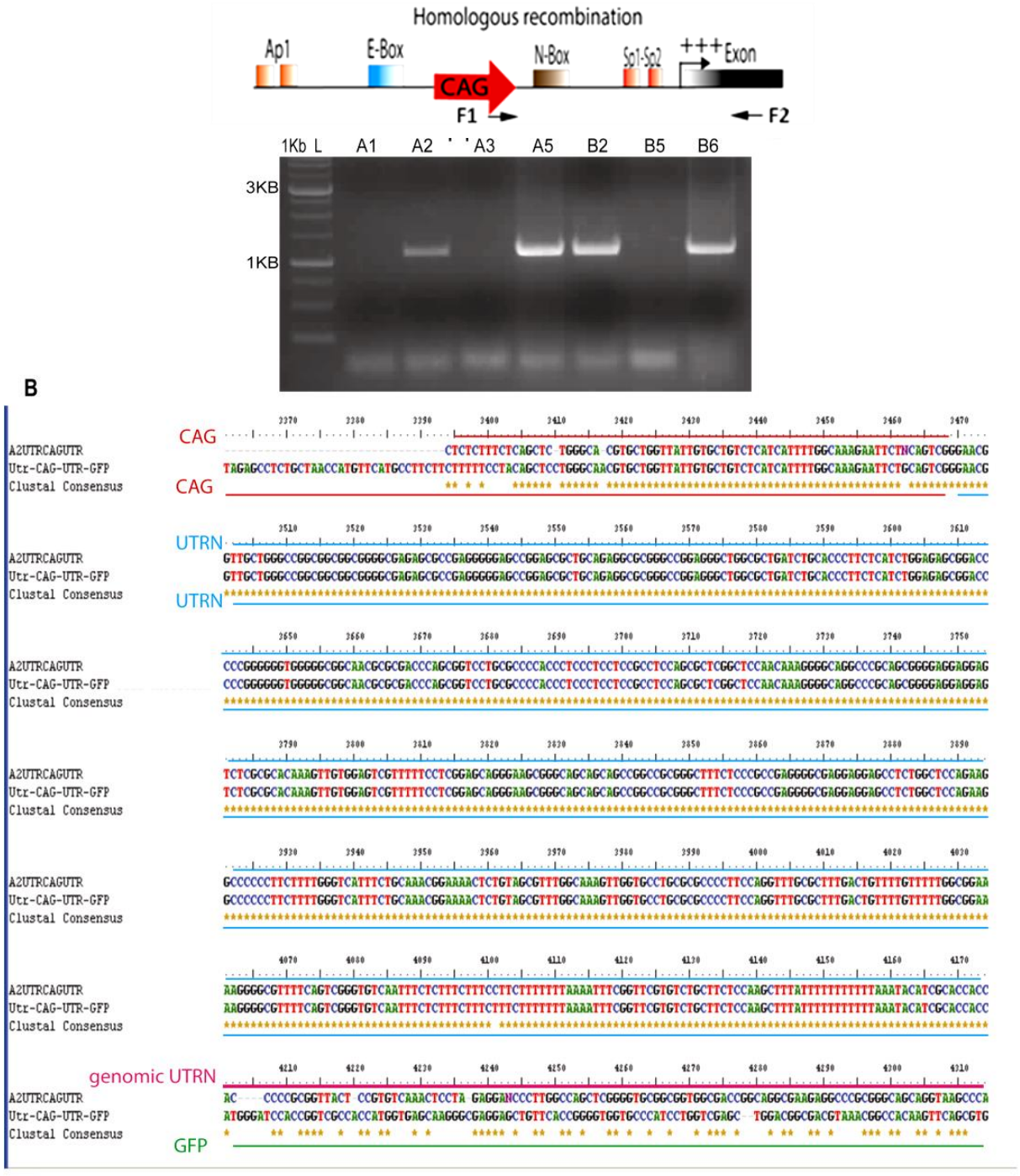
Homologous recombination
Ap1
E-Box
CAG
N-Box
Sp1-Sp2
+++Exon
F1
F2
1Kb L
A1
A2
A3
A5
B2
B5
B6
3KB
1KB
B
CAG
A2UTRCAGUTR
Utr-CAG-UTR-GFP
Clustal Consensus
UTRN
genomic UTRN
GFP

Figure 15 Integration of CAG promoter into the endogenous human utrophin A promoter

(A) The analysis by real-time PCR of the utrophin gene mRNA expression from selected clones of HEK 293T cells treated with CRISPR-Cas9 + Donor plasmid and non-treated control cells (Ctr-). The gene expression ratio between utrophin and GAPDH is shown as the mean ± SEM from three independent experiments performed in triplicate. *$P < 0.05$ and **$P < 0.01$ and ***$P<0.001$ indicate statistical significance by t-test.

(B) Western blot analysis of utrophin protein levels in HEK 293T cells treated with (CRISPR-Cas9 + Donor plasmid) and untreated control cells (Ctr-). Vinculin detection was used to normalize the amount of loaded protein.

Figure 15

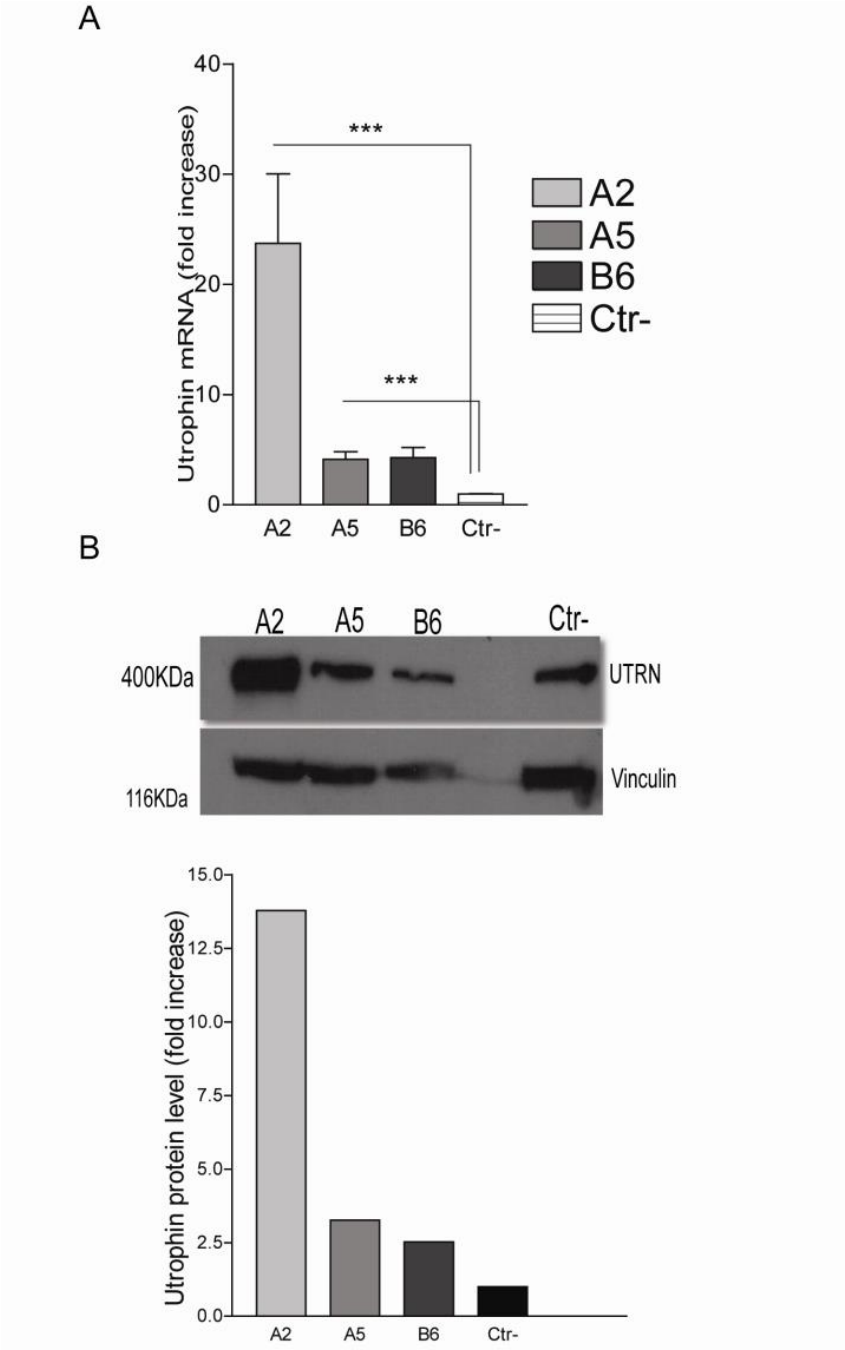
A
40
30
20
10
0
Utrophin mRNA (fold increase)
***
***
A2
A5
B6
Ctr-
A2
A5
B6
Ctr-
B
A2
A5
B6
Ctr-
400KDa
UTRN
116KDa
Vinculin
15.0
12.5
10.0
7.5
5.0
2.5
0.0
Utrophin protein level (fold increase)
A2
A5
B6
Ctr-

Figure 16 Analysis of the top 4 off-target hits predicted to be located in genes

(A) Identification of the sequence, score, position and primers used to amplify the 4 off-target loci.

(B) Sequencing of the off-target regions shows no modification in these genes.

Figure 16

A

sequence	score	mismatches	UCSC gene	locus	Primers	
ACGCTGACCAGGGAACCTGCCGG	0.1	4MMs [10:17:19:20]	NM_001008211	chr10:-13142194	For off target1 Rev off target1	CAGGGAGCGGCTGGCTGT CTCTCCCACCAGGTCAGGACCC
ACGCTCAGGCGGAAACGTAGCAG	0.2	4MMs [6:8:9:13]	NM_173483	chr19:-15662158	For off target2 Rev off target2	TAACCCTCACCCAGCGTGG GCGGTGCCTGGTCATCCA
ACGCTGGCCCGGGACCCGAGGGG	0.0	4MMs [7:15:17:18]	NM_006332	chr19:+18284519	For off target3 Rev off target3	CCTGGGCAGGGCTGATTG CCTGTCGCCGTCCCTACCTT
ACCCTGACCCGGGCACTGAGGGG	0.0	4MMs [3:14:17:18]	NM_020818	chr14:+94088868	For Off target4 Rev off target 4	CTCTTCTCCCTCCGTCCCCA CGGATTCCTCAGCTCCATCC

B

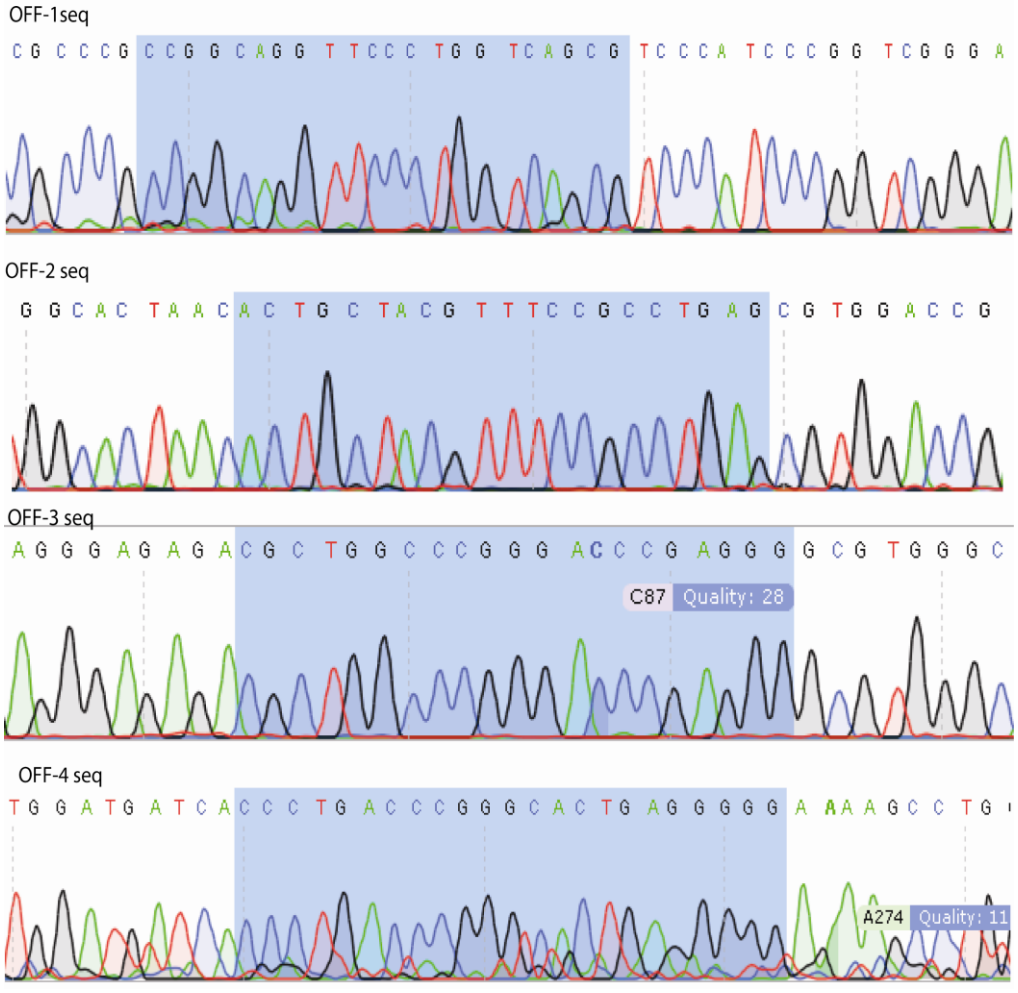

Chapter 6 Discussion

Zinc Finger Proteins to mediate human utrophin up-regulation

Zinc Finger Proteins: engineered DNA-recognition domains

Utrophin gene, located at the autosomal chromosome number 6, encodes a protein displaying a high degree of sequence similarity to dystrophin [186]. Unlike dystrophin which is expressed only in muscle and brain in adult, utrophin is widely expressed during development, but becomes restricted to the neuromuscular junction (NMJ) and myotendinous junction in normal adult; however, in dystrophin-deficient muscle, utrophin is also localised at the sarcolemma compensating the lack of dystrophin [277]. In fact, the therapeutic effect of up-regulating extra-synaptic utrophin was tested by Tinsley et *al* in 1996 [199], and revealed that mini-utrophin over-expression in transgenic *mdx* mice is sufficient to rescue the dystrophic *mdx* phenotype. The human utrophin A promoter has several DNase I accessible sites including one region within 400bp of the transcription start site [234], suggesting that these regions might provide good targets for ZFPs. The ZFP "Jazz" was the first designed artificial transcription factor able to bind and activate the transcription of utrophin A promoter [278, 279]; "Jazz" was synthesised using the list of the recognition code selected by Choo and Klug [280, 281]. In previous work our lab has designed a panel of ZFPs based on the recognition modules described by Liu *et al* [282]. The produced ZFPs were able to target and up-regulate murine utrophin gene expression [234]. Our goal for this study was to identify a panel of ZFPs that could activate transcription of the endogenous human utrophin gene. In fact, we have successfully engineered a new panel of ZFPs based on the knowledge of utrophin A promoter's structure and based on the software provided

by the zinc finger consortium [283]. We first used our previous results of DNase I hypersensitivity mapping analysis to identify accessible regions of the utrophin A promoter [234, 267]. Then, using the zinc finger consortium software we designed a panel of ZFPs that are predicted to target and bind human utrophin A promoter. The Figure 3C shows an example of the predicted 9-bp sequences targeted by an artificial ZFP; for example, the predicted sequence **GAG-GGG-GAG** is targeted by coupling the predicted three zinc fingers F1-F2-F3. The F1 finger is represented by four possible fingers (ZF113), (ZF115), (ZF135) and (ZF136) that are predicted to target the triplet GAG. The zinc finger F1 (ZF115) has seven amino acids that constitute the recognition helix positions −1 to +6 relative to the start of the α-helix that contacts DNA in the finger, which is composed of the following amino acids **QSFNLRR**. Then, the finger F2 (ZF134) that targets the sequence GGG and its helix is composed of **RRSHLTR** amino acids. Finally, the F3 (ZF135) that targets also the sequence GAG, but has the **RHSNLIR** amino acids on the F3 helix. Sanger sequencing results shown in Figure 5C confirm that the alpha helix of the predicted zinc fingers match the produced one.

Trans-activation of the human utrophin A promoter

Zinc finger-based transcription factors consist of a transcriptional effector domain fused to the engineered zinc finger DNA binding domain. Depending on the effector domain, ZFPs can up- or down regulate gene expression and thus represent powerful tools in gene expression modification and allow novel approaches in clinical practice. ZFP targeting strategies combined with analysis of chromatin structure present an efficient tool for identifying artificial transcription factors and specifically regulating endogenous genes [284]. In this study, zinc finger-based transcription factors are designed using the modular assembly method, which

assumes that a single domain (module) can recognize a specific DNA triplet regardless of the position of the triplet within the target site or the identities of adjacent neighboring fingers [228]. The designed modules are simply joined together to make a ZFP that should bind the target sequence. Although modular assembly is relatively simple to accomplish, ZFPs generated using this method have been shown to have a high failure rate *in vivo* [285, 286]. In order to target and activate utrophin A promoter, the VP16 domain of the herpes simplex virus is fused to the zinc finger DNA binding domain, which will activate gene expression by facilitating the assembly of a RNA polymerase II pre-initiation complex and interact with chromatin-remodeling enzymes [287]. First, the artificial zinc finger proteins were screened on an episomal utrophin promoter reporter construct (Figure 6A). The analysis of the beta galactosidase activity revealed that the increase of its activity was dependent on the presence of certain ZFPs. The differences in beta galactosidase activity reflect the activation potential of each tested ZFP. Moreover, the specific activity of each ZFP was deduced by normalizing the beta galactosidase activity against the level of VP16 expression. The activity of each ZFP depends on the target site sequence accessibility and its α-helix composition. The preliminary screening of several ZFP constructs led to the characterisation of potential ZFPs that are able to induce beta galactosidase up-regulation. The targeted region **GAG-GGG-GAG** near the target sequence of Sp1, which is a natural zinc finger binding site, has more activation potential than the other targeted regions of human utrophin A, and overlaps with the murine region targeted in previous work with the ZFP51 (Figure 3A) [234].

The up-regulation of the endogenous utrophin gene

Although beta galactosidase results have shown a potential activity of certain ZFPs as transcription factors on the episomal reporter construct, the selected cells expressing the most potent ZFPs have shown only a 1.3 fold increase in the endogenous utrophin mRNA levels (Figure 7B). Similar results have been observed at other loci [284], which might highlight the effect of the micro-environment composition around the target sequence. It is known that chromatin structure can be influenced in a variety of ways, mainly DNA methylation, which occurs on cytosine residues primarily in the context of a CpG site, can prevent the binding of trans factors [288]. Because the human utrophin A promoter is highly rich with CpG islands and has several DNA methylation spots, the endogenous chromatin environment could be made unavailable via DNA methylation, or other epigenetic factors such as H3K27-3Me (three methylations), which might explain the moderate increase of utrophin mRNA expression. According to the literature, it is known that for some transcription factors (such as E2F, CREB and USF) methylation at specific CpGs will inhibit protein binding and then inhibit transcription [289]. It has been shown that zinc finger protein Sp1 binding is inhibited by ^{m}Cp^{m}CpG methylation [290]. Moreover, artificial transcription factors can synergize with chromatin remodeling drugs to reactivate gene expression [291]. To further improve the regulatory effects of ZFP, we considered epigenetic factors such as DNA methylation. Therefore, we treated the stably selected ZF51-IRES-GFP-293T HEK cells for 5 days with 40 uM of azacytidine, which is a chemical analogue of the cytosine nucleoside; azacytidine incorporation into DNA leads to a covalent binding with DNA methyl-transferases; as a result, the utrophin promoter will presumably be less methylated, then the ZFP may have better binding to the DNA and induce the

endogenous utrophin A promoter activation. Figure 7C shows that treatment of the HEK 293T cells harboring the best predicted ZFP (ZF51) with azacytidine leads to a slight increase in endogenous utrophin mRNA expression. Thus, targeting endogenous utrophin promoter with ZFPs cannot be sufficiently upregulated to overcome lack of dystrophin as shown in similar studies. For example, a 6 zinc finger protein was engineered and coupled with the transcriptional activation domain derived from the multivalent adaptor protein Che-1/AATF. Expression of the 6 zinc finger protein in mammalian cells promoted only 1.9 fold increase of endogenous utrophin transcription [292]. Moreover, a new study tried the same principle of utrophin A promoter upregulation using the death CRISPR/Cas9 system fused to multiple copies of VP16 activator (dCas9-VP160); treatment of dystrophin-deficient myoblasts with the dCas9-VP160 led also to an increase of endogenous utrophin expression varying from 1.7- to 2.7, especially when targeting the utrophin A promoter [293]. According to above data, utrophin promoter A is tightly repressed and despite the increase of zinc finger protein number or modification of the activator domain substantial upregulation of the endogenous utrophin could not be achieved. Therefore, we pursued other means to upregulate utrophin transcription.

Zinc Finger Nuclease mediates utrophin A cleavage

Engineering of ZFN targeting utrophin A promoter

All through the ZFP section, we have shown that zinc finger proteins can be reprogrammed to target any DNA sequence; therefore, a fusion protein comprising such a programmable DNA-binding domain coupled to a non-specific nuclease could be used as a genome editing tool. In fact, Zinc Finger Nuclease (ZFNs) combine both properties: 1) the DNA binding specificity and flexibility of ZFPs and 2) a cleavage activity of the modified FokI domains that function as

obligate homodimers [242]. Recently, ZFNs have been used in gene editing of specific targets for either gene knockout or gene integration [243]. Applications of gene editing using ZFNs can be useful in several fields including biotechnology (cellular and animal engineering), agriculture (crops and animals improvement) [244, 245], and medicine (gene therapy) [246, 247]. We therefore sought to investigate whether a ZFN genome editing tool combined with a donor vector carrying a strong promoter flanked in between the utrophin A promoter sequences could induce gene targeting *in vitro*. Indeed, a recent study has shown the efficacy of ZFN correcting haemophilia B in mouse, resulting in measurable circulating levels of factor IX; this therapeutic strategy was sufficient to restore haemostasis in the mouse [294]. We hypothesized that the insertion of a strong promoter such as the cytomegalovirus enhancer chicken beta-actin (CAG) via HDR mechanism precisely at the upstream region of the utrophin gene, might lead to the permanent up-regulation of the endogenous utrophin gene. First we generated a pair of ZFN targeting the human utrophin A promoter according to the Zinc Finger Nuclease consortium (Figure 8). The 2.3Kb utrophin A promoter has the majority of the regulatory elements including the N-box and Sp1-Sp3 sites and the +1 transcription initiation site (+1); the targeted sequence CAC-TCC-CTC is located upstream the (+1) site implying that when the HDR is occurring the CAG insertion will be positioned specifically before the (+1) transcription initiation site, thus guarantying the upregulation of endogenous utrophin. The predicted ZFNs were then cloned into the psyc-97 plasmid [295], which has the self-cleaving 2A peptide. The psyc-97-ZFNs will generate a bicistronic construct encoding both ZFNs under the control of the CMV promoter (Figure 9A, B).

Effect of ZFN on utrophin A promoter

The T7E1 assay showed that the ZFN pair is highly active, driving small insertions and/or deletions (indels), characteristic of DSB repair by NHEJ, and results in up to 25% cleavage at the targeted sequence as shown in Figure 9C. Unlike control treated cells, the denatured and reannealed PCR products amplified from genomic DNA of cells expressing the ZFN show extra bands once treated with the T7E1 endonuclease confirming indel mutations at the targeted sequence. Since the ZFN strategy has shown some difficulty in the design, and the characterization of the ZFN treated cells, we tried in parallel a new system of genome editing based on RNA-DNA recognition that is easier to manipulate.

CRISPR/Cas9 system mediated HDR in HEK 293T cells

The CRISPR/cas9 tool, which is a genome editing nuclease guided by a single guided RNA (sgRNA) has shown a significant potential in curing monogenic diseases [296]. CRISPR-Cas9 system has shown the ability of correcting genomic mutations in *mdx* mouse model, which opens up new frontiers in treating DMD [168]. Recently, several groups have tried to edit the dystrophin gene using the CRISP/Cas9 technology. Long *et al* used CRISPR/Cas9-mediated genome editing to correct the dystrophin gene mutation in the germ line of *mdx* mice, and then monitored muscle structure and function [168].Moreover, Ousterout *et al* designed multiplexed sgRNAs to restore the dystrophin reading frame by targeting the mutational hotspot at exons 45–55, which can correct up to 62% of DMD mutations [169]. Similarly, another group has demonstrated the feasibility of using a single CRISPR pair to correct the reading frame for the majority of DMD patients [297]. However, immunological response against dystrophin, and the wide range of mutations in dystrophin gene are some of the limitations for dystrophin repair.

Since one of the most promising approaches for DMD therapy is based on increasing the levels of the utrophin gene, we pursued CRISPR-Cas9 technology to insert precisely a strong promoter into utrophin A promoter resulting in permanent up-regulation of endogenous utrophin. Thus, we present a universal approach for inserting a strong promoter such as Cytomegalovirus Enhancer/Chicken β-Actin (CAG) promoter upstream the +1 transcription initiation site of human utrophin A promoter using CRISPR-Cas9 system and a dsDNA donor template, which contains the CAG promoter, flanked between homologous utrophin A promoter sequences; as a result, we were able through homologous direct repair mechanism to significantly increase the endogenous utrophin expression in HEK 293T cells.

Engineering of CRISPR/Cas9 system targeting utrophin A promoter

The CRISPR/Cas9 system induces DSBs, which can be repaired by one of the two different pathways either NHEJ or HDR. According to Figure 10, the sgRNA recognizes the genomic utrophin A promoter region and will guide the nuclease Cas9, which in turn will make DSB on the target genomic DNA. The DSB will trigger the DNA repair mechanism such as NHEJ or HDR. During the NHEJ repair pathway, the DSB is repaired by random indel mutations at the site of the junction. Unlike NHEJ, the HDR pathway can introduce precise point mutations or insertions in the presence of a repair template in the form of a donor plasmid, which allows high fidelity and precise editing.

Promoter selection for homology direct repair

Many constitutive promoters have been found to be very active in muscle cells including (Rous sarcoma virus (RSV) and the cytomegalovirus enhancer (CMV) [298]. However, both promoter activities decreased in muscle of young adult and old mice after sixty days post injection [299].

The muscle specific creatine kinase (MCK) promoter has been also used to over-express dystrophin in DMD gene therapy [300]; however, the activity of MCK promoter was measured using only histological observation. Recently, a study has examined six constitutive promoters commonly used in mammalian systems, including the simian virus 40 early promoter (SV40), cytomegalovirus immediate-early promoter (CMV), human Ubiquitin C promoter (UBC), human elongation factor 1α promoter (EF1A), mouse phosphoglycerate kinase 1 promoter (PGK), and chicken β-Actin promoter coupled with CMV early enhancer (CAG) in different cell types including mouse myoblasts (C2C12). The results showed that CAG promoter is a consistently strong promoter in all the cell types [301]. In order to confirm that insertion of a strong promoter such as CAG will lead to the up-regulation of the downstream gene, we cloned the CAG promoter in the utrophin A promoter region linked to a luciferase reporter gene. The insertion of the CAG promoter at the utrophin A region led to very high up-regulation of mRNA expression and activity of luciferase as shown in Figure 11.

CRISPR/Cas9 mediates utrophin DNA Double Stranded Break

The first step for performing targeted genome editing is the induction of a DNA double-stranded break at the genomic locus [302]. For this purpose, we engineered CRISPR Cas9+sgRNA expression plasmids, and tested their ability of cleaving the human utrophin A promoter DNA (Figure 12). The analysis of the T7E1 assay showed the presence of an extra band of 700bp indicating mismatches at this region. It is known that the *s.pyogenes* Cas9 (SpCas9) makes a blunt cut between the 17th and 18th bases in the target sequence (3 bp 5′ of the PAM) [303, 304]. In fact, Sanger sequencing showed that CRISPR/Cas9 system can induce DNA double-strand breaks in the human utrophin A promoter genomic locus as confirmed by the deletion of one or

two bp near the 5′ of the PAM sequence (Figure 12). On the figure 13D most sequenssed clones have shown a deletion of one bp except clone 2 which has a deletion of 3 base pair and insertion of one base pair.

CRISPR/Cas9 induces CAG insertion into endogenous utrophin A promoter

The introduction of targeted genomic sequence changes into living cells has become a powerful tool for therapy of genetic diseases. In the present study, we have designed a donor plasmid, which has the CMV early enhancer/chicken beta actin (CAG) promoter flanked by the human utrophin A promoter sequences. The co-transfection of the donor plasmid and the CRISRP/Cas9 plasmid in HEK 293T cells will trigger the HDR mechanism, which will lead to the insertion of CAG promoter at the endogenous utrophin A promoter. In fact, the PCR screening of co-transfected HEK 293T cells shows that CRISPR/Cas9 allows the selection of 4 positive clones out of 7, which means about 57% efficient endogenous knock-in of the (CAG) promoter into utrophin A promoter region after selection (Figure 14). Moreover, the insertion of CAG promoter leads to a permanent increase of utrophin expression, which might reach up to 25 fold increase in the clone A2 (Figure 15). The endogenous utrophin expression in clone A2 is 5 time higher than the clones A5 and B6; this differnce in fold increase could be explained by the fact that the clone A2 has insertion of the CAG promoter in utrophin A promoter at both chromosoms; in contrast, clones A5 and B6 might have insertion of the CAG promoter only in one chromosome.

Off-target cleavage

Off-target cleavage is a serious concern for CRISPR/Cas9-mediated genome engineering [305]. Once we showed that CRISPR/Cas9 system can target and cleave the human utrophin A

promoter sequence, we next studied the Cas9 off-target activities. To potentially identify mutations induced at off-target sites, we performed *in silico* analysis using the CRISPR design tools, which predict and score off-targets for the CRISPR/Cas9 system. Figure 16 shows the four predicted off-targets with at least 4 mismatches in comparison to the original target sites. PCR amplification of the predicted off-target sites followed by Sanger sequencing has shown no indel mutations on the off-target sites (Figure 16). The above results illustrated the effectiveness of CRISPR/Cas9 system in modifying and up-regulating the endogenous utrophin gene with high efficiency and specificity. Since there is no homology between the donor plasmid and the other 23 off target sites, they will be repaired only with the NHEJ mechanism, and their repair won't affect cell activity since they are located in non-coding regions.

Conclusion and Future directions

Human Induced Pluripotents Stem (IPS) cells approach

In conclusion, these results show proof-of-principle for the development of genome editing tool able to increase levels of endogenous utrophin for the therapy of DMD. In this regard, modification of human utrophin A promoter using CRISPR/Cas9 system in induced pluripotent stem cells (IPS) might help in increasing utrophin expression in DMD patients after cell transplant. Because of the heterogeneity in the dystrophin mutations, correction of dystrophin in DMD IPS cells using CRISPR/cas9 system might not be applicable to all DMD patients [170]. However, the modification of utrophin A promoter in DMD IPS cells can target all patients regardless of the type of dystrophin mutation. In summary, the up-regulation of the utrophin protein in patient-derived IPS cells using CRISPR/Cas9 system might be effective and might have minimal effects on off-target mutagenesis. Our efficient and precise utrophin up-regulation

method using CRISPR technologies should provide a framework for future *ex vivo* gene therapy using patient-specific human IPS cells.

References

1. McNally, E.M. and P. Pytel, *Muscle diseases: The muscular dystrophies.* Annual Review of Pathology-Mechanisms of Disease, 2007. **2**: p. 87-109.
2. Tyler, K.L., *Origins and early descriptions of "Duchenne muscular dystrophy".* Muscle & Nerve, 2003. **28**(4): p. 402-422.
3. Mendell, J.R., et al., *Evidence-Based Path to Newborn Screening for Duchenne Muscular Dystrophy.* Annals of Neurology, 2012. **71**(3): p. 304-313.
4. Emery, A.E., *Duchenne muscular dystrophy--Meryon's disease.* Neuromuscul Disord, 1993. **3**(4): p. 263-6.
5. Becker, P.E. and F. Kiener, *[A new x-chromosomal muscular dystrophy].* Arch Psychiatr Nervenkr Z Gesamte Neurol Psychiatr, 1955. **193**(4): p. 427-48.
6. Koenig, M., et al., *The molecular basis for Duchenne versus Becker muscular dystrophy: correlation of severity with type of deletion.* Am J Hum Genet, 1989. **45**(4): p. 498-506.
7. Wein, N., L. Alfano, and K.M. Flanigan, *Genetics and Emerging Treatments for Duchenne and Becker Muscular Dystrophy.* Pediatric Clinics of North America, 2015. **62**(3): p. 723-+.
8. Yahyaoui, M., et al., *[Polyradiculoneuritis. Analysis of a homogeneous series of 33 cases].* Maroc Med, 1981. **3**(1): p. 555-61.
9. Emanuel, B.S., E.H. Zackai, and S.H. Tucker, *Further evidence for Xp21 location of Duchenne muscular dystrophy (DMD) locus: X;9 translocation in a female with DMD.* J Med Genet, 1983. **20**(6): p. 461-3.
10. Demartinville, B., et al., *Localization of DNA-Sequences in Region Xp21 of the Human X-Chromosome - Search for Molecular Markers Close to the Duchenne Muscular-Dystrophy Locus.* American Journal of Human Genetics, 1985. **37**(2): p. 235-249.
11. Sarfarazi, M., et al., *Genetic linkage relationship between the Xg blood group system and two X chromosome DNA polymorphisms in families with Duchenne and Becker muscular dystrophy.* Hum Genet, 1983. **65**(2): p. 169-71.
12. Monaco, A.P., et al., *Isolation of candidate cDNAs for portions of the Duchenne muscular dystrophy gene.* Nature, 1986. **323**(6089): p. 646-50.
13. Koenig, M., et al., *Complete cloning of the Duchenne muscular dystrophy (DMD) cDNA and preliminary genomic organization of the DMD gene in normal and affected individuals.* Cell, 1987. **50**(3): p. 509-17.
14. Boyce, F.M., et al., *Dystrophin is transcribed in brain from a distant upstream promoter.* Proc Natl Acad Sci U S A, 1991. **88**(4): p. 1276-80.
15. Dsouza, V.N., et al., *A Novel Dystrophin Isoform Is Required for Normal Retinal Electrophysiology.* Human Molecular Genetics, 1995. **4**(5): p. 837-842.
16. Lidov, H.G.W., S. Selig, and L.M. Kunkel, *Dp140 - a Novel 140-Kda Cns Transcript from the Dystrophin Locus.* Human Molecular Genetics, 1995. **4**(3): p. 329-335.
17. Byers, T.J., H.G.W. Lidov, and L.M. Kunkel, *An Alternative Dystrophin Transcript Specific to Peripheral-Nerve.* Nature Genetics, 1993. **4**(1): p. 77-81.
18. Lederfein, D., et al., *A 71-Kilodalton Protein Is a Major Product of the Duchenne Muscular-Dystrophy Gene in Brain and Other Nonmuscle Tissues.* Proceedings of the

National Academy of Sciences of the United States of America, 1992. **89**(12): p. 5346-5350.
19. Feener, C.A., M. Koenig, and L.M. Kunkel, *Alternative Splicing of Human Dystrophin Messenger-Rna Generates Isoforms at the Carboxy Terminus.* Nature, 1989. **338**(6215): p. 509-511.
20. Surono, A., et al., *Six novel transcripts that remove a huge intron ranging from 250 to 800 kb are produced by alternative splicing of the 5' region of the dystrophin gene in human skeletal muscle.* Biochemical and Biophysical Research Communications, 1997. **239**(3): p. 895-899.
21. Moser, H., *Duchenne muscular dystrophy: pathogenetic aspects and genetic prevention.* Hum Genet, 1984. **66**(1): p. 17-40.
22. Koenig, M., et al., *The molecular basis for Duchenne versus Becker muscular dystrophy: correlation of severity with type of deletion.* Am J Hum Genet, 1989. **45**(4): p. 498-506.
23. Lenk, U., et al., *Point Mutations at the Carboxy-Terminus of the Human Dystrophin Gene - Implications for an Association with Mental-Retardation in Dmd Patients.* Human Molecular Genetics, 1993. **2**(11): p. 1877-1881.
24. Monaco, A.P., et al., *An explanation for the phenotypic differences between patients bearing partial deletions of the DMD locus.* Genomics, 1988. **2**(1): p. 90-5.
25. Ervasti, J.M., et al., *Deficiency of a glycoprotein component of the dystrophin complex in dystrophic muscle.* Nature, 1990. **345**(6273): p. 315-9.
26. Gumerson, J.D. and D.E. Michele, *The Dystrophin-Glycoprotein Complex in the Prevention of Muscle Damage.* Journal of Biomedicine and Biotechnology, 2011.
27. Watkins, S.C., et al., *Immunoelectron microscopic localization of dystrophin in myofibres.* Nature, 1988. **333**(6176): p. 863-6.
28. Koenig, M., A.P. Monaco, and L.M. Kunkel, *The complete sequence of dystrophin predicts a rod-shaped cytoskeletal protein.* Cell, 1988. **53**(2): p. 219-28.
29. O'Brien, K.F. and L.M. Kunkel, *Dystrophin and muscular dystrophy: past, present, and future.* Mol Genet Metab, 2001. **74**(1-2): p. 75-88.
30. Koenig, M. and L.M. Kunkel, *Detailed analysis of the repeat domain of dystrophin reveals four potential hinge segments that may confer flexibility.* J Biol Chem, 1990. **265**(8): p. 4560-6.
31. Macias, M.J., et al., *Structure of the WW domain of a kinase-associated protein complexed with a proline-rich peptide.* Nature, 1996. **382**(6592): p. 646-9.
32. Rentschler, S., et al., *The WW domain of dystrophin requires EF-hands region to interact with beta-dystroglycan.* Biol Chem, 1999. **380**(4): p. 431-42.
33. Anderson, J.T., R.P. Rogers, and H.W. Jarrett, *Ca2+-calmodulin binds to the carboxyl-terminal domain of dystrophin.* J Biol Chem, 1996. **271**(12): p. 6605-10.
34. Blake, D.J., et al., *Coiled-coil regions in the carboxy-terminal domains of dystrophin and related proteins: potentials for protein-protein interactions.* Trends Biochem Sci, 1995. **20**(4): p. 133-5.
35. Blake, D.J., et al., *Coiled-Coil Regions in the Carboxy-Terminal Domains of Dystrophin and Related Proteins - Potentials for Protein-Protein Interactions.* Trends in Biochemical Sciences, 1995. **20**(4): p. 133-135.

36. Pasternak, C., S. Wong, and E.L. Elson, *The Mechanical Function of Dystrophin in Muscle-Cells.* Molecular Biology of the Cell, 1992. **3**: p. A192-A192.
37. Campbell, K.P. and S.D. Kahl, *Association of dystrophin and an integral membrane glycoprotein.* Nature, 1989. **338**(6212): p. 259-62.
38. Yoshida, M., et al., *Dissociation of the complex of dystrophin and its associated proteins into several unique groups by n-octyl beta-D-glucoside.* Eur J Biochem, 1994. **222**(3): p. 1055-61.
39. Ishikawa-Sakurai, M., et al., *ZZ domain is essentially required for the physiological binding of dystrophin and utrophin to beta-dystroglycan.* Human Molecular Genetics, 2004. **13**(7): p. 693-702.
40. Jung, D., et al., *Identification and Characterization of the Dystrophin Anchoring Site on Beta-Dystroglycan.* Journal of Biological Chemistry, 1995. **270**(45): p. 27305-27310.
41. Brenman, J.E., et al., *Interaction of nitric oxide synthase with the postsynaptic density protein PSD-95 and alpha1-syntrophin mediated by PDZ domains.* Cell, 1996. **84**(5): p. 757-67.
42. Guiraud, S., et al., *Advances in genetic therapeutic strategies for Duchenne muscular dystrophy.* Experimental Physiology, 2015. **100**(12): p. 1458-1467.
43. Banks, G.B. and J.S. Chamberlain, *The value of mammalian models for duchenne muscular dystrophy in developing therapeutic strategies.* Curr Top Dev Biol, 2008. **84**: p. 431-53.
44. Bulfield, G., et al., *X chromosome-linked muscular dystrophy (mdx) in the mouse.* Proc Natl Acad Sci U S A, 1984. **81**(4): p. 1189-92.
45. Sicinski, P., et al., *The Molecular-Basis of Muscular-Dystrophy in the Mdx Mouse - a Point Mutation.* Science, 1989. **244**(4912): p. 1578-1580.
46. Lynch, G.S., et al., *Force and power output of fast and slow skeletal muscles from mdx mice 6-28 months old.* J Physiol, 2001. **535**(Pt 2): p. 591-600.
47. Rafael, J.A., et al., *Testing of SHIRPA, a mouse phenotypic assessment protocol, on Dmd(mdx) and Dmd(mdx3cv) dystrophin-deficient mice.* Mamm Genome, 2000. **11**(9): p. 725-8.
48. Tanabe, Y., K. Esaki, and T. Nomura, *Skeletal muscle pathology in X chromosome-linked muscular dystrophy (mdx) mouse.* Acta Neuropathol, 1986. **69**(1-2): p. 91-5.
49. Grady, R.M., et al., *Skeletal and cardiac myopathies in mice lacking utrophin and dystrophin: A model for Duchenne muscular dystrophy.* Cell, 1997. **90**(4): p. 729-738.
50. Deconinck, A.E., et al., *Utrophin-dystrophin-deficient mice as a model for Duchenne muscular dystrophy.* Cell, 1997. **90**(4): p. 717-727.
51. Cooper, B.J., et al., *The Homolog of the Duchenne Locus Is Defective in X-Linked Muscular-Dystrophy of Dogs.* Nature, 1988. **334**(6178): p. 154-156.
52. Sharp, N.J., et al., *An error in dystrophin mRNA processing in golden retriever muscular dystrophy, an animal homologue of Duchenne muscular dystrophy.* Genomics, 1992. **13**(1): p. 115-21.
53. Winand, N.J., et al., *Deletion of the dystrophin muscle promoter in feline muscular dystrophy.* Neuromuscul Disord, 1994. **4**(5-6): p. 433-45.
54. Gaschen, L., et al., *Cardiomyopathy in dystrophin-deficient hypertrophic feline muscular dystrophy.* J Vet Intern Med, 1999. **13**(4): p. 346-56.

55. Collins, C.A. and J.E. Morgan, *Duchenne's muscular dystrophy: animal models used to investigate pathogenesis and develop therapeutic strategies.* International Journal of Experimental Pathology, 2003. **84**(4): p. 165-172.
56. Fan, N.N. and L.X. Lai, *Genetically Modified Pig Models for Human Diseases.* Journal of Genetics and Genomics, 2013. **40**(2): p. 67-73.
57. Klymiuk, N., et al., *Dystrophin-deficient pigs provide new insights into the hierarchy of physiological derangements of dystrophic muscle.* Human Molecular Genetics, 2013. **22**(21): p. 4368-4382.
58. Nakamura, K., et al., *Generation of muscular dystrophy model rats with a CRISPR/Cas system.* Scientific Reports, 2014. **4**.
59. Deconinck, N. and B. Dan, *Pathophysiology of duchenne muscular dystrophy: current hypotheses.* Pediatr Neurol, 2007. **36**(1): p. 1-7.
60. Rafii, M.S., et al., *Biglycan binds to alpha- and gamma-sarcoglycan and regulates their expression during development.* J Cell Physiol, 2006. **209**(2): p. 439-47.
61. Helbling-Leclerc, A., et al., *Mutations in the laminin alpha 2-chain gene (LAMA2) cause merosin-deficient congenital muscular dystrophy.* Nat Genet, 1995. **11**(2): p. 216-8.
62. Hayashi, Y.K., et al., *Mutations in the integrin alpha7 gene cause congenital myopathy.* Nat Genet, 1998. **19**(1): p. 94-7.
63. Mokri, B. and A.G. Engel, *Duchenne dystrophy: electron microscopic findings pointing to a basic or early abnormality in the plasma membrane of the muscle fiber.* Neurology, 1975. **25**(12): p. 1111-20.
64. Rowland, L.P., *Pathogenesis of muscular dystrophies.* Arch Neurol, 1976. **33**(5): p. 315-21.
65. Emery, A.E., *Muscle histology and creatine kinase levels in the foetus in Duchenne muscular dystrophy.* Nature, 1977. **266**(5601): p. 472-3.
66. Petrof, B.J., et al., *Dystrophin protects the sarcolemma from stresses developed during muscle contraction.* Proc Natl Acad Sci U S A, 1993. **90**(8): p. 3710-4.
67. Franco, A. and J.B. Lansman, *Calcium Entry through Stretch-Inactivated Ion Channels in Mdx Myotubes.* Nature, 1990. **344**(6267): p. 670-673.
68. De Backer, F., et al., *Long-term study of Ca(2+) homeostasis and of survival in collagenase-isolated muscle fibres from normal and mdx mice.* J Physiol, 2002. **542**(Pt 3): p. 855-65.
69. Bodensteiner, J.B. and A.G. Engel, *Intracellular calcium accumulation in Duchenne dystrophy and other myopathies: a study of 567,000 muscle fibers in 114 biopsies.* Neurology, 1978. **28**(5): p. 439-46.
70. Duncan, C.J., *Role of intracellular calcium in promoting muscle damage: a strategy for controlling the dystrophic condition.* Experientia, 1978. **34**(12): p. 1531-5.
71. Bertorini, T.E., et al., *Calcium and Magnesium Content in Fetuses at Risk and Prenecrotic Duchenne Muscular-Dystrophy.* Neurology, 1984. **34**(11): p. 1436-1440.
72. Mongini, T., et al., *Free Cytoplasmic Ca++ at Rest and after Cholinergic Stimulus Is Increased in Cultured Muscle-Cells from Duchenne Muscular-Dystrophy Patients.* Neurology, 1988. **38**(3): p. 476-480.
73. Turner, P.R., et al., *Increased Protein-Degradation Results from Elevated Free Calcium Levels Found in Muscle from Mdx Mice.* Nature, 1988. **335**(6192): p. 735-738.

74. Collet, C., et al., *Intracellular calcium signals measured with indo-1 in isolated skeletal muscle fibres from control and mdx mice.* J Physiol, 1999. **520 Pt 2**: p. 417-29.
75. Leijendekker, W.J., et al., *Regulation of cytosolic calcium in skeletal muscle cells of the mdx mouse under conditions of stress.* Br J Pharmacol, 1996. **118**(3): p. 611-6.
76. Gillis, J.M., *Membrane abnormalities and Ca homeostasis in muscles of the mdx mouse, an animal model of the Duchenne muscular dystrophy: a review.* Acta Physiol Scand, 1996. **156**(3): p. 397-406.
77. Imbert, N., et al., *Abnormal Calcium Homeostasis in Duchenne Muscular-Dystrophy Myotubes Contracting in-Vitro.* Cell Calcium, 1995. **18**(3): p. 177-186.
78. Rivetbastide, M., et al., *Changes in Cytosolic Resting Ionized Calcium Level and in Calcium Transients during in-Vitro Development of Normal and Duchenne Muscular-Dystrophy Cultured Skeletal-Muscle Measured by Laser Cytofluorometry Using Indo-1.* Cell Calcium, 1993. **14**(7): p. 563-571.
79. Hopf, F.W., et al., *A critical evaluation of resting intracellular free calcium regulation in dystrophic mdx muscle.* American Journal of Physiology-Cell Physiology, 1996. **271**(4): p. C1325-C1339.
80. Tutdibi, O., et al., *Increased calcium entry into dystrophin-deficient muscle fibres of MDX and ADR-MDX mice is reduced by ion channel blockers.* Journal of Physiology-London, 1999. **515**(3): p. 859-868.
81. Mule, F. and R. Serio, *Increased calcium influx is responsible for the sustained mechanical tone in colon from dystrophic (mdx) mice.* Gastroenterology, 2001. **120**(6): p. 1430-1437.
82. Fong, P., et al., *Increased Activity of Calcium Leak Channels in Myotubes of Duchenne Human and Mdx Mouse Origin.* Science, 1990. **250**(4981): p. 673-676.
83. Robert, V., et al., *Alteration in calcium handling at the subcellular level in mdx myotubes.* Journal of Biological Chemistry, 2001. **276**(7): p. 4647-4651.
84. Vandebrouck, A., et al., *Regulation of store-operated calcium entries and mitochondrial uptake by minidystrophin expression in cultured myotubes.* Faseb Journal, 2005. **19**(12): p. 136-+.
85. Nethery, D., et al., *PLA(2) dependence of diaphragm mitochondrial formation of reactive oxygen species.* Journal of Applied Physiology, 2000. **89**(1): p. 72-80.
86. Tidball, J.G. and M. Wehling-Henricks, *The role of free radicals in the pathophysiology of muscular dystrophy.* J Appl Physiol (1985), 2007. **102**(4): p. 1677-86.
87. Austin, L., et al., *Potential oxyradical damage and energy status in individual muscle fibres from degenerating muscle diseases.* Neuromuscul Disord, 1992. **2**(1): p. 27-33.
88. Dudley, R.W., et al., *Dynamic responses of the glutathione system to acute oxidative stress in dystrophic mouse (mdx) muscles.* Am J Physiol Regul Integr Comp Physiol, 2006. **291**(3): p. R704-10.
89. Whitehead, N.P., et al., *N-Acetylcysteine ameliorates skeletal muscle pathophysiology in mdx mice.* J Physiol, 2008. **586**(Pt 7): p. 2003-14.
90. Buetler, T.M., et al., *Green tea extract decreases muscle necrosis in mdx mice and protects against reactive oxygen species.* Am J Clin Nutr, 2002. **75**(4): p. 749-53.

91. Martins, A.S., et al., *Reactive oxygen species contribute to Ca2+ signals produced by osmotic stress in mouse skeletal muscle fibres.* Journal of Physiology-London, 2008. **586**(1): p. 197-210.
92. Kuznetsov, A.V., et al., *Impaired mitochondrial oxidative phosphorylation in skeletal muscle of the dystrophin-deficient mdx mouse.* Molecular and Cellular Biochemistry, 1998. **183**(1-2): p. 87-96.
93. Lamb, G.D. and G.S. Posterino, *Effects of oxidation and reduction on contractile function in skeletal muscle fibres of the rat.* Journal of Physiology-London, 2003. **546**(1): p. 149-163.
94. Tidball, J.G., *Inflammatory processes in muscle injury and repair.* American Journal of Physiology-Regulatory Integrative and Comparative Physiology, 2005. **288**(2): p. R345-R353.
95. Love, N.R., et al., *Amputation-induced reactive oxygen species are required for successful Xenopus tadpole tail regeneration.* Nature Cell Biology, 2013. **15**(2): p. 222-228.
96. Otto, A., et al., *Canonical Wnt signalling induces satellite-cell proliferation during adult skeletal muscle regeneration.* Journal of Cell Science, 2008. **121**(17): p. 2939-2950.
97. Le Grand, F., et al., *Wnt7a Activates the Planar Cell Polarity Pathway to Drive the Symmetric Expansion of Satellite Stem Cells.* Cell Stem Cell, 2009. **4**(6): p. 535-547.
98. Dumont, N.A., et al., *Dystrophin expression in muscle stem cells regulates their polarity and asymmetric division.* Nature Medicine, 2015. **21**(12): p. 1455-+.
99. Troy, A., et al., *Coordination of satellite cell activation and self-renewal by Par-complex-dependent asymmetric activation of p38alpha/beta MAPK.* Cell Stem Cell. **11**(4): p. 541-53.
100. Haslett, J.N., et al., *Gene expression comparison of biopsies from Duchenne muscular dystrophy (DMD) and normal skeletal muscle.* Proc Natl Acad Sci U S A, 2002. **99**(23): p. 15000-5.
101. Yamada, M., et al., *Matrix metalloproteinase-2 mediates stretch-induced activation of skeletal muscle satellite cells in a nitric oxide-dependent manner.* Int J Biochem Cell Biol, 2008. **40**(10): p. 2183-91.
102. Buono, R., et al., *Nitric Oxide Sustains Long-Term Skeletal Muscle Regeneration by Regulating Fate of Satellite Cells Via Signaling Pathways Requiring Vangl2 and Cyclic GMP.* Stem Cells, 2012. **30**(2): p. 197-209.
103. Grozdanovic, Z. and H.G. Baumgarten, *Nitric oxide synthase in skeletal muscle fibers: a signaling component of the dystrophin-glycoprotein complex.* Histol Histopathol, 1999. **14**(1): p. 243-56.
104. Fleming, I. and R. Busse, *NO: the primary EDRF.* Journal of Molecular and Cellular Cardiology, 1999. **31**(1): p. 5-14.
105. Wehling, M., M.J. Spencer, and J.G. Tidball, *A nitric oxide synthase transgene ameliorates muscular dystrophy in mdx mice.* J Cell Biol, 2001. **155**(1): p. 123-31.
106. Alderton, J.M. and R.A. Steinhardt, *How calcium influx through calcium leak channels is responsible for the elevated levels of calcium-dependent proteolysis in dystrophic myotubes.* Trends in Cardiovascular Medicine, 2000. **10**(6): p. 268-272.

107. Wrogemann, K. and S.D. Pena, *Mitochondrial calcium overload: A general mechanism for cell-necrosis in muscle diseases.* Lancet, 1976. **1**(7961): p. 672-4.
108. Millay, D.P., et al., *Calcium influx is sufficient to induce muscular dystrophy through a TRPC-dependent mechanism.* Proceedings of the National Academy of Sciences of the United States of America, 2009. **106**(45): p. 19023-19028.
109. Carafoli, E. and M. Molinari, *Calpain: A protease in search of a function?* Biochemical and Biophysical Research Communications, 1998. **247**(2): p. 193-203.
110. Raymackers, J.M., et al., *Consequence of parvalbumin deficiency in the mdx mouse: histological, biochemical and mechanical phenotype of a new double mutant.* Neuromuscul Disord, 2003. **13**(5): p. 376-87.
111. Alderton, J.M. and R.A. Steinhardt, *Calcium influx through calcium leak channels is responsible for the elevated levels of calcium-dependent proteolysis in dystrophic myotubes.* Journal of Biological Chemistry, 2000. **275**(13): p. 9452-9460.
112. Spencer, M.J., D.E. Croall, and J.G. Tidball, *Calpains Are Activated in Necrotic Fibers from Mdx Dystrophic Mice.* Journal of Biological Chemistry, 1995. **270**(18): p. 10909-10914.
113. Wallace, G.Q. and E.M. McNally, *Mechanisms of Muscle Degeneration, Regeneration, and Repair in the Muscular Dystrophies.* Annual Review of Physiology, 2009. **71**: p. 37-57.
114. Malik, V., L.R. Rodino-Klapac, and J.R. Mendell, *Emerging drugs for Duchenne muscular dystrophy.* Expert Opinion on Emerging Drugs, 2012. **17**(2): p. 261-277.
115. Mendell, J.R., et al., *Gene therapy for muscular dystrophy: Lessons learned and path forward.* Neuroscience Letters, 2012. **527**(2): p. 90-99.
116. Manzur, A.Y., et al., *Glucocorticoid corticosteroids for Duchenne muscular dystrophy.* Cochrane Database Syst Rev, 2008(1): p. CD003725.
117. Ricotti, V., et al., *Steroids in Duchenne muscular dystrophy.* Neuromuscular Disorders, 2013. **23**(8): p. 696-697.
118. Kirschner, J., et al., *Treatment of Duchenne muscular dystrophy with ciclosporin A: a randomised, double-blind, placebo-controlled multicentre trial.* Lancet Neurology, 2010. **9**(11): p. 1053-1059.
119. Muntoni, F., et al., *Steroids in Duchenne muscular dystrophy: from clinical trials to genomic research.* Neuromuscul Disord, 2002. **12 Suppl 1**: p. S162-5.
120. McIntosh, L., et al., *Nuclear magnetic resonance spectroscopy study of muscle growth, mdx dystrophy and glucocorticoid treatments: correlation with repair.* NMR Biomed, 1998. **11**(1): p. 1-10.
121. Pasquini, F., et al., *The effect of glucocorticoids on the accumulation of utrophin by cultured normal and dystrophic human skeletal muscle satellite cells.* Neuromuscul Disord, 1995. **5**(2): p. 105-14.
122. Anderson, J.E. and C. Vargas, *Correlated NOS-Imu and myf5 expression by satellite cells in mdx mouse muscle regeneration during NOS manipulation and deflazacort treatment.* Neuromuscul Disord, 2003. **13**(5): p. 388-96.
123. Fisher, I., et al., *Prednisolone-induced changes in dystrophic skeletal muscle.* FASEB J, 2005. **19**(7): p. 834-6.

124. Merlini, L., et al., *Early corticosteroid treatment in 4 duchenne muscular dystrophy patients: 14-year follow-up.* Muscle & Nerve, 2012. **45**(6): p. 796-802.
125. Finder, J.D., et al., *Respiratory care of the patient with Duchenne muscular dystrophy: ATS consensus statement.* Am J Respir Crit Care Med, 2004. **170**(4): p. 456-65.
126. Passamano, L., et al., *Improvement of survival in Duchenne Muscular Dystrophy: retrospective analysis of 835 patients.* Acta Myol. **31**(2): p. 121-5.
127. Messina, S., et al., *Nuclear factor kappa-B blockade reduces skeletal muscle degeneration and enhances muscle function in Mdx mice.* Exp Neurol, 2006. **198**(1): p. 234-41.
128. Grounds, M.D., et al., *Strategies to protect dystrophic muscle from necrosis: anti-TNF alpha (Remicade (R)) therapy and over-expression of IGF-1.* Neuromuscular Disorders, 2004. **14**(8-9): p. 625-625.
129. Asai, A., et al., *Primary role of functional ischemia, quantitative evidence for the two-hit mechanism, and phosphodiesterase-5 inhibitor therapy in mouse muscular dystrophy.* PLoS One, 2007. **2**(8): p. e806.
130. Burkin, D.J., et al., *Enhanced expression of the alpha 7 beta 1 integrin reduces muscular dystrophy and restores viability in dystrophic mice.* Journal of Cell Biology, 2001. **152**(6): p. 1207-1218.
131. Bogdanovich, S., et al., *Myostatin (GDF8) blockage improves muscle function in MDX mouse.* Journal of the Neurological Sciences, 2002. **199**: p. S65-S65.
132. Wagner, K.R., et al., *Loss of myostatin attenuates severity of muscular dystrophy in mdx mice.* Annals of Neurology, 2002. **52**(6): p. 832-836.
133. Dent, K.M., et al., *Improved molecular diagnosis of dystrophinopathies in an unselected clinical cohort.* Am J Med Genet A, 2005. **134**(3): p. 295-8.
134. Palmer, E., J.M. Wilhelm, and F. Sherman, *Phenotypic suppression of nonsense mutants in yeast by aminoglycoside antibiotics.* Nature, 1979. **277**(5692): p. 148-50.
135. Malik, V., et al., *Gentamicin-Induced Readthrough of Stop Codons in Duchenne Muscular Dystrophy.* Annals of Neurology, 2010. **67**(6): p. 771-780.
136. Keys, T.F., et al., *Renal toxicity during therapy with gentamicin or tobramycin.* Mayo Clin Proc, 1981. **56**(9): p. 556-9.
137. Bidou, L., et al., *Sense from nonsense: therapies for premature stop codon diseases.* Trends in Molecular Medicine, 2012. **18**(11): p. 679-688.
138. Bushby, K., et al., *Ataluren Treatment of Patients with Nonsense Mutation Dystrophinopathy.* Muscle & Nerve, 2014. **50**(4): p. 477-487.
139. Bladen, C.L., et al., *The TREAT-NMD DMD Global Database: Analysis of More than 7,000 Duchenne Muscular Dystrophy Mutations.* Human Mutation, 2015. **36**(4): p. 395-402.
140. Dunckley, M.G., et al., *Modification of splicing in the dystrophin gene in cultured Mdx muscle cells by antisense oligoribonucleotides.* Hum Mol Genet, 1998. **7**(7): p. 1083-90.
141. Lu, Q.L., et al., *Functional amounts of dystrophin produced by skipping the mutated exon in the mdx dystrophic mouse.* Nature Medicine, 2003. **9**(8): p. 1009-1014.
142. Goyenvalle, A., et al., *Rescue of severely affected dystrophin/utrophin-deficient mice through scAAV-U7snRNA-mediated exon skipping.* Human Molecular Genetics, 2012. **21**(11): p. 2559-2571.

143. Aartsma-Rus, A., et al., *Entries in the Leiden Duchenne muscular dystrophy mutation database: an overview of mutation types and paradoxical cases that confirm the reading-frame rule.* Muscle Nerve, 2006. **34**(2): p. 135-44.
144. van Deutekom, J.C.T., et al., *Antisense-induced exon skipping restores dystrophin expression in DMD patient derived muscle cells.* Human Molecular Genetics, 2001. **10**(15): p. 1547-1554.
145. Anderson, W.F., *September 14, 1990: the beginning.* Hum Gene Ther, 1990. **1**(4): p. 371-2.
146. Lehrman, S., *Virus treatment questioned after gene therapy death.* Nature, 1999. **401**(6753): p. 517-8.
147. Hacein-Bey-Abina, S., et al., *A serious adverse event after successful gene therapy for X-linked severe combined immunodeficiency.* N Engl J Med, 2003. **348**(3): p. 255-6.
148. Acsadi, G., et al., *Human dystrophin expression in mdx mice after intramuscular injection of DNA constructs.* Nature, 1991. **352**(6338): p. 815-8.
149. Ragot, T., et al., *Efficient adenovirus-mediated transfer of a human minidystrophin gene to skeletal muscle of mdx mice.* Nature, 1993. **361**(6413): p. 647-50.
150. Vincent, N., et al., *Long-term correction of mouse dystrophic degeneration by adenovirus-mediated transfer of a minidystrophin gene.* Nat Genet, 1993. **5**(2): p. 130-4.
151. Chamberlain, J.S., *Dystrophin levels required for genetic correction of Duchenne muscular dystrophy.* Basic and Applied Myology, 1997. **7**(3-4): p. 251-255.
152. Liu, F., et al., *Transfer of full-length Dmd to the diaphragm muscle of Dmd(mdx/mdx) mice through systemic administration of plasmid DNA.* Mol Ther, 2001. **4**(1): p. 45-51.
153. Zhang, G., et al., *Intraarterial delivery of naked plasmid DNA expressing full-length mouse dystrophin in the mdx mouse model of duchenne muscular dystrophy.* Hum Gene Ther, 2004. **15**(8): p. 770-82.
154. Romero, N.B., et al., *Phase I study of dystrophin plasmid-based gene therapy in Duchenne/Becker muscular dystrophy.* Hum Gene Ther, 2004. **15**(11): p. 1065-76.
155. Kumar-Singh, R. and J.S. Chamberlain, *Encapsidated adenovirus minichromosomes allow delivery and expression of a 14 kb dystrophin cDNA to muscle cells.* Hum Mol Genet, 1996. **5**(7): p. 913-21.
156. Kochanek, S., et al., *A new adenoviral vector: Replacement of all viral coding sequences with 28 kb of DNA independently expressing both full-length dystrophin and beta-galactosidase.* Proceedings of the National Academy of Sciences of the United States of America, 1996. **93**(12): p. 5731-5736.
157. Chen, H.H., et al., *Persistence in muscle of an adenoviral vector that lacks all viral genes.* Proceedings of the National Academy of Sciences of the United States of America, 1997. **94**(5): p. 1645-1650.
158. Acsadi, G., et al., *A Differential Efficiency of Adenovirus-Mediated in-Vivo Gene-Transfer into Skeletal-Muscle Cells of Different Maturity.* Human Molecular Genetics, 1994. **3**(4): p. 579-584.
159. Thirion, C., et al., *Strategies for muscle-specific targeting of adenoviral gene transfer vectors.* Neuromuscular Disorders, 2002. **12**: p. S30-S39.

160. Yuasa, K., et al., *Adeno-associated virus vector-mediated gene transfer into dystrophin-deficient skeletal muscles evokes enhanced immune response against the transgene product.* Gene Therapy, 2002. **9**(23): p. 1576-1588.
161. Zincarelli, C., et al., *Analysis of AAV serotypes 1-9 mediated gene expression and tropism in mice after systemic injection.* Mol Ther, 2008. **16**(6): p. 1073-80.
162. Wang, B., et al., *A canine minidystrophin is functional and therapeutic in mdx mice.* Gene Ther, 2008. **15**(15): p. 1099-106.
163. Wang, B., J. Li, and X. Xiao, *Adeno-associated virus vector carrying human minidystrophin genes effectively ameliorates muscular dystrophy in mdx mouse model.* Proc Natl Acad Sci U S A, 2000. **97**(25): p. 13714-9.
164. Mendell, J.R., et al., *Brief Report: Dystrophin Immunity in Duchenne's Muscular Dystrophy.* New England Journal of Medicine, 2010. **363**(15): p. 1429-1437.
165. Koo, T., et al., *Triple Trans-Splicing Adeno-Associated Virus Vectors Capable of Transferring the Coding Sequence for Full-Length Dystrophin Protein into Dystrophic Mice.* Human Gene Therapy, 2014. **25**(2): p. 98-108.
166. Urnov, F.D., et al., *Genome editing with engineered zinc finger nucleases.* Nature Reviews Genetics, 2010. **11**(9): p. 636-646.
167. Wyman, C. and R. Kanaar, *DNA double-strand break repair: all's well that ends well.* Annu Rev Genet, 2006. **40**: p. 363-83.
168. Long, C.Z., et al., *Prevention of muscular dystrophy in mice by CRISPR/Cas9-mediated editing of germline DNA.* Science, 2014. **345**(6201): p. 1184-1188.
169. Ousterout, D.G., et al., *Multiplex CRISPR/Cas9-based genome editing for correction of dystrophin mutations that cause Duchenne muscular dystrophy.* Nature Communications, 2015. **6**.
170. Li, H.L., et al., *Precise correction of the dystrophin gene in duchenne muscular dystrophy patient induced pluripotent stem cells by TALEN and CRISPR-Cas9.* Stem Cell Reports, 2015. **4**(1): p. 143-54.
171. Gilchrist, S.C., et al., *Immune response to full-length dystrophin delivered to Dmd muscle by a high-capacity adenoviral vector.* Mol Ther, 2002. **6**(3): p. 359-68.
172. Watt, D.J., et al., *Incorporation of Donor Muscle Precursor Cells into an Area of Muscle Regeneration in the Host Mouse.* Journal of the Neurological Sciences, 1982. **57**(2-3): p. 319-331.
173. Morgan, J.E. and T.A. Partridge, *Cell Transplantation and Gene-Therapy in Muscular-Dystrophy.* Bioessays, 1992. **14**(9): p. 641-645.
174. Vilquin, J.T., et al., *Myoblast Allotransplantation in Mice - Degree of Success Varies Depending on the Efficacy of Various Immunosuppressive Treatments.* Transplantation Proceedings, 1994. **26**(6): p. 3372-3373.
175. Mendell, J.R., et al., *Myoblast transfer in the treatment of Duchenne's muscular dystrophy.* N Engl J Med, 1995. **333**(13): p. 832-8.
176. Karpati, G., et al., *Myoblast transfer in Duchenne muscular dystrophy.* Ann Neurol, 1993. **34**(1): p. 8-17.
177. Tremblay, J.P., et al., *Myoblast Transplantation between Monozygotic Twin Girl Carriers of Duchenne Muscular-Dystrophy.* Neuromuscular Disorders, 1993. **3**(5-6): p. 583-592.

178. Hong, F., et al., *Cyclosporine blocks muscle differentiation by inducing oxidative stress and by inhibiting the peptidylprolyl-cis-trans-isomerase activity of cyclophilin A: cyclophilin A protects myoblasts from cyclosporine-induced cytotoxicity.* Faseb Journal, 2002. **16**(10): p. 1633-+.
179. Gussoni, E., et al., *Dystrophin expression in the mdx mouse restored by stem cell transplantation.* Nature, 1999. **401**(6751): p. 390-394.
180. Ichim, T.E., et al., *Mesenchymal stem cells as anti-inflammatories: Implications for treatment of Duchenne muscular dystrophy.* Cellular Immunology, 2010. **260**(2): p. 75-82.
181. Takahashi, K., et al., *Induction of pluripotent stem cells from adult human fibroblasts by defined factors.* Cell, 2007. **131**(5): p. 861-872.
182. Sebastiano, V., et al., *In Situ Genetic Correction of the Sickle Cell Anemia Mutation in Human Induced Pluripotent Stem Cells Using Engineered Zinc Finger Nucleases.* Stem Cells, 2011. **29**(11): p. 1717-1726.
183. Kazuki, Y., et al., *Complete Genetic Correction of iPS Cells From Duchenne Muscular Dystrophy.* Molecular Therapy, 2010. **18**(2): p. 386-393.
184. Pearce, M., et al., *The Utrophin and Dystrophin Genes Share Similarities in Genomic Structure.* Human Molecular Genetics, 1993. **2**(11): p. 1765-1772.
185. Love, D.R., et al., *An Autosomal Transcript in Skeletal-Muscle with Homology to Dystrophin.* Nature, 1989. **339**(6219): p. 55-58.
186. Tinsley, J.M., et al., *Primary Structure of Dystrophin-Related Protein.* Nature, 1992. **360**(6404): p. 591-593.
187. Khurana, T.S., et al., *Immunolocalization and developmental expression of dystrophin related protein in skeletal muscle.* Neuromuscul Disord, 1991. **1**(3): p. 185-94.
188. Man, N.T., et al., *Localization of the Dmdl Gene-Encoded Dystrophin-Related Protein Using a Panel of 19 Monoclonal-Antibodies - Presence at Neuromuscular-Junctions, in the Sarcolemma of Dystrophic Skeletal-Muscle, in Vascular and Other Smooth Muscles, and in Proliferating Brain-Cell Lines.* Journal of Cell Biology, 1991. **115**(6): p. 1695-1700.
189. Ohlendieck, K., et al., *Dystrophin-Related Protein Is Localized to Neuromuscular-Junctions of Adult Skeletal-Muscle.* Neuron, 1991. **7**(3): p. 499-508.
190. Khurana, T.S., E.P. Hoffman, and L.M. Kunkel, *Identification of a Chromosome-6-Encoded Dystrophin-Related Protein.* Journal of Biological Chemistry, 1990. **265**(28): p. 16717-16720.
191. Burton, E.A., et al., *A second promoter provides an alternative target for therapeutic up-regulation of utrophin in Duchenne muscular dystrophy.* Proceedings of the National Academy of Sciences of the United States of America, 1999. **96**(24): p. 14025-14030.
192. Gramolini, A.O., G. Belanger, and B.J. Jasmin, *Distinct regions in the 3' untranslated region are responsible for targeting and stabilizing utrophin transcripts in skeletal muscle cells.* J Cell Biol, 2001. **154**(6): p. 1173-83.
193. Gramolini, A.O., et al., *Increased expression of utrophin in a slow vs. a fast muscle involves posttranscriptional events.* Am J Physiol Cell Physiol, 2001. **281**(4): p. C1300-9.

194. Weir, A.P., et al., *A- and B-utrophin have different expression patterns and are differentially up-regulated in mdx muscle.* Journal of Biological Chemistry, 2002. **277**(47): p. 45285-45290.
195. Tinsley, J.M., et al., *Primary structure of dystrophin-related protein.* Nature, 1992. **360**(6404): p. 591-3.
196. Peters, M.F., et al., *Differential membrane localization and intermolecular associations of alpha-dystrobrevin isoforms in skeletal muscle.* J Cell Biol, 1998. **142**(5): p. 1269-78.
197. Clerk, A., et al., *Dystrophin-Related Protein, Utrophin, in Normal and Dystrophic Human Fetal Skeletal-Muscle.* Histochemical Journal, 1993. **25**(8): p. 554-561.
198. Karpati, G., et al., *Localization and Quantitation of the Chromosome-6-Encoded Dystrophin-Related Protein (Utrophin) in Pathological Human Muscle.* Neurology, 1993. **43**(4): p. A294-A295.
199. Tinsley, J., et al., *Expression of full-length utrophin prevents muscular dystrophy in mdx mice.* Nat Med, 1998. **4**(12): p. 1441-4.
200. Tinsley, J.M., et al., *Amelioration of the dystrophic phenotype of mdx mice using a truncated utrophin transgene.* Nature, 1996. **384**(6607): p. 349-353.
201. Gilbert, T., et al., *Adenovirus-mediated utrophin gene transfer mitigates the dystrophic phenotype of mdx mouse muscles.* Human Gene Therapy, 1999. **10**(8): p. 1299-1310.
202. Dennis, C.L., et al., *Molecular and functional analysis of the utrophin promoter.* Nucleic Acids Res, 1996. **24**(9): p. 1646-52.
203. Perkins, K.J. and K.E. Davies, *The role of utrophin in the potential therapy of Duchenne muscular dystrophy.* Neuromuscular Disorders, 2002. **12**: p. S78-S89.
204. Gramolini, A.O., et al., *Induction of utrophin gene expression by heregulin in skeletal muscle cells: role of the N-box motif and GA binding protein.* Proc Natl Acad Sci U S A, 1999. **96**(6): p. 3223-7.
205. Basu, U., et al., *Heregulin-induced epigenetic regulation of the utrophin-A promoter.* FEBS Lett, 2007. **581**(22): p. 4153-8.
206. Basu, U., et al., *Translational regulation of utrophin by miRNAs.* PLoS One. **6**(12): p. e29376.
207. Galvagni, F., S. Capo, and S. Oliviero, *Sp1 and Sp3 physically interact and co-operate with GABP for the activation of the utrophin promoter.* J Mol Biol, 2001. **306**(5): p. 985-96.
208. Miura, P., et al., *Pharmacological activation of PPARbeta/delta stimulates utrophin A expression in skeletal muscle fibers and restores sarcolemmal integrity in mature mdx mice.* Hum Mol Genet, 2009. **18**(23): p. 4640-9.
209. Chakkalakal, J.V., et al., *Expression of utrophin A mRNA correlates with the oxidative capacity of skeletal muscle fiber types and is regulated by calcineurin/NFAT signaling.* Proc Natl Acad Sci U S A, 2003. **100**(13): p. 7791-6.
210. Chakkalakal, J.V., et al., *Stimulation of calcineurin signaling attenuates the dystrophic pathology in mdx mice.* Hum Mol Genet, 2004. **13**(4): p. 379-88.
211. Selsby, J.T., et al., *Rescue of dystrophic skeletal muscle by PGC-1alpha involves a fast to slow fiber type shift in the mdx mouse.* PLoS One, 2012. **7**(1): p. e30063.
212. Courdier-Fruh, I., et al., *Glucocorticoid-mediated regulation of utrophin levels in human muscle fibers.* Neuromuscul Disord, 2002. **12 Suppl 1**: p. S95-104.

213. St-Pierre, S.J., et al., *Glucocorticoid treatment alleviates dystrophic myofiber pathology by activation of the calcineurin/NF-AT pathway.* FASEB J, 2004. **18**(15): p. 1937-9.
214. Krag, T.O.B., et al., *Heregulin ameliorates the dystrophic phenotype in mdx mice.* Proceedings of the National Academy of Sciences of the United States of America, 2004. **101**(38): p. 13856-13860.
215. Voisin, V. and S. de la Porte, *[Pharmacological treatments for Duchenne and Becker dystrophies]*. J Soc Biol, 2005. **199**(1): p. 17-28.
216. Sonnemann, K.J., et al., *Functional substitution by TAT-utrophin in dystrophin-deficient mice.* PLoS Med, 2009. **6**(5): p. e1000083.
217. Gauthier-Rouviere, C. and A. Bonet-Kerrache, *RhoA leads to up-regulation and relocalization of utrophin in muscle fibers.* Biochem Biophys Res Commun, 2009. **384**(3): p. 322-8.
218. Tinsley, J.M., et al., *Daily Treatment with SMTC1100, a Novel Small Molecule Utrophin Upregulator, Dramatically Reduces the Dystrophic Symptoms in the mdx Mouse.* PLoS One, 2011. **6**(5).
219. Wang, Q., et al., *A method of utrophin up-regulation through RNAi-mediated knockdown of the transcription factor EN1.* J Int Med Res, 2011. **39**(1): p. 161-71.
220. Vaquerizas, J.M., et al., *A census of human transcription factors: function, expression and evolution.* Nat Rev Genet, 2009. **10**(4): p. 252-63.
221. Kornberg, R.D., *Structure of chromatin.* Annu Rev Biochem, 1977. **46**: p. 931-54.
222. Klug, A., *From macromolecules to biological assemblies. Nobel Lecture, 8 December 1982.* Biosci Rep, 1983. **3**(5): p. 395-430.
223. Weintraub, H. and M. Groudine, *Chromosomal Subunits in Active Genes Have an Altered Conformation.* Science, 1976. **193**(4256): p. 848-856.
224. Pelham, H.R.B. and D.D. Brown, *A Specific Transcription Factor That Can Bind Either the 5s Rna Gene or 5s Rna.* Proceedings of the National Academy of Sciences of the United States of America-Biological Sciences, 1980. **77**(7): p. 4170-4174.
225. Miller, J., A.D. Mclachlan, and A. Klug, *Repetitive Zinc-Binding Domains in the Protein Transcription Factor Iiia from Xenopus Oocytes.* Embo Journal, 1985. **4**(6): p. 1609-1614.
226. Diakun, G.P., L. Fairall, and A. Klug, *Exafs Study of the Zinc-Binding Sites in the Protein Transcription Factor-Iiia.* Nature, 1986. **324**(6098): p. 698-699.
227. Pavletich, N.P. and C.O. Pabo, *Zinc Finger DNA Recognition - Crystal-Structure of a Zif268-DNA Complex at 2.1-A.* Science, 1991. **252**(5007): p. 809-817.
228. Cathomen, T. and J.K. Joung, *Zinc-finger nucleases: The next generation emerges.* Molecular Therapy, 2008. **16**(7): p. 1200-1207.
229. Joung, J.K., E.I. Ramm, and C.O. Pabo, *A bacterial two-hybrid selection system for studying protein-DNA and protein-protein interactions.* Proc Natl Acad Sci U S A, 2000. **97**(13): p. 7382-7.
230. Ihara, H., et al., *In vitro selection of zinc finger DNA-binding proteins through ribosome display.* Biochem Biophys Res Commun, 2006. **345**(3): p. 1149-54.
231. Bae, K.H. and J.S. Kim, *One-step selection of artificial transcription factors using an in vivo screening system.* Mol Cells, 2006. **21**(3): p. 376-80.

232. Blancafort, P., L. Magnenat, and C.F. Barbas, *Scanning the human genome with combinatorial transcription factor libraries.* Nature Biotechnology, 2003. **21**(3): p. 269-274.
233. Ledford, H., *Targeted gene editing enters clinic.* Nature, 2011. **471**(7336): p. 16-16.
234. Lu, Y.F., et al., *Targeting Artificial Transcription Factors to the Utrophin A Promoter EFFECTS ON DYSTROPHIC PATHOLOGY AND MUSCLE FUNCTION.* Journal of Biological Chemistry, 2008. **283**(50): p. 34720-34727.
235. Mattei, E., et al., *The artificial gene Jazz, a transcriptional regulator of utrophin, corrects the dystrophic pathology in mdx mice.* Transgenic Research, 2010. **19**(2): p. 342-342.
236. Chamberlain, J.S., *Gene therapy of muscular dystrophy.* Hum Mol Genet, 2002. **11**(20): p. 2355-62.
237. Orr-Weaver, T.L., J.W. Szostak, and R.J. Rothstein, *Yeast transformation: a model system for the study of recombination.* Proc Natl Acad Sci U S A, 1981. **78**(10): p. 6354-8.
238. Plessis, A., et al., *Site-specific recombination determined by I-SceI, a mitochondrial group I intron-encoded endonuclease expressed in the yeast nucleus.* Genetics, 1992. **130**(3): p. 451-60.
239. Folger, K., K. Thomas, and M.R. Capecchi, *Analysis of homologous recombination in cultured mammalian cells.* Cold Spring Harb Symp Quant Biol, 1984. **49**: p. 123-38.
240. Liang, F., et al., *Homology-directed repair is a major double-strand break repair pathway in mammalian cells.* Proceedings of the National Academy of Sciences of the United States of America, 1998. **95**(9): p. 5172-5177.
241. van Gent, D.C., J.H. Hoeijmakers, and R. Kanaar, *Chromosomal stability and the DNA double-stranded break connection.* Nat Rev Genet, 2001. **2**(3): p. 196-206.
242. Miller, J.C., et al., *An improved zinc-finger nuclease architecture for highly specific genome editing.* Nat Biotechnol, 2007. **25**(7): p. 778-85.
243. Cathomen, T. and J.K. Joung, *Zinc-finger nucleases: the next generation emerges.* Mol Ther, 2008. **16**(7): p. 1200-7.
244. Doyon, Y., et al., *Heritable targeted gene disruption in zebrafish using designed zinc-finger nucleases.* Nature Biotechnology, 2008. **26**(6): p. 702-708.
245. Galli, C., et al., *Genetic engineering including superseding microinjection: new ways to make GM pigs.* Xenotransplantation, 2010. **17**(6): p. 397-410.
246. Cradick, T.J., et al., *Zinc-finger Nucleases as a Novel Therapeutic Strategy for Targeting Hepatitis B Virus DNAs.* Molecular Therapy, 2010. **18**(5): p. 947-954.
247. Overlack, N., et al., *Gene Repair of an Usher Syndrome Causing Mutation by Zinc-Finger Nuclease Mediated Homologous Recombination.* Investigative Ophthalmology & Visual Science, 2012. **53**(7): p. 4140-4146.
248. Sander, J.D. and J.K. Joung, *CRISPR-Cas systems for editing, regulating and targeting genomes.* Nature Biotechnology, 2014. **32**(4): p. 347-355.
249. Ishino, Y., et al., *Nucleotide sequence of the iap gene, responsible for alkaline phosphatase isozyme conversion in Escherichia coli, and identification of the gene product.* J Bacteriol, 1987. **169**(12): p. 5429-33.

250. Mojica, F.J., et al., *Biological significance of a family of regularly spaced repeats in the genomes of Archaea, Bacteria and mitochondria.* Mol Microbiol, 2000. **36**(1): p. 244-6.
251. Bolotin, A., et al., *Clustered regularly interspaced short palindrome repeats (CRISPRs) have spacers of extrachromosomal origin.* Microbiology, 2005. **151**(Pt 8): p. 2551-61.
252. Pourcel, C., G. Salvignol, and G. Vergnaud, *CRISPR elements in Yersinia pestis acquire new repeats by preferential uptake of bacteriophage DNA, and provide additional tools for evolutionary studies.* Microbiology, 2005. **151**(Pt 3): p. 653-63.
253. Barrangou, R., et al., *CRISPR provides acquired resistance against viruses in prokaryotes.* Science, 2007. **315**(5819): p. 1709-12.
254. Jinek, M., et al., *A Programmable Dual-RNA-Guided DNA Endonuclease in Adaptive Bacterial Immunity.* Science, 2012. **337**(6096): p. 816-821.
255. Deol, J.R., et al., *Gene Therapy for Duchenne Muscular Dystrophy Using a Gutted Adenovirus Expressing Utrophin.* Molecular Therapy, 2006. **13**: p. S354-S355.
256. Di Certo, M.G., et al., *The artificial gene Jazz, a transcriptional regulator of utrophin, corrects the dystrophic pathology in mdx mice.* Hum Mol Genet, 2010. **19**(5): p. 752-60.
257. Wright, D.A., et al., *Standardized reagents and protocols for engineering zinc finger nucleases by modular assembly.* Nat Protoc, 2006. **1**(3): p. 1637-52.
258. Sander, J.D., et al., *ZiFiT (Zinc Finger Targeter): an updated zinc finger engineering tool.* Nucleic Acids Res. **38**(Web Server issue): p. W462-8.
259. Jiang, W.Y., et al., *RNA-guided editing of bacterial genomes using CRISPR-Cas systems.* Nature Biotechnology, 2013. **31**(3): p. 233-239.
260. Moorwood, C., et al., *Drug discovery for Duchenne muscular dystrophy via utrophin promoter activation screening.* PLoS One, 2011. **6**(10): p. e26169.
261. Vaquerizas, J.M., et al., *A census of human transcription factors: function, expression and evolution.* Nature Reviews Genetics, 2009. **10**(4): p. 252-263.
262. Diakun, G.P., L. Fairall, and A. Klug, *EXAFS study of the zinc-binding sites in the protein transcription factor IIIA.* Nature, 1986. **324**(6098): p. 698-9.
263. Lachenmann, M.J., et al., *The hidden thermodynamics of a zinc finger.* Journal of Molecular Biology, 2002. **316**(4): p. 969-989.
264. Choo, Y., I. Sanchezgarcia, and A. Klug, *In-Vivo Repression by a Site-Specific DNA-Binding Protein Designed against an Oncogenic Sequence.* Nature, 1994. **372**(6507): p. 642-645.
265. Sander, J.D., et al., *ZiFiT (Zinc Finger Targeter): an updated zinc finger engineering tool.* Nucleic Acids Res, 2010. **38**(Web Server issue): p. W462-8.
266. Sander, J.D., et al., *ZiFiT (Zinc Finger Targeter): an updated zinc finger engineering tool.* Nucleic Acids Research, 2010. **38**: p. W462-W468.
267. Perkins, K.J., E.A. Burton, and K.E. Davies, *The role of basal and myogenic factors in the transcriptional activation of utrophin promoter A: implications for therapeutic up-regulation in Duchenne muscular dystrophy.* Nucleic Acids Research, 2001. **29**(23): p. 4843-4850.
268. Stocksley, M.A., et al., *A 1.3 kb promoter fragment confers spatial and temporal expression of utrophin A mRNA in mouse skeletal muscle fibers.* Neuromuscul Disord, 2005. **15**(6): p. 437-49.

269. Lu, Y., et al., *Targeting artificial transcription factors to the utrophin A promoter: effects on dystrophic pathology and muscle function.* J Biol Chem, 2008. **283**(50): p. 34720-7.
270. Stresemann, C. and F. Lyko, *Modes of action of the DNA methyltransferase inhibitors azacytidine and decitabine.* Int J Cancer, 2008. **123**(1): p. 8-13.
271. Joung, J.K. and J.D. Sander, *INNOVATION TALENs: a widely applicable technology for targeted genome editing.* Nature Reviews Molecular Cell Biology, 2013. **14**(1): p. 49-55.
272. Rouet, P., F. Smih, and M. Jasin, *Expression of a Site-Specific Endonuclease Stimulates Homologous Recombination in Mammalian-Cells.* Proceedings of the National Academy of Sciences of the United States of America, 1994. **91**(13): p. 6064-6068.
273. Kim, Y.G., J. Cha, and S. Chandrasegaran, *Hybrid restriction enzymes: zinc finger fusions to Fok I cleavage domain.* Proc Natl Acad Sci U S A, 1996. **93**(3): p. 1156-60.
274. Mani, M., et al., *Binding of two zinc finger nuclease monomers to two specific sites is required for effective double-strand DNA cleavage.* Biochemical and Biophysical Research Communications, 2005. **334**(4): p. 1191-1197.
275. Kim, J.H., et al., *High cleavage efficiency of a 2A peptide derived from porcine teschovirus-1 in human cell lines, zebrafish and mice.* PLoS One, 2011. **6**(4): p. e18556.
276. Fine, E.J., et al., *An online bioinformatics tool predicts zinc finger and TALE nuclease off-target cleavage.* Nucleic Acids Research, 2014. **42**(6).
277. Matsumura, K., et al., *Association of Dystrophin-Related Protein with Dystrophin-Associated Proteins in Mdx Mouse Muscle.* Nature, 1992. **360**(6404): p. 588-591.
278. Corbi, N., et al., *The artificial zinc finger coding gene 'Jazz' binds the utrophin promoter and activates transcription.* Gene Ther, 2000. **7**(12): p. 1076-83.
279. Galvagni, F., S. Capo, and S. Oliviero, *Sp1 and Sp3 physically interact and co-operate with GABP for the activation of the utrophin promoter.* Journal of Molecular Biology, 2001. **306**(5): p. 985-996.
280. Choo, Y. and A. Klug, *Toward a code for the interactions of zinc fingers with DNA: selection of randomized fingers displayed on phage.* Proc Natl Acad Sci U S A, 1994. **91**(23): p. 11163-7.
281. Choo, Y. and A. Klug, *Selection of DNA-Binding Sites for Zinc Fingers Using Rationally Randomized DNA Reveals Coded Interactions.* Proceedings of the National Academy of Sciences of the United States of America, 1994. **91**(23): p. 11168-11172.
282. Liu, Q., Z.Q. Xia, and C.C. Case, *Validated zinc finger protein designs for all 16 GNN DNA triplet targets.* Journal of Biological Chemistry, 2002. **277**(6): p. 3850-3856.
283. Fu, F., et al., *Zinc Finger Database (ZiFDB): a repository for information on C2H2 zinc fingers and engineered zinc-finger arrays.* Nucleic Acids Research, 2009. **37**: p. D279-D283.
284. Liu, P.Q., et al., *Regulation of an endogenous locus using a panel of designed zinc finger proteins targeted to accessible chromatin regions - Activation of vascular endothelial growth factor A.* Journal of Biological Chemistry, 2001. **276**(14): p. 11323-11334.
285. Ramirez, C.L., et al., *Unexpected failure rates for modular assembly of engineered zinc fingers.* Nature Methods, 2008. **5**(5): p. 374-375.
286. Joung, J.K., D.F. Voytas, and T. Cathomen, *Genome editing with modularly assembled zinc-finger nucleases reply.* Nature Methods, 2010. **7**(2): p. 91-92.

287. Herrera, F.J. and S.J. Triezenberg, *VP16-dependent association of chromatin-modifying coactivators and underrepresentation of histones at immediate-early gene promoters during herpes simplex virus infection.* Journal of Virology, 2004. **78**(18): p. 9689-9696.
288. Marchal, C. and B. Miotto, *Emerging concept in DNA methylation: role of transcription factors in shaping DNA methylation patterns.* J Cell Physiol, 2015. **230**(4): p. 743-51.
289. Qiao, H. and J.M. May, *CpG methylation at the USF-binding site mediates cell-specific transcription of human ascorbate transporter SVCT2 exon 1a.* Biochemical Journal, 2011. **440**: p. 73-84.
290. Clark, S.J., J. Harrison, and P.L. Molloy, *Sp1 binding is inhibited by (m)Cp(m)CpG methylation.* Gene, 1997. **195**(1): p. 67-71.
291. Beltran, A.S., et al., *Reprogramming epigenetic silencing: artificial transcription factors synergize with chromatin remodeling drugs to reactivate the tumor suppressor mammary serine protease inhibitor.* Mol Cancer Ther, 2008. **7**(5): p. 1080-90.
292. Onori, A., et al., *UtroUp is a novel six zinc finger artificial transcription factor that recognises 18 base pairs of the utrophin promoter and efficiently drives utrophin upregulation.* Bmc Molecular Biology, 2013. **14**.
293. Wojtal, D., et al., *Spell Checking Nature: Versatility of CRISPR/Cas9 for Developing Treatments for Inherited Disorders.* American Journal of Human Genetics, 2016. **98**(1): p. 90-101.
294. Li, H.J., et al., *In vivo genome editing restores haemostasis in a mouse model of haemophilia.* Nature, 2011. **475**(7355): p. 217-U128.
295. Kim, J.H., et al., *High Cleavage Efficiency of a 2A Peptide Derived from Porcine Teschovirus-1 in Human Cell Lines, Zebrafish and Mice.* Plos One, 2011. **6**(4).
296. Lu, X.J., et al., *CRISPR-Cas9: a new and promising player in gene therapy.* Journal of Medical Genetics, 2015. **52**(5): p. 289-296.
297. Young, C.S., et al., *A Single CRISPR-Cas9 Deletion Strategy that Targets the Majority of DMD Patients Restores Dystrophin Function in hiPSC-Derived Muscle Cells.* Cell Stem Cell. **18**(4): p. 533-40.
298. Wolff, J.A., et al., *Conditions Affecting Direct Gene-Transfer into Rodent Muscle Invivo.* Biotechniques, 1991. **11**(4): p. 474-485.
299. Acsadi, G., et al., *Dystrophin expression in muscles of mdx mice after adenovirus-mediated in vivo gene transfer.* Hum Gene Ther, 1996. **7**(2): p. 129-40.
300. Dunant, P., et al., *Expression of dystrophin driven by the 1.35 kb MCK promoter ameliorates muscular dystrophy in fast, but not in slow muscles of transgenic mdx mice.* Neuromuscular Disorders, 2003. **13**(7-8): p. 632-632.
301. Qin, J.Y., et al., *Systematic Comparison of Constitutive Promoters and the Doxycycline-Inducible Promoter.* Plos One, 2010. **5**(5).
302. Carroll, D., *Genome engineering with zinc-finger nucleases.* Genetics, 2011. **188**(4): p. 773-82.
303. Jinek, M., et al., *A programmable dual-RNA-guided DNA endonuclease in adaptive bacterial immunity.* Science, 2012. **337**(6096): p. 816-21.
304. Ran, F.A., et al., *Genome engineering using the CRISPR-Cas9 system.* Nat Protoc, 2013. **8**(11): p. 2281-308.

305. Cradick, T.J., et al., *CRISPR/Cas9 systems targeting beta-globin and CCR5 genes have substantial off-target activity.* Nucleic Acids Res, 2013. **41**(20): p. 9584-92.